

# Modelling of Relaxation Phenomena in Transformer Oil-Paper-Pressboard Insulation to determine the Dielectric Response Behaviour under DC and Impulse Voltages

Devika Poduval



# Modelling of Relaxation Phenomena in Transformer Oil-Paper-Pressboard Insulation to determine the Dielectric Response Behaviour under DC and Impulse voltages

by

## Devika Poduval

to obtain the degree of Master of Science  
at the Delft University of Technology,  
to be defended publicly on October 30th, 2020 .

Student number:	4901827	
Project duration:	December 1, 2019 – October 30, 2020	
Responsible supervisor:	Prof. Ir. Peter Vaessen,	TU Delft
Daily supervisor:	Dr. Ir. Armando Rodrigo Mor,	TU Delft
Company supervisor:	Ir. Mark Wilkinson	Royal Smit Transformers B.V.
Thesis committee:	Prof. Ir. Peter Vaessen,	TU Delft
	Dr. Ir. Armando Rodrigo Mor,	TU Delft
	Dr. Ir. Rudi Santbergen	TU Delft

*This thesis is confidential and cannot be made public until October 30, 2021*

An electronic version of this thesis is available at <http://repository.tudelft.nl/>.



# Acknowledgement

Firstly, I would like to thank my supervisor, Dr.Armando Rodrigo Mor for allowing me to work on this research topic in collaboration with Royal Smit Transformers. His timely feedback has always helped me to think critically and motivated me to work hard on the thesis. I would also like to thank Mr.Mark Wilkinson of Royal Smit Transformers for his support and guidance.

I want to thank the support of Ing.Paul Van Nes and Dr.Luis Carlos Castro Heredia of TU Delft High voltage laboratory who helped me with all the testing for my thesis research. Without their help, this thesis would not have been possible. I am also truly grateful to TU Delft High Voltage laboratory manager Ir.Radek Heller for his support and encouragement. I want to extend my respect and gratitude to Prof.Peter Vaessen for reviewing my thesis report and for giving critical comments. I am much obliged to Dr.Rudi Santbergen for taking time to be a part of the thesis committee and for reviewing my report. It was a privilege to associate and work with all these brilliant minds, and this has helped me tune into a better learner.

No words can ever be strong enough to express my gratitude to my beloved parents, my husband and daughter for their unconditional love, support and patience during my study at TU delft. Lastly, I would like to thank my friends, especially Sai Medha Subramanian, Nived Abhay, Adeep Santhosh and Shruti Seshadri who have always supported and encouraged me in all my endeavours.

# Abstract

The factory acceptance tests are extremely important for the deployment and service life of Extra-high voltage transformers (EHV) and reactors. An essential part of such tests is Lightning Impulse (LI) tests which are intended to ensure that the transformer insulation withstands the transient lightning overvoltages which may occur while in service. These tests are usually done with negative polarity to prevent air side flashovers.

In recent years, there has been an increasing demand for additional positive polarity lightning impulse tests to secure the reliability and life of the transformers. The transformer, during its service life, is subjected to massive electrical stresses due to lightning strikes and switching impulses. As a consequence, this may lead to the degradation of the transformer insulation. During lightning impulse tests, ionisations might occur in the pressboard/insulating liquid insulation system, which would lead to the development of space charges. The space charges generated may have an influence on the withstand behaviour of the insulation corresponding to applied impulse voltage. There is also a possibility of field enhancements due to the effect of space charge, especially when tested consecutively with opposite polarity. During the acceptance tests on transformers at SGB-SMIT transformers, a waiting period of one hour is given between the negative polarity LI and positive polarity LI. This arbitrary waiting time is given under the assumption that this will allow any 'trapped' charges to decay and provide relaxation time for the slower polarisation processes. So the main question is whether this waiting period allows sufficient time for the decay of charges in the transformer insulation. For this analysis, the relaxation time characteristics of the transformer insulation system were investigated by estimation of the time dependency of depolarisation currents in the oil, paper/pressboard insulation.

In this thesis, the characteristic of the time-domain dielectric response and the time dependency of the currents due to depolarisation of charges under DC and impulse voltage was investigated by the polarisation-depolarisation current (PDC) measurements on the test samples. The PDC method is a non-destructive diagnostic method for evaluating transformer insulation in the time domain.

A test set up was built to represent a simplified model of transformer insulation comprising of mineral oil, paper and pressboard. The measurements of discharge voltage over time were conducted on the test samples of oil, paper and pressboard to understand the time-dependency of polarisation-depolarisation processes occurring within the transformer insulation. Two dominant time constants of decay were estimated for oil, paper and pressboard samples. The results from the discharge voltage measurement were compared with the analytical solution of the output voltage of the equivalent R-C circuit of the test sample which revealed that there were more than two polarisation phenomena occurring within the composite test sample of oil, paper and pressboard. Later, to mitigate the inconsistencies with the simplified R-C model, it was extended and modified based on the linear dielectric response theory to study the dielectric response behaviour of transformer insulation under DC voltage for longer charging times ( $t_c=10,000$  seconds).

The modified R-C model was envisioned and developed in PSPICE simulation environment. The model incorporates the effect of the individual polarisation processes occurring within the constituent dielectrics of transformer oil-paper-pressboard insulation. The dielectric properties like conductivity and dielectric response function  $f(t)$  can be estimated reasonably accurately with this modified R-C model. A comparison of the maximum and minimum values of the polarisation currents of the composite test sample obtained from the simulated model and from dielectric testing was conducted. The results demonstrated that relative errors were limited to a maximum of 8 %.

The time-domain polarisation and depolarisation behaviour of composite transformer insulation was analysed under DC and impulse voltages from simulations of PDC measurements using PSPICE simulation software. It was observed that for the same thickness of solid insulation, as the oil-gap increases, the magnitude of the depolarisation current at the end of the discharging period (10,000 seconds) also increases. For identical oil-gaps, as the thickness of the pressboard in the composite test sample of oil-paper-pressboard

was increased, the depolarisation currents show a delayed response to decay to a minimum value at the end of discharging duration. The time dependency of depolarisation currents at the end of discharging time of one hour was realised for impulse voltages. The study of the depolarisation currents under the influence of impulse voltage revealed that the charge induced field at the end of the discharging period of one hour does not exceed the permissible threshold electric field of 2 kV/mm inside the transformer insulation. In the future, the model could be developed into a valuable diagnostic tool for studying the dielectric responses of complex transformer insulation under the influence of different parameters like moisture content, ageing products, geometrical configuration and temperature.

# Contents

Acknowledgement	ii
Abstract	iii
List of Figures	viii
List of Tables	xi
1 Introduction	1
1.1 Motivation	1
1.2 Research Questions	2
1.3 Research Methodology	2
1.4 Research outline	3
2 Dielectric tests and Dielectric response analysis	4
2.1 Transformer insulation	4
2.2 Interfacial charge accumulation in transformer insulation	5
2.2.1 Polarisation and depolarisation	5
2.2.2 Detrapping of charges	6
2.3 Dielectric response analysis	7
2.3.1 Dielectric response measurements	8
2.3.2 Dielectric spectroscopy in time domain	8
2.3.3 Frequency domain spectroscopy	9
2.4 Overview of dielectric tests conducted on transformer insulation	10
2.5 Impulse voltage testing of transformer insulation	12
2.6 Conclusion	12
3 Dielectric relaxation in time domain	14
3.1 Introduction	14
3.1.1 Theory	14
3.2 Discharge voltage measurements	15
3.2.1 Test samples used for discharge voltage measurement	15
3.2.2 Proposed model for discharge voltage measurement	16
3.2.3 Equipment used for measurements	17
3.2.4 Electrostatic voltmeter for discharge voltage measurement	17
3.2.5 Preparation of the test samples	18
3.2.6 Procedure	19
3.3 Estimation of the time constants of the discharge voltage curve	22
3.3.1 Estimated values of time constants of the discharge voltage curve	24
3.4 Observations and Discussions	25
3.4.1 Effect of the oil-gap distance on the time constant values	26
3.4.2 Effect of the temperature on the time constant values	27
3.4.3 Effect of the moisture content on the time constant values	28
3.5 Summary	29
3.6 Conclusion	29
4 Simplified R-C model	30
4.1 R-C equivalent model of transformer insulation	30
4.1.1 Modelling of simplified R-C equivalent circuit	31
4.1.2 Analysis of the simplified R-C model	33
4.2 Modified equivalent R-C model of the insulation system	35
4.2.1 Basic relations of the linear dielectric response theory	36

4.3	Identification of the circuit parameters of the equivalent R-C model . . . . .	36
4.4	Dielectric response in time domain . . . . .	37
4.4.1	Relation between polarisation current and the dielectric response function $f(t)$ . . . . .	37
4.4.2	Estimation of depolarisation current and its relation with dielectric response function $f(t)$ . . . . .	39
4.5	Dielectric response of multi-layered insulation . . . . .	39
4.5.1	Polarisation current through multi-layered insulation of oil, paper and pressboard . . . . .	40
4.6	Summary . . . . .	41
5	DC measurements of polarisation currents . . . . .	42
5.1	Dielectric measurements using IDAX 300 . . . . .	42
5.2	Overview of the dielectric measurements on individual test samples . . . . .	43
5.2.1	Test cells used for the measuring test samples of oil, paper and pressboard . . . . .	44
5.2.2	Test Conditions . . . . .	46
5.2.3	IDAX test results of individual samples of oil, paper and pressboard . . . . .	47
5.3	Overview of the tests performed on the composite test samples . . . . .	49
5.3.1	Test conditions . . . . .	52
5.3.2	Optimal charging time $t_c$ . . . . .	53
5.3.3	IDAX test results of composite insulation of oil, paper and pressboard . . . . .	53
5.4	Summary . . . . .	58
6	Simulation of the modified R-C model . . . . .	59
6.1	Introduction . . . . .	59
6.2	Building the linear dielectric model for oil, paper and pressboard samples using PSPICE . . . . .	60
6.2.1	Identifying the model parameters of individual dielectric model. . . . .	60
6.2.2	Modelling the individual R-C circuit of oil, paper and pressboard . . . . .	62
6.3	Comparison of the polarisation currents obtained from DC tests and the simulated PSPICE models . . . . .	63
6.3.1	Analysis of the depolarisation currents obtained from PSPICE model . . . . .	64
6.3.2	Analysis of the dielectric response function $f(t)$ obtained from PSPICE model . . . . .	67
6.4	Building of the PSPICE model of extended R-C circuit of composite insulation of oil, paper and pressboard . . . . .	68
6.4.1	Identification the model parameters of extended R-C circuit. . . . .	68
6.4.2	Comparison of the polarisation currents obtained from DC tests and the simulated PSPICE model . . . . .	71
6.5	Analysis of the time dependency of depolarisation currents . . . . .	78
6.5.1	Analysis of the time dependency of dielectric response function $f(t)$ in the composite insulation . . . . .	81
6.6	Analysis of the time dependency of the depolarisation currents in the composite insulation under impulse voltage . . . . .	82
6.6.1	Building one stage Marx generator in PSPICE . . . . .	82
6.6.2	Measurement of the depolarisation currents under the influence of the 1.2/50 $\mu s$ impulse voltage. . . . .	83
6.7	Observations and Discussions . . . . .	87
6.8	Conclusion . . . . .	90
7	Conclusions and Future Recommendations . . . . .	91
7.1	Conclusions. . . . .	91
7.2	Future Recommendations . . . . .	93
A	APPENDIX . . . . .	94
A.1	Exponential curve fitting using curve fitting tool on discharge voltage curves. . . . .	94
B	APPENDIX . . . . .	97
B.1	Dissipation factor ( $\tan \delta$ ) of the test samples . . . . .	97
B.1.1	Values of dissipation factor obtained from DC measurements on individual test samples of oil, paper and pressboard . . . . .	97

B.2	Values of dissipation factor obtained from DC measurements on composite test samples of oil, paper and pressboard . . . . .	97
B.3	Estimated Values of oil to paper/pressboard ratio in the composite test samples of oil, paper and pressboard . . . . .	99
C	APPENDIX . . . . .	101
C.1	MATLAB CODE FOR CALCULATING THE MODEL PARAMETERS . . . . .	101
C.2	MATLAB CODE FOR CALCULATING THE RELATIVE PERMITTIVITY OF COMPOSITE INSULATION . . . . .	102
	Bibliography . . . . .	103

# List of Figures

2.1	Oil distribution transformers made by SGB-SMIT Group . . . . .	5
2.2	Voltage and current waveforms representing polarisation and depolarisation [10] . . . . .	6
2.3	Test arrangement for polarisation-depolarisation measurements [8] . . . . .	9
2.4	Return voltage curve [10] . . . . .	9
2.5	IDAX 300 used for Frequency domain spectroscopy [1] . . . . .	10
3.1	Polarisation phenomenon . . . . .	15
3.2	Equipment used for measurement along with Test set-up . . . . .	16
3.3	Test set up with sample . . . . .	16
3.4	Schematic diagram of the test aquarium with samples and the measurement set-up . . . . .	17
3.5	Test set with sample paper-pressboard is kept in vacuum oven . . . . .	18
3.6	Vacuum Oven used for vacuum treatment of pressboard and paper . . . . .	18
3.7	Vacuum oven used for degassing and vacuum treatment of oil . . . . .	19
3.8	Discharge voltage vs time obtained at $T=39^{\circ}C$ . . . . .	20
3.9	Discharge voltage vs time at $T=22^{\circ}C$ ; $d=3.2$ cm . . . . .	21
3.10	Discharge voltage vs time at $T=22^{\circ}$ , after the the test aquarium with samples was kept open and exposed to ambient air for 4 days; $d=3.2$ cm . . . . .	22
3.11	Discharge voltage vs Time ; Distance between the electrodes ' $d'$ '= 3.2 cm ; $T=39^{\circ}C$ . . . . .	23
3.12	Exponential curve fit is used on the plot of discharge voltage curve varying with time . . . . .	23
3.13	Comparison of plots of discharge voltage vs time to study the effect of oil-gap . . . . .	26
3.14	Discharge voltage vs time obtained at $T=39^{\circ}C$ and $T=22^{\circ}C$ . . . . .	27
3.15	Comparison of plots of discharge voltage vs time to study the effect of moisture in the composite test sample . . . . .	28
4.1	Cross-section of the transformer insulation between low and high voltage windings [12] . . . . .	30
4.2	R-C equivalent circuit of sample in time domain . . . . .	31
4.3	R-C equivalent circuit of sample in s-domain . . . . .	32
4.4	Simplified R-C equivalent circuit of sample in s-domain . . . . .	32
4.5	Comparison between measured discharge voltage plot and the simulated discharge voltage plot . . . . .	34
4.6	Modified R-C equivalent circuit of the insulation system . . . . .	35
4.7	Equivalent circuit of the linear dielectric [12] . . . . .	36
4.8	Extended model of linear multi-layer dielectric . . . . .	39
4.9	Extended circuit of the multi-layered dielectric . . . . .	40
5.1	IDAX 300 [1] . . . . .	42
5.2	2914 Tettex test cell for solid insulants . . . . .	44
5.3	Schematic diagram of test object and guarded measuring electrode . . . . .	45
5.4	Oil test cell . . . . .	45
5.5	Low voltage electrode of oil test cell . . . . .	46
5.6	Oil test cell dimensions . . . . .	46
5.7	Polarisation current vs Time plot for oil . . . . .	48
5.8	Polarisation current vs Time plot for paper sample of thickness 0.25 mm . . . . .	48
5.9	Polarisation current vs Time for pressboard sample of thickness 1 mm . . . . .	48
5.10	Polarisation current vs Time for pressboard sample of thickness 2 mm . . . . .	49
5.11	Test aquarium with measuring electrode . . . . .	50
5.12	Paper and pressboard samples screwed to the metallic parallel plate . . . . .	50
5.13	Test aquarium with test dielectrics . . . . .	51
5.14	Polarisation current vs Time for composite insulation of oil, paper and pressboard sample ; $d=9.5$ mm . . . . .	54

5.15	Polarisation current vs Time for composite insulation of oil, paper and pressboard sample ; $d=$ 14.5 mm . . . . .	54
5.16	Polarisation current vs Time for composite insulation of oil, paper and pressboard sample ; $d =$ 19.5 mm . . . . .	54
5.17	Polarisation current vs Time for composite insulation of oil, paper and pressboard sample ; $d=$ 15.5 mm . . . . .	55
5.18	Polarisation current vs Time for composite insulation of oil, paper and pressboard sample ; $d =$ 20.5 mm . . . . .	56
5.19	Polarisation current vs Time for composite insulation of oil, paper and pressboard sample ; $d =$ 25.5 mm . . . . .	56
5.20	Polarisation current vs Time for composite insulation of oil, paper and pressboard sample ; $d =$ 12 mm . . . . .	57
5.21	Polarisation current vs Time for composite insulation of oil, paper and pressboard sample ; $d =$ 17 mm . . . . .	57
5.22	Polarisation current vs Time for composite insulation of oil, paper and pressboard sample ; $d =$ 22 mm . . . . .	58
6.1	Analysis flowchart . . . . .	59
6.2	Linear dielectric model . . . . .	60
6.3	Linear dielectric model for individual test samples of oil, paper and pressboard . . . . .	61
6.4	PSPICE model of individual dielectric . . . . .	62
6.5	Comparison of the polarisation current varying over time obtained from DC tests and the PSPICE models . . . . .	63
6.6	Comparison of the polarisation current varying over time obtained from DC tests and the PSPICE models . . . . .	63
6.7	Polarisation and depolarisation current varying over time for oil . . . . .	65
6.8	Polarisation and depolarisation current varying over time for pressboard sample of 1 mm thick- ness . . . . .	65
6.9	Depolarisation current varying over time for individual dielectrics of oil, paper and pressboard .	66
6.10	Dielectric response function $f(t)$ for individual dielectrics of oil, paper and pressboard; Plot of $f(t)$ starts from $t= 10,000$ seconds. . . . .	67
6.11	Modified extended R-C circuit of composite insulation of oil, paper and pressboard . . . . .	68
6.12	Polarisation current in composite insulation of oil, paper and pressboard . . . . .	69
6.13	Comparison between $i_{pol}(t)$ values from IDAX and simulated PSPICE model; Distance between the electrodes = 9.5 mm . . . . .	72
6.14	Comparison between $i_{pol}(t)$ values from IDAX and simulated PSPICE model; Distance between the electrodes = 14.5 mm . . . . .	72
6.15	Comparison between $i_{pol}(t)$ values from IDAX and simulated PSPICE model; Distance between the electrodes=19.5 mm . . . . .	73
6.16	Comparison between $i_{pol}(t)$ values from IDAX and simulated PSPICE model; Distance be- tween the electrodes= 15.5 mm . . . . .	74
6.17	Comparison between measured $i_{pol}(t)$ values from IDAX and simulated PSPICE model; Dis- tance between the electrodes =20.5 mm . . . . .	74
6.18	Comparison between $i_{pol}(t)$ values from IDAX and simulated PSPICE model; Distance between the electrodes =25.5 mm . . . . .	75
6.19	Comparison between measured $i_{pol}(t)$ values from IDAX and simulated PSPICE model; Dis- tance between the electrodes = 12 mm . . . . .	76
6.20	Comparison between $i_{pol}(t)$ values from IDAX and simulated PSPICE model; Distance between the electrodes = 17 mm . . . . .	76
6.21	Comparison between $i_{pol}(t)$ values from IDAX and simulated PSPICE model; Distance between the electrodes = 22 mm . . . . .	77
6.22	Polarisation Currents and Depolarisation Currents; Thickness of pressboard in composite insu- lation= 1 mm . . . . .	78
6.23	Polarisation Currents and Depolarisation Currents;Thickness of pressboard in composite insu- lation= 2 mm . . . . .	78

6.24	Polarisation Currents and Depolarisation Currents;Thickness of pressboard in composite insulation=5 mm . . . . .	78
6.25	Estimated $f(t)$ plots from the depolarisation current plots measured from $t= 10,000$ to $20,000$ seconds ; Figure (b) Dielectric function $f(t)$ of composite test samples was zoomed in for better analysis . . . . .	81
6.26	One stage Marx generator . . . . .	82
6.27	Impulse circuit built in PSPICE . . . . .	83
6.28	$1.2/50\mu$ s impulse voltage . . . . .	84
6.29	Impulse circuit connected to the extended R-C circuit . . . . .	84
6.30	Polarisation and Depolarisation current under the influence of the applied impulse voltage . . .	85
A.1	Exponential curve fitting using curve fitting tool on discharge voltage curve varying over time .	94
A.2	Exponential curve fitting using curve fitting tool on discharge voltage curve varying over time .	95
A.3	Exponential curve fitting using curve fitting tool on discharge voltage curve varying over time .	95
A.4	Exponential curve fitting using curve fitting tool on discharge voltage curve varying over time .	95
A.5	Exponential curve fitting using curve fitting tool on discharge voltage curve varying over time .	96
B.1	Test aquarium with test dielectrics . . . . .	99

# List of Tables

1.1	Research Methodology . . . . .	2
1.2	Chapter summary . . . . .	3
2.1	LI Test Sequence performed as a part of factory acceptance test for transformers (400-500 kV) . . . . .	11
3.1	Equipment used for measurement of discharge voltage . . . . .	17
3.2	Test case-I: Measurement of discharge voltage taken at T= 39°C . . . . .	20
3.3	Time constants obtained at T=22°C for different charging times $t_c$ ; $d=3.2$ cm . . . . .	21
3.4	Test case-III: Measurement of discharge voltage taken at T= 22°, after the the test aquarium with samples was kept open and exposed to ambient air for 4 days; $d=3.2$ cm . . . . .	22
3.5	Time constants obtained at T=39°C for different charging times $t_c$ ; Distance between the electrodes $d'=3.2$ cm . . . . .	24
3.6	Time constants and R-square values obtained at T=22°C for different charging times $t_c$ . Distance between the electrodes $d'=3.2$ cm . . . . .	25
3.7	Time constants and R-square values obtained at room temperature of T = 22°C after the test aquarium with samples was kept open and exposed to ambient air for 4 days; Distance between the electrodes $d'=3.2$ cm . . . . .	25
3.8	Time constants obtained at Temperature of T= 39°C for charging time $t_c=1$ min and 5 min. . . . .	26
3.9	Time constants obtained at T=22°C; $d=3.2$ cm . . . . .	27
3.10	Time constants obtained at T=22°C (Same oil temperature but in the second case the test samples were exposed to moisture for four days). Distance between the electrodes $d'=3.2$ cm . . . . .	28
4.1	Dielectric time constants of the oil, paper and pressboard . . . . .	34
5.1	Measurement specifications of IDAX 300 . . . . .	43
5.2	Specifications of PDC measurements using IDAX 300 . . . . .	43
5.3	Test samples and measured parameters obtained from IDAX 300 . . . . .	44
5.4	Ambient test conditions for individual samples . . . . .	47
5.5	Measured values of capacitance $C_m$ and insulation resistance $R_m$ obtained from IDAX 300 . . . . .	47
5.6	Computed parameters of distance between electrodes $d'$ , oil-gap and oil-solid insulation ratio); Thickness of pressboard in composite insulation = 1 mm . . . . .	51
5.7	Ambient test conditions for composite test samples; Thickness of pressboard in the sample = 1 mm . . . . .	52
5.8	Ambient test conditions for composite test samples; Thickness of pressboard in the sample = 2 mm . . . . .	52
5.9	Ambient test conditions for composite test samples; Thickness of pressboard in the sample = 5 mm . . . . .	52
5.10	Test case:1 Measured parameters from IDAX; Thickness of pressboard in composite insulation = 1 mm . . . . .	53
5.11	Measured parameters from IDAX; Thickness of pressboard in composite insulation = 2 mm . . . . .	55
5.12	Measured parameters from IDAX; Thickness of pressboard in composite insulation = 5 mm . . . . .	57
6.1	Estimated model parameters . . . . .	62
6.2	Relative error % between the maximum values of polarisation currents obtained from IDAX and the simulated PSPICE model . . . . .	64
6.3	Relative error % between the minimum values of polarisation currents obtained from IDAX and the simulated PSPICE model . . . . .	64
6.4	Dissipation factor measured at 50 Hz . . . . .	66
6.5	Maximum and minimum values of depolarisation currents of individual test samples . . . . .	67

6.6	Comparison between measured values of maximum values of polarisation values from IDAX and the simulated model in PSPICE; Thickness of pressboard in the composite insulation = 1 mm	73
6.7	Comparison between measured values of minimum values of polarisation current from IDAX and the simulated model in PSPICE; Thickness of pressboard in the composite insulation= 1 mm	73
6.8	Comparison between measured values of maximum values of polarisation values from IDAX and the simulated model in PSPICE; Thickness of pressboard in the composite insulation= 2 mm	75
6.9	Comparison between measured values of minimum values of polarisation current from IDAX and the simulated model in PSPICE; Thickness of pressboard in the composite insulation= 2 mm	75
6.10	Comparison between measured values of maximum values of polarisation values from IDAX and the simulated model in PSPICE; Thickness of pressboard in the composite insulation= 5 mm	77
6.11	Comparison between measured values of minimum values of polarisation current from IDAX and the simulated model in PSPICE; Thickness of pressboard in the composite insulation= 5 mm	77
6.12	Maximum and minimum values of depolarisation currents from PSPICE model;Thickness of pressboard in the sample= 1mm	79
6.13	Maximum and minimum values of depolarisation currents measured from the PSPICE model; Thickness of pressboard in the sample= 1 mm	79
6.14	Maximum and minimum values of depolarisation currents measured from the PSPICE model; Thickness of pressboard in the sample= 2 mm	80
6.15	Maximum and minimum values of depolarisation currents measured from the PSPICE model; Thickness of pressboard in the sample= 2 mm	80
6.16	Maximum and minimum values of depolarisation currents measured from the PSPICE model; Thickness of pressboard in the sample = 5 mm	80
6.17	Maximum and minimum values of depolarisation currents measured from the PSPICE model; Thickness of pressboard in the sample =5 mm	81
6.18	Test case:1 Maximum and minimum values of depolarisation currents;Thickness of pressboard in the sample = 1 mm	85
6.19	Test case:2 Maximum and minimum values of depolarisation currents ; Thickness of pressboard in the sample= 1 mm	85
6.20	Test case:3 Maximum and minimum values of depolarisation currents ; Thickness of pressboard in the sample= 2 mm	86
6.21	Test case:4 Maximum and minimum values of depolarisation currents ; Thickness of pressboard in the sample= 2 mm	86
6.22	Test case:5 Maximum and minimum values of depolarisation currents ; Thickness of pressboard in the sample = 5 mm	86
6.23	Test case:6 Maximum and minimum values of depolarisation currents ; Thickness of pressboard in the sample = 5 mm	87
6.24	Comparison of minimum value of depolarisation current obtained from composite test samples with sample oil-gap distance $d_{oil}$ with different thickness of solid insulation	88
6.25	Comparison of minimum value of depolarisation current obtained from composite test samples with sample oil-gap with different thickness of solid insulation	88
6.26	Depolarisation current values $i_{depol}(t)$ at the end of discharging time of $t_d$ ; Applied voltage= 500 V	89
B.1	Tan delta values for individual test samples	97
B.2	Test case:1 Tan $\delta$ values for the composite test sample of oil, paper and pressboard; Thickness of pressboard = 1 mm	98
B.3	Test case:2 Tan $\delta$ values for the composite test sample of oil, paper and pressboard; Thickness of pressboard = 2 mm	98
B.4	Test case:3 Tan $\delta$ values for the composite test sample of oil, paper and pressboard; Thickness of pressboard = 5 mm	98
B.5	Estimation of oil to paper-pressboard ratio ( Rounded off to nearest decimal point); Thickness of pressboard in composite insulation = 1 mm	99
B.6	Estimation of oil to paper-pressboard ratio (Rounded off to nearest decimal point); Thickness of pressboard in composite insulation = 2 mm	100
B.7	Estimation of oil to paper-pressboard ratio (Rounded off to nearest decimal point) ;Thickness of pressboard in composite insulation = 5 mm	100





# 1

## Introduction

The first chapter briefly describes the motivation behind this project, followed by the research questions that this thesis attempts to answer. Finally, an outline of the approach adopted to answer the research objectives of the thesis is also presented.

### 1.1. Motivation

Insulation is regarded as one of the essential components of a transformer. The dielectric tests guarantee the effectiveness of the insulation system of a transformer and are conducted to qualify a transformer's ability to operate safely during nominal operating voltage. However, the power frequency withstand tests alone are not usually sufficient to ensure the dielectric withstand capability of a transformer.

For extended service life and to secure the integrity of transformers, the lightning Impulse (LI) testing is included as a part of the factory acceptance test for extra-high voltage transformers and reactors. The LI tests are intended to ensure that the transformer insulation is capable of withstanding the transient lightning over-voltages which may occur while in service. These tests are generally performed with negative polarity to prevent air side flashovers in the external insulation. Additional positive polarity lightning impulse tests are also occasionally conducted along with negative LI tests as per the demand of the customers, typically for the TSOs (Transmission system operators) in the Netherlands, Germany and Switzerland.

It is likely that during lightning impulse tests, ionisations might occur in the pressboard/insulating liquid insulation system, which would lead to the development of space charges. The space charges generated may have an influence on the withstand behaviour of the insulation corresponding to applied impulse voltage. There is also a possibility of field enhancements due to the effect of space charge, especially when tested with positive and negative polarity LI consecutively.

Generally, as an industry standard, a waiting period of one hour is given between the application of opposite polarity LI, i.e. while administering both positive and negative lightning impulse tests in a consecutive order. This waiting time is given in order to allow any 'trapped' charges to decay and to allow relaxation time for the slower polarisation processes. This research tries to answer whether the waiting period of one hour is sufficient for the charges in the transformer insulation system to 'de-trap' and depolarise. The electric field generated due to remnant charges in the dielectric may have adverse effects on the dielectric strength of the insulation. A thorough analysis of the theoretical background is required to understand the physical processes occurring within the constituent dielectrics of transformer insulation under the influence of the applied electric field. Henceforth for this investigation, the time dependency of polarisation-depolarisation currents in the transformer insulation system under DC and impulse voltages were studied.

A test set up was built to represent a simplified model of transformer insulation to study the polarisation-depolarisation processes occurring within the transformer insulation. For the analysis of the transformer insulation system consisting of oil-paper and pressboard insulation, the measurement of discharge voltage of the system was also carried out initially to understand the time-dependency of depolarisation processes occurring inside the transformer insulation.

## 1.2. Research Questions

This thesis aims to find answers for the following research questions:

- How to determine the time dependency of physical processes of polarisation and depolarisation, occurring within the transformer oil-paper-pressboard insulation under the influence of the applied electric field?
- How to develop a model which will help to determine the dielectric response behaviour of transformer insulation under DC and impulse voltages?
- What experimental procedure would help to verify the newly developed model ? How can the developed model be validated with the experimental outcome ?
- What results can be derived from the developed model regarding the time dependency of depolarisation currents of the transformer oil-paper-pressboard insulation system under DC and Impulse voltages ?

## 1.3. Research Methodology

The following Table 1.1 provides an overview of the research work carried out during this thesis . In order to effectively answer the research questions , the inventory of thesis work was divided into three phases:

<b>PHASE- 1</b>	- Literature review on the inventory of effects occurring in the Transformer insulation during dielectric tests.
	- Develop a test set up to investigate the dielectric behaviour of the transformer insulation under DC voltage.
<b>PHASE- 2</b>	- Analysis of the test results and comparison with the equivalent R-C circuit model of the test sample.
	- Prepare a modified equivalent circuit model of the sample under test.
	- Conduct time domain dielectric measurements on the individual test samples and on composite test samples comprising of oil, paper and pressboard.
<b>PHASE- 3</b>	- Identify the model parameters of the equivalent R-C circuit.
	- Build an extended R-C equivalent models of the test samples using PSPICE simulation software.
	- Analysis of the dielectric behaviour of transformer insulation under under DC and impulse voltage.

Table 1.1: Research Methodology

## 1.4. Research outline

The thesis report is organised as follows:

Chapter 1 provides an introduction to the research project and gives a description of the research questions. It also give an overview of the research methodology used in this thesis. Chapter 2 discusses the literature review conducted for the thesis and provides an outline of the relevant background to this thesis.

An overview of the dielectric relaxation behaviour of discharge voltage of the composite insulation of oil, paper and pressboard is presented in Chapter 3. Along with that, an evaluation of the time constants of decay of the discharge voltage of the composite test samples is also conferred in Chapter 3. A simplified R-C model of the test sample of oil, paper and pressboard is analytically solved, and the need for a modified R-C equivalent circuit for representing the transformer insulation is described in Chapter 4.

Chapter 5 outlines the DC measurements of the polarisation currents of the individual dielectrics- oil, paper and pressboard and also of the test samples containing a combination of oil, paper and pressboard conducted in the High voltage Laboratory, TU Delft. The parameters of the extended R-C equivalent model were identified and derived from these dielectric measurements.

Chapter 6 details the building of the linear dielectric models representing the individual dielectrics of oil, paper and pressboard in PSPICE simulation platform. It also describes the modelling of extended R-C circuits of the composite test samples of oil, paper and pressboard using PSPICE simulation software. Lastly, Chapter 7 summarises the conclusions and answers the main research questions of this thesis. and discusses some of the future recommendations in this field of research. The following Table 1.2 lists the chapters and corresponding chapter names included in this thesis report.

<b>Chapters</b>	<b>Chapter Name</b>
<b>Chapter-1</b>	Introduction
<b>Chapter-2</b>	Dielectric tests and dielectric response analysis
<b>Chapter-3</b>	Dielectric response in time domain
<b>Chapter-4</b>	Simplified R-C model of transformer insulation
<b>Chapter-5</b>	DC measurements of polarisation currents
<b>Chapter-6</b>	Simulation of extended R-C model of transformer insulation
<b>Chapter-7</b>	Conclusions and future recommendations

Table 1.2: Chapter summary

# 2

## Dielectric tests and Dielectric response analysis

This chapter starts with an introduction to the commonly used dielectric materials of oil, paper and pressboard as the transformer insulation and an overview of their properties and functions are described briefly. To understand the breakdown mechanism of the transformer insulation, a thorough review of dielectric response characteristics such as polarisation, depolarisation and other subsequent phenomena within the transformer insulation is crucial. Firstly, a discussion on the interfacial charge accumulation inside the transformer insulation under DC voltages is presented. Relevant background information regarding the polarisation, depolarisation and detrapping of charges is also included under this section. After that, the related research papers on dielectric diagnostics methods is reviewed. Following that, an outline of time-domain dielectric spectroscopy is given. Lastly, different dielectric tests and the need for the impulse voltage testing of transformer insulation has been explained in the final section.

### 2.1. Transformer insulation

The oil-paper-pressboard insulation is widely used in majority of power transformers. The transformer oil which serves as liquid insulation must possess sufficient dielectric strength, thermal conductivity, and chemical stability [7]. Additionally, it must also serve the function of cooling the windings and extraction of the heat dissipated by the conductors. The dielectric properties of the oil-paper insulation system are maintained by proper drying of oil and drying and impregnation of paper/pressboard. Moisture content and contaminants in the oil significantly reduce the dielectric strength of the oil. The minimum value of breakdown voltage (BDV) of transformer oil is 30-40 kV for a test gap of 2.5 mm. A higher BDV value confirms a lower concentration of contaminants [13]. The breakdown voltage of transformer oil shows a decreasing trend with ageing [27].

The solid insulation employed in the transformer are paper and pressboard and mainly involves barriers, spacers, clamps and winding insulation. The barriers prevent particle-induced breakdown by interrupting the short-circuiting bridges in the liquid insulation. This helps in improving the breakdown strength of the oil. The barriers are made of pressboard, usually of few millimetres thickness [32], [49]. The cellulose insulation comprising of paper and pressboard contributes to better thermal performance of the transformer by forming cooling ducts for the oil. It also provides mechanical support to the windings. The cellulose-based paper widely used for conductor insulation in oil-filled transformers is called kraft paper. Thermally upgraded paper (Thermal class E (120 °C) as per IEC 554-3-5 with a thickness of 50 - 125 microns) and diamond dotted epoxy paper are the different grades of cellulose paper used as transformer insulation [5]. Heat and moisture are the key factors known to cause the degeneration of the paper insulation. Due to ageing, contaminants build up in the transformer oil, and by-products of oxidation processes form deposits and adversely affect the mechanical strength of paper insulation.



(a) Oil Distribution transformer [20]

(b) Solid insulation used in transformers [49]

Figure 2.1: Oil distribution transformers made by SGB-SMIT Group

## 2.2. Interfacial charge accumulation in transformer insulation

The space charge trapping and accumulation is fundamental in multi-dielectric media under high fields due to significant charge injection and conductivity mismatch between constituent dielectrics. Whenever there is a jump in the  $\epsilon/\sigma$  values especially in case of layered dielectric such as impregnated paper/pressboard in oil, there will be space charge accumulation and trapping of charges.

In a dielectric, under the influence of high electric field, free charges may be injected into the bulk of the material from electrodes or can be generated by ionisation. Furthermore, these charges can get trapped in the trapping centers in the dielectric. When the trapping rate is greater than the de-trapping rate, it will lead to the accumulation of charges in the bulk of the dielectric [62]. If the charge injection from the electrodes is more than the dielectric can conduct, then homo charges are formed near the electrodes. Similarly, hetero charges are formed if the dielectric transports charges faster than the electrodes could supply [33].

As the polarisation-depolarisation measurements are carried out at low electric fields, the effect of charge injection would be negligible. Hence, the polarisation- depolarisation measurements are mainly influenced by the ionic charge carriers trapped at the mineral oil and paper/ pressboard interface [43].

### 2.2.1. Polarisation and depolarisation

On applying a DC voltage  $U$  across a dielectric of capacitance  $C$ , a capacitive current  $i_c$  starts to flow which is given by

$$i_c = C \frac{dU}{dt} \quad (2.1)$$

Afterwards, the current through the dielectric is expected to fall to a small magnitude of current called the leakage current  $i_l$ . Instead, the current starts to decay slowly. This current is called the polarisation current, and it flows until a steady-state conduction current is reached. The polarisation current is governed by the orientation of the dipoles in response to the electric field generated due to the applied DC voltage [33].

When the DC voltage is switched off and the test dielectric is shorted, the dipoles relax and return back to the original state due to which a current  $i_d$  flows, which can be characterised as depolarisation current. Due to the conductivity difference between oil and paper, ionic charges may accumulate at the interfacial region of oil-paper insulation system. During depolarisation, a part of accumulated charges gets detrapped and contributes to depolarisation current. The time taken by the depolarisation current to fall back to zero after the removal of applied DC voltage will give an approximate idea about the standing behaviour of the materials inside the transformer [51], [12].

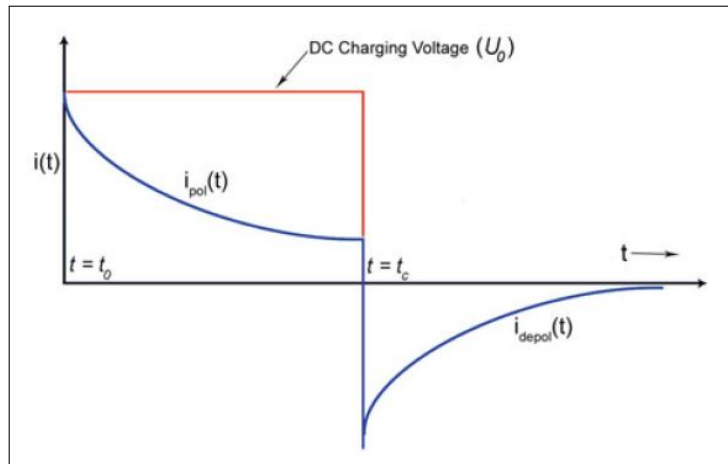


Figure 2.2: Voltage and current waveforms representing polarisation and depolarisation [10]

### 2.2.2. Detrapping of charges

In the presence of an electric field, charges are introduced in a dielectric in two possible ways: by ionisation and by charge injection from electrodes. Generally, the compounds in mineral oil and cellulose material (like pressboard) become easily ionised under the presence of the electric field. Migration of such ions from positive to the negative electrode produces the conduction current [62].

Available literature [63],[24], [42] has reported that the oil-paper interface region functions like a potential barrier, where the positive charges get trapped. The trapping of charges proceeds until the trapped charges obtain adequate energy to cross the barrier and contribute to the conduction process again. In the transformer insulation, many intermittent layers of oil and paper exist, creating a vast interface region which forms potential trap-centres for charges.

Several factors influence the interfacial charge trapping, which includes the conductivity difference of oil and cellulose, the presence of moisture and ageing of the transformer insulation. The process of trapping of charges can be considered as a mode of energy storage restraining the charge build-up to specific sites. The trapped charges receive the energy to overcome the interfacial potential barrier (trap energy or trap depth) through various processes including thermal collisions, photon bombardment and electric field. Also, the various polar compounds present in oil and surface imperfections of the pressboard samples create ideal traps for the ionic charges to get trapped at the oil-pressboard interface even at low fields. Drifting and accumulation of charges at the electrode during polarisation and ionic charge carrier trapping during flow electrification (Sloshing of oil over the pressboard surface) are the other factors contributing to the trapping of charges in the transformer insulation. The process of procuring necessary trap energy by a bound carrier to get released is known as detrapping. The trapped charges may remain bounded depending on trap depths, for many hours to several days, and may cause localised field enhancement. Such trapped charge centres eventually lead to lowered dielectric strength of oil-paper composite insulation [14].

In oil-paper insulation systems, under the influence of the DC electric field, the space charges start to accumulate at the interface. During the study of the electrical field strength of transformer insulation, the combined effect of the electrical field strength and temperature on space charge behaviours were examined by the authors Runhao Zou et al [63]. For this, space/interface charge simulation based on the bipolar charge transport model and a simulation parameter using FEM for the multi-layer oil-paper insulation system was proposed. The authors conclude that temperature plays a more significant influence on the charge density and the total charge quantity than the electrical field strength.

J.Hornak et al. also make use of the finite element method (FEM) models to demonstrate the different space charge behaviour and its influence on the intensity of the electric field to monitor the interactions of space charge inside the insulation structure. The interfacial charge can distort the local electrical field of the oil-paper insulation system, which leads to insulation breakdown or cause material degradation. The

interfacial charge density and the total charge quantity at steady-state both increases exponentially with the electrical field strength and temperature [24].

The accumulation of space charge at the oil-paper interface is a critical issue for the insulation diagnostics of transformers. This interfacial charge mainly accumulates due to the difference in conductivity values of oil and paper. Accumulation of interfacial charge leads to localised field enhancement, with the additional possibility of occurrence of partial discharges and accelerated insulation ageing. The authors D.Mishra et al. in their paper present that though the assessment of interfacial charge is critical, it is a tedious process to estimate interfacial space charge behaviour from the transformer diagnostics methods currently in use [42].

When a DC field electric field is applied to oil-paper insulation, the dipole groups present within the insulation orient themselves in the direction of the applied field. As a result, the energy content of the dipoles is increased. The charging current flowing through the dielectric material during this process is termed as polarisation current. After the polarisation process is completed, on the removal of the applied field and short-circuiting the terminals of the dielectric/oil-paper insulation, the dipoles give up the acquired energy and return to their initial position. This relaxation of dipoles appears in the form of depolarisation current flowing through the dielectric. The polarisation-depolarisation current (PDC) measurement is an offline non-invasive technique that falls under Time-Domain Spectroscopy (TDS).

It has been reported that under low fields [42], the ionisation occurring in the compounds of mineral oil and pressboard causes ions to migrate gradually from the positive electrode to the negative electrode, producing conduction current. The oil paper interface has a considerable number of broken bonds, and chain folds at the microscopic level. Owing to the low mobility of the positive charges when compared to the negative charges, the positive charges are easily trapped in these regions of broken bonds and chain folds. As a consequence, the interface region serves as a potential barrier.

Localised field enhancements may happen if the charges are unable to overcome the potential barrier and may stay trapped for several hours or days.

The positive charges remain trapped in the interfacial region until they acquire sufficient energy to cross the interface and contribute to the conduction process again. The charge trapping is also influenced by critical factors like the difference of conductivities of oil and paper, moisture and ageing. Localised field enhancements may happen if the charges are unable to overcome the potential barrier and may stay trapped for several hours or days. In such cases, eventually, the energy stored in the trapped charge centers reduces the reaction activation barrier and promotes degradation of insulation.

During the depolarisation process, the charges in the trap sites get detrapped by receiving the required energy through mainly thermal oscillations, as there is virtually no scope of photonic bombardment or high electric field inside the insulation during depolarisation period. This generates a de-trapping current, which also contributes to the depolarisation current. The authors also note that the de-trapping time constant is in the same range as those of the dipolar relaxation time constants, it is difficult to separate the two currents by employing conventional approach [61], [42].

The older the insulation material, the slower the detrapping process. The same is true for insulation with higher moisture content. With ageing and higher moisture content, more ions are formed which gets trapped in the interfacial region, leading to space charge buildup. The ionic mobility may get affected, and as a result, the ions would take to more considerable detrapping time. The authors conclude that the time constant of detrapping current is related to the paper conductivity, oil conductivity, dissipation factor and age of the insulation [42].

### **2.3. Dielectric response analysis**

The reliability of power transformers is very significant for the availability of power generation and transmission systems. An insulation breakdown within a power transformer can lead to the failure of the transformer, which in turn may cause substantial financial losses due to a power outage and consequent damages. Hence it is imperative to implement better diagnostic methods for assessing the insulation condition of the power transformers, to lower the risks of failures and unforeseen power interruptions [12].

Thermal, electromechanical and chemical stresses influence ageing of the oil-paper insulation system of power transformers. Under the influence of these stresses, the cellulose insulation turns brittle, and the endurance against mechanical stress becomes considerably low. Moisture is produced in the solid insulation due to breaking of glucose molecule chains in cellulose, which additionally acts as a catalyst to initiate breakdown. Furthermore, the breakdown voltage of the insulating oil and paper is reduced with an increased moisture content of the oil. The conductivity of oil-paper insulation is closely related to the moisture content and different ageing byproducts in the insulation. Hence parameters like conductivity of the oil and the solid insulation material can be efficiently used for the condition estimation of the oil-paper insulation.

U.Gafvert et al. published their conclusions on polarisation-depolarisation current measurements to evaluate the condition of the insulation systems of different power transformers. With PDC measurements, it is possible to separate and independently assess the dielectric response of oil and paper components based on material properties of the insulation. Such an evaluation is not possible under the method of return voltage measurement. Henceforth the PDC measurements are considered as a better-preferred approach than the return voltage measurement [18], [17]. U.Gafvert in his previous works along with E.Ildstad successfully modelled the return voltage of an oil-pressboard insulation system with knowledge of the dielectric response function  $f(t)$ , permittivity and conductivity of materials involved [19].

D.Houhanessian et al. conferred the results of polarisation-depolarisation current measurements of pressboard samples at different moisture content and temperature [25].

Leibfried et al. conducted an assessment of solid insulation of the transformer on the basis of moisture content. The authors also described the application of the PDC technique on new and aged power transformers for evaluating the insulation condition. The status of insulation could be adequately analysed by reviewing the dielectric response parameters [35].

### **2.3.1. Dielectric response measurements**

The analysis of the dielectric response of transformer insulation systems can be carried out in both time domain and frequency domain. In the time domain, the approaches used for quantifying the dielectric response are :

1. Investigation of polarisation and depolarisation currents (PDC).
2. Analysis of recovery voltage and the polarisation spectrum (RVM).

In the frequency domain, the determination of dielectric response is conducted by employing dielectric spectroscopic instruments and is known as frequency domain spectroscopy (FDS). Insulation spectroscopy is carried out by conducting the measurements of the complex capacitance and its derived quantity- the dissipation factor  $\tan\delta$  over an extended frequency range (0.1 mHz - 1 kHz).

### **2.3.2. Dielectric spectroscopy in time domain**

#### **1. Polarisation and depolarisation current (PDC) measurements**

The dielectric response of the insulation could be estimated by applying a step voltage  $U_0$  to the test object, and this voltage must be constant and without any distortion. The polarisation current is measured until a steady DC voltage is reached. When the test device is short-circuited, then the measurements of the depolarisation currents could be taken. It should also be noted that strong electrical fields inside the insulating material may make the circuit to be nonlinear. Therefore it should be assured that the DC voltage source is set to produce a stable DC voltage [59].

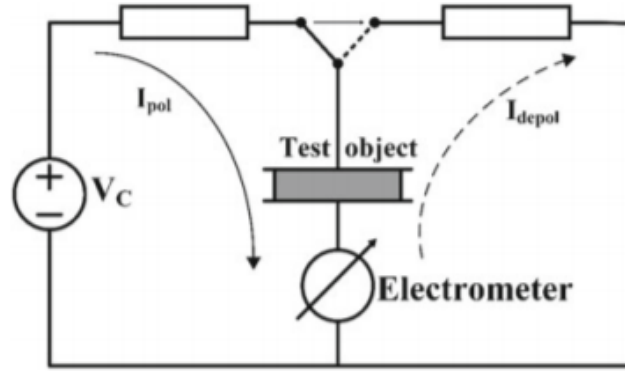


Figure 2.3: Test arrangement for polarisation-depolarisation measurements [8]

## 2. Return voltage method

The measurement of return voltages is another technique to quantify the dielectric response of materials. A constant DC voltage  $U_0$  charges the test object for a charging time  $t_c$  seconds. The test object is then grounded for a discharging time of  $t_d$ . Afterwards, the ground potential is removed, and the test object is kept in an open circuit condition. For times  $t > t_d$ , the test object is charged by the depolarisation current. Consequently, a recovery voltage  $U_r(t)$  caused by the residual polarisation starts to appear across the test object. The principle of the measurement is given as in figure: 2.4 .

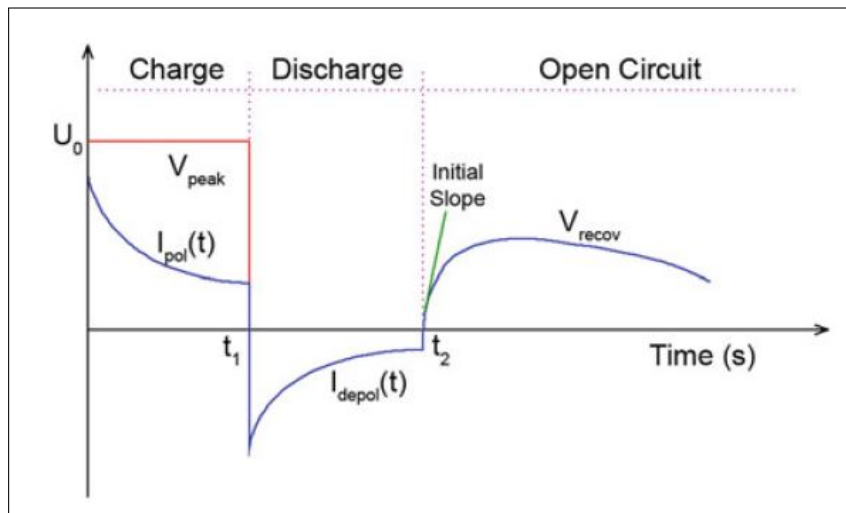


Figure 2.4: Return voltage curve [10]

### 2.3.3. Frequency domain spectroscopy

Frequency domain spectroscopy (FDS) is a non-destructive method of evaluating the condition of the oil-paper insulation system of transformers. In FDS method, a sinusoidal voltage is applied across the terminals of the test insulation and the amplitude and phase of the response current flowing through the insulation is recorded [9]. The complex capacitance, complex permittivity and dissipation factor of the insulation are determined from the measured current values over a wide frequency range. The parameters affecting FDS measurements are the geometry of the insulation system such as the relative dimensions of spacers, barriers and oil ducts and external factors like operating temperature and moisture content. The FDS results for the estimation of moisture content in solid insulation is better interpreted by numerical modelling. In this method, the insulation under test is regarded as a black box accessible only through its terminals. The method provides an overall condition assessment of the insulation system but is not suitable to recognize the local defects in the transformer insulation system [1], [9].



Figure 2.5: IDAX 300 used for Frequency domain spectroscopy [1]

The capacitance and  $\tan \delta$  measurements are efficient diagnostic tools for monitoring the insulation status. The capacitance of the dielectric is dependent on the dielectric material characteristics and the physical configuration of electrodes. The voids and impurities in insulation will lower the effective distance between the electrodes. The higher the measured capacitance value, the greater will be the possibility of partial discharges (PD) and insulation deterioration [9].

The information concerning the source of any defects in the insulation could be given by the power dissipation factor indicated by the  $\tan \delta$  value. Therefore the  $\tan \delta$  measurement is a useful approach for the condition diagnosis of any insulation system. A higher value of  $\tan \delta$  shows the presence of the moisture in the insulation. Otherwise, it could also be an indication of deterioration of the insulation. Both capacitance and  $\tan \delta$  values are dependent on the test frequency. Hence, the periodic evaluation of capacitance values and  $\tan \delta$  values will help to identify undesirable conditions of PD, moisture and also the presence of any conductive contaminants in the insulation.

## 2.4. Overview of dielectric tests conducted on transformer insulation

Insulation is one of the essential constructional elements of a transformer as any form of defect in the insulation could initiate the failure of the transformer. Previously the low-frequency tests were considered adequate to demonstrate the dielectric strength of the transformer insulation. But later, when the failures due to lightning and switching phenomena became more apparent, the impulse testing apparatus was developed.

The distribution of impulse voltage stress over the distribution winding is different from that experienced under low-frequency voltages and hence, it was realized that the low-frequency tests were not sufficient to test the dielectric strength. The waveforms simulated during the impulse tests are similar to those encountered while in service. Further research in the period of 1950s, led to the development of switching impulse tests for Extra high voltage (EHV) levels as transient voltages produced as a result of various switching operations have to be considered for the design of both internal and external transformer insulation. The dielectric tests are intended to verify the dielectric strength of transformer insulation. Some of the main dielectric tests are:

1. Full-wave lightning impulse tests for line terminals (LI)  
These tests are designed to verify the withstand capacity of transformer insulation against fast rise transients occurring during lightning strikes. The impulse is applied to the line terminals and causes non-uniform stresses in the winding of the transformer under test.
2. Chopped-wave lightning impulse tests for line terminals (LIC)  
These tests are intended to verify the withstand capability of transformer insulation against high-frequency voltage phenomena that may occur during its service. A chopped wave LI produces a higher peak value and also, contains higher frequency components than a full-wave lightning impulse.
3. Switching Impulse test for line terminals (SI)  
These tests are designed to verify the withstand capacity of transformer insulation against slow rise transients occurring due to the switching operations while in service. This test checks the withstand capacity of the line terminal and the connected windings against the switching impulse.

4. Induced voltage withstand test (IVW)

These tests are intended to verify the alternating voltage (AC) withstand the strength of the line terminal and their connected windings to earth and other windings and the withstand strength between the phases.

The lightning impulse voltage can be defined as a unidirectional voltage which rises very quickly to a maximum value and then decays slowly. The standard lightning impulse, according to IEC 60060, is characterised by the time to peak value of  $1.2 \mu s \pm 30 \%$  and time to half value of  $50 \mu s \pm 20 \%$ . The impulse testing of the power transformers is usually performed with the full-wave and chopped wave impulses with chopping time ranging from 2-6  $\mu s$  as per the requirements of IEC standard 60076-3. Additionally, references are made to IEC 60060-1, for the general definitions and test requirements of lightning Impulse tests.

With regard to the initial discussion with former company supervisor Ir.Luc Dorpmanns, it was pointed out that during recent years, there is a high demand for the additional positive polarity lightning impulse tests, along with negative polarity LI tests. Referring to IEC standards 60060 and 60076 [3], [4], the following Table 2.1 provides information regarding the LI tests carried out at SGB-SMIT transformers as a part of the acceptance tests conducted at their transformer manufacturing company in Nijmegen. Typically the RFW LI is applied at 50% of the Full wave (FW) LI voltage, and the Chopped wave (CW) is applied at 110% of the FW LI voltage. The Reduced chopped wave (RCW) is performed at 50 % of CW LI voltage.

Lightning Impulse (LI) type	Voltage (kV)	Polarity of the applied LI
Reduced Full wave (RFW)	712.5	Negative
Reduced chopped wave (RCW)	783.75	Negative
Full wave (FW)	1425	Negative
Chopped full wave (CFW)	1567.5	Negative
Chopped full wave (CFW)	1567.5	Negative
Full wave (FW)	1425	Negative
Reduced Full wave (RFW)	712.5	Positive
Full wave (FW)	1425	Positive

Table 2.1: LI Test Sequence performed as a part of factory acceptance test for transformers (400-500 kV)

During lightning impulse tests ionisations might occur in the pressboard/insulating liquid insulation system which would lead to the generation of space charges. The space charges generated may have an influence on the withstand behaviour of the insulation corresponding to applied impulse voltage especially when tested consecutively with opposite polarity.

Generally, a waiting period of one hour is given between the negative polarity LI and positive polarity LI. This waiting time is given in order to allow any 'trapped' charges to decay and for allow relaxation time for the slower polarisation processes. So the main question is whether this waiting period is required between the application of lightning Impulses of opposite polarity or could the waiting time be of shorter duration. For this analysis, the influence of charge accumulation and charge decay occurring in the transformer insulation system (oil-paper/press board interface) is studied.

## 2.5. Impulse voltage testing of transformer insulation

Lightning impulse test is a type test, and this performed to evaluate instrument transformer insulation strength to withstand lightning impulse voltages. This dielectric test aids to demonstrate that the insulation can withstand impulses that strike it externally due to lightning during its service period. High voltage surges resembling lightning simulated in laboratories are commonly known as high voltage impulses. The lightning impulse (LI) test is conducted to evaluate the dielectric integrity of the winding when subjected to voltages as specified by the LI test standards IEC 60076 and IEC 60060. It characterises the time-voltage behaviour of the transformer insulation against a specific waveform. Due to the transient characteristic of the phenomena, an oscillating voltage distribution occurs. This voltage, in turn, can produce a voltage to ground of up to twice the magnitude of the applied wave. The impulse voltage distribution during lightning impulse tests is dependent on the winding capacitance, whereas the low-frequency voltage distributes throughout the winding uniformly on volts per turns basis.

Ueta et al. verified the insulation performance of an oil-immersed power transformer against lightning surges by applying a lightning impulse (LI) voltage superimposed with ac voltage. The turn -to- turn insulation and section-to-section insulation inside the winding of a shell-type transformer was tested with LI superimposed with ac voltage. It was noted that the breakdown voltage and LI partial discharge inception voltage (LI PDIV) owing to the superimposed voltage did not differ from the values of the breakdown voltage and LI PDIV when the LI has applied alone. As the breakdown is determined by the dielectric strength of the oil-impregnated paper, the breakdown voltage was not affected by the presence of the ac voltage. In the case when the oil-impregnated paper to oil component ratio is low, the oil gap is primarily responsible for the breakdown. Contrarily when the impregnated paper to oil ratio was increased, then the oil-impregnated paper was primarily responsible for the breakdown [58].

The author Liu in [40] has mentioned that the effect due to space charges is not dominant in a uniform electric field. For the same gap distance, the breakdown voltage of natural ester and synthetic ester under negative polarity LI is almost comparable to that under positive polarity LI. On the contrary, in a non-uniform field, the polarity effect is significant as under negative polarity LI breakdown voltages result in a lower discharge inception voltage but a higher breakdown voltage than when under positive polarity [40], [38]. [40], [39].

The dielectric strength of external insulation ( between the bushing and tank) is lower at the positive polarity impulse than the strength of internal insulation. Also, the testing with LI of positive polarity will result in lower breakdown voltage of transformer insulation. Hence the impulse tests are normally performed with negative polarity to prevent air side flashovers in the external insulation.

The authors Wenxia Sima et al. investigated the accumulative effect of repeated lightning impulses on the oil-impregnated paper (OIP) used in power transformers. The pulsed electro-acoustic technique was employed to investigate space charges in OIP samples. By varying the applied time, amplitude and interval time of the applied lightning impulses, the behaviour of charges in OIP under different conditions were analysed by the authors. The charge injection and transport phenomenon during lightning impulse accumulation were also studied. The increase in the frequency of application of the lightning impulses, application of higher voltage, and short interval time between the impulses contributed to the accumulation and transport of space charges [56].

## 2.6. Conclusion

The low-frequency dielectric response is found in a comparably shorter time duration using the time-domain measurements. Another advantage of time-domain measurements is that the setting up of a testing platform is comparatively easy. Conversely, it is complicated to carry out the high-frequency dielectric response measurements as a minimal time delay is unavoidable due to the mechanical switching of high voltage and rise time of the high voltage source when conventional test setup is employed. The narrow bandwidth of the current measuring instrument also adds to this problem. Henceforth, it could be summarised that the frequency-domain spectroscopy is suitable for high-frequency measurements and the time domain methods are ideal for low-frequency dielectric response computations.

Though the return voltage diagnostic method is more manageable for on-site set up and is less noise-sensitive, the input impedance of the testing instrument, the geometric and electrical characteristics of the

connecting cable etc. contribute to the leakage currents and hence influences the output measurements of RVM. Besides, the dielectric response of return voltage depends on the charging time duration  $t_c$  and on the time duration  $t_d$  during which the test object is shorted (discharging duration). The total test duration in case of RVM is also relatively longer. The conversion of the measured data to the frequency domain is less complex using PDC diagnostic methodology than the transformation of measured data from the return voltage method to the frequency domain [15].

After a thorough investigation of the available literature on the dielectric response analysis, the polarisation and depolarisation current (PDC) method was selected to study the time dependency of the dielectric response of composite liquid-solid transformer insulation in this thesis.

# 3

## Dielectric relaxation in time domain

The chapter sets the stage for the analysis of dielectric response characteristics of oil, paper and pressboard, which are the most commonly used insulation in distribution transformers. The dielectric relaxation in the time domain was studied with the help of discharge voltage method where a DC voltage was applied on the test sample for a specific charging duration and removed. The chapter also presents an overview of the test set up employed for the discharge voltage measurements. The decay of the voltage across the test sample was observed, and the time constants of decay of the discharge voltage were estimated.

The first section provides a brief introduction to the theory of dielectric polarisation and depolarisation. The proposed model for the measurement of discharge voltage is also addressed in the same section. Following that, the details concerning the test set up, samples and the test procedure have been described. The discharge voltage measurements conducted on the composite test samples of oil, paper and pressboard have been discussed in the next section. Finally, the observations made from the results of the discharge voltage measurements have been presented.

### 3.1. Introduction

For the condition assessment and analysis of dielectric behaviour of oil-paper insulation, many methods like Polarisation-depolarisation current (PDC) measurement, Frequency dielectric spectroscopy (FDS) and Recovery voltage method (RVM) are in practice. All of these methods primarily rely on the dielectric properties of the insulation system [23].

For the estimation of the time dependency of dielectric behaviour of the transformer insulation, the method of discharge voltage measurement was conducted on the test sample consisting of oil, paper and pressboard. It uses DC voltage to effectively understand the relaxation behaviour of the polarisation processes occurring inside the transformer insulation. Firstly, the test samples of transformer oil (Nynas NITRO), paper and pressboard were dried and vacuum treated. The test samples of paper and pressboard were screwed on the HV electrode and impregnated in oil. The samples of pressboard and paper were of cross-sectional area  $15 \times 15 \text{ cm}^2$  with thickness as 3 mm and 0.25 mm respectively. A DC voltage of 2 kV was applied to the HV electrode for a set charging time  $t_c$  and then removed. The electrostatic voltmeter measures the decaying voltage, and this data was displayed and recorded using the LabVIEW environment [figure 3.4].

#### 3.1.1. Theory

When a DC voltage was applied to the dielectric, the electric charges in the dielectric shift from their average equilibrium positions in response to the electric field generated, causing dielectric polarisation. The positive charges shift in the direction of the electric field, while negative charges are displaced in the opposite direction [60].

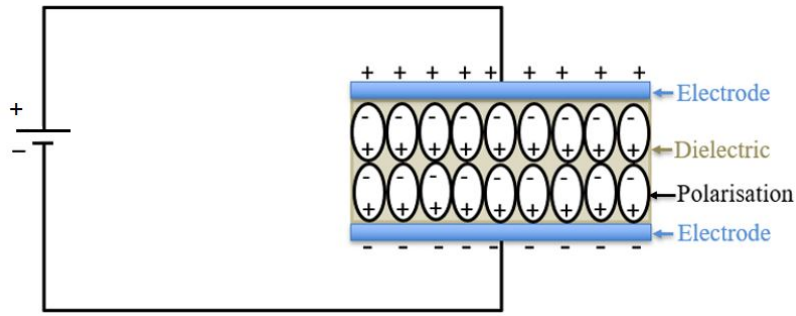


Figure 3.1: Polarisation phenomenon

There are mainly four types of polarisations occurring in dielectrics- electronic polarisation, ionic polarisation, orientational polarisation and space charge polarisation. For transformer insulation, the most relevant polarisation processes are electron polarisation and space charge polarisation [36].

On applying a voltage to the dielectric, ionic polarisation and electronic polarisation are completed in a short time, but other types of polarisation, such as space charge polarisation take a longer duration to complete. The current drawn by the insulation during this charging period is recorded and is known as polarisation current. The polarisation current can be considered as the summation of two current components, the first component being the charging current due to the alignment of dipoles in the insulation and the other being the conduction current.

After the DC voltage is removed, the formerly activated polarisation processes now give rise to the discharging current in the opposite direction. This discharging current can be characterised as the depolarisation current and is caused by the relaxation of previously polarised dipoles in the insulation. Unlike the polarisation current, the depolarisation current is not influenced by the conductivity component of current. The recorded voltage during this period of depolarisation can be defined as the 'Discharge voltage'.

## 3.2. Discharge voltage measurements

This section describes the discharge voltage measurements conducted on the composite dielectric consisting of oil, paper and pressboard. The first subsection provides an overview of the details regarding the test samples of oil, paper and pressboard, which is used in the test set up. A schematic diagram of the proposed test set up for the discharge voltage measurement is also given under this section. Following this, a brief discussion is given on the preparation of the samples for testing. In the final subsection, the procedure for measuring the discharge voltage varying over time is presented, and an overview of the different test cases of discharge voltage measurements and the corresponding plots is given.

The main purpose of measurement of discharge voltage is to study the faster and slower polarisation processes occurring in the composite insulation of oil, paper and pressboard. From the analysis of the plots of discharge voltage vs time, the time constants representing the fast and slower polarisation processes can be obtained. A longer time constant would mean that there is slower polarisation process occurring within the insulation and may be an indication of the interfacial charges taking longer time to detrapp and depolarise.

### 3.2.1. Test samples used for discharge voltage measurement

The test-samples inside the test aquarium represent the simplified model of a transformer insulation with liquid insulation as transformer oil (Nynas NYTRO) and solid insulation consisting of paper and pressboard [figure 3.3]. The pressboard and paper were of same cross-sectional area ( $15 \times 15 \text{ cm}^2$ ) with thickness as 3 mm and 0.25 mm respectively. The solid test samples were impregnated in transformer oil. The test set up was vacuum treated for 24 hours and degassed at  $65^\circ\text{C}$ .

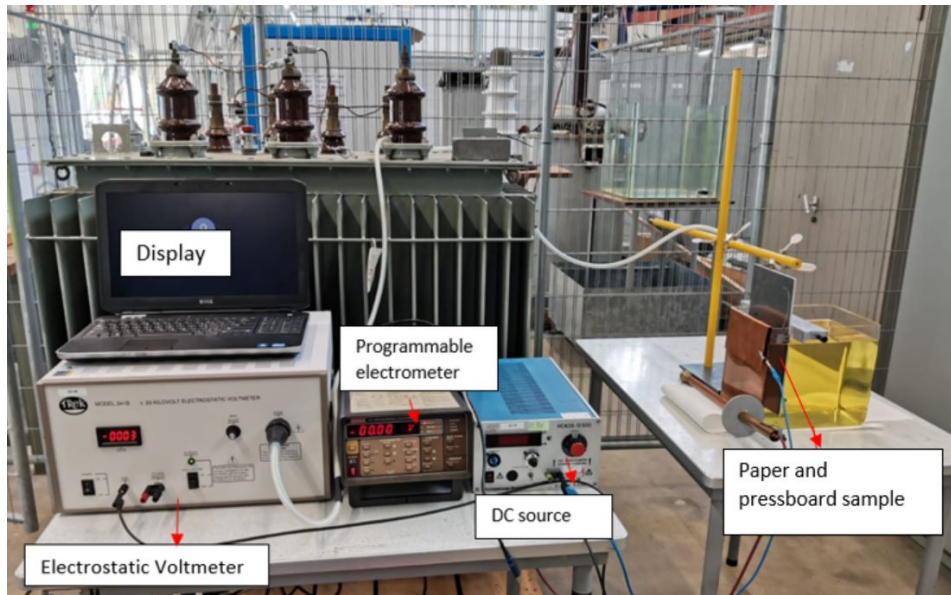


Figure 3.2: Equipment used for measurement along with Test set-up

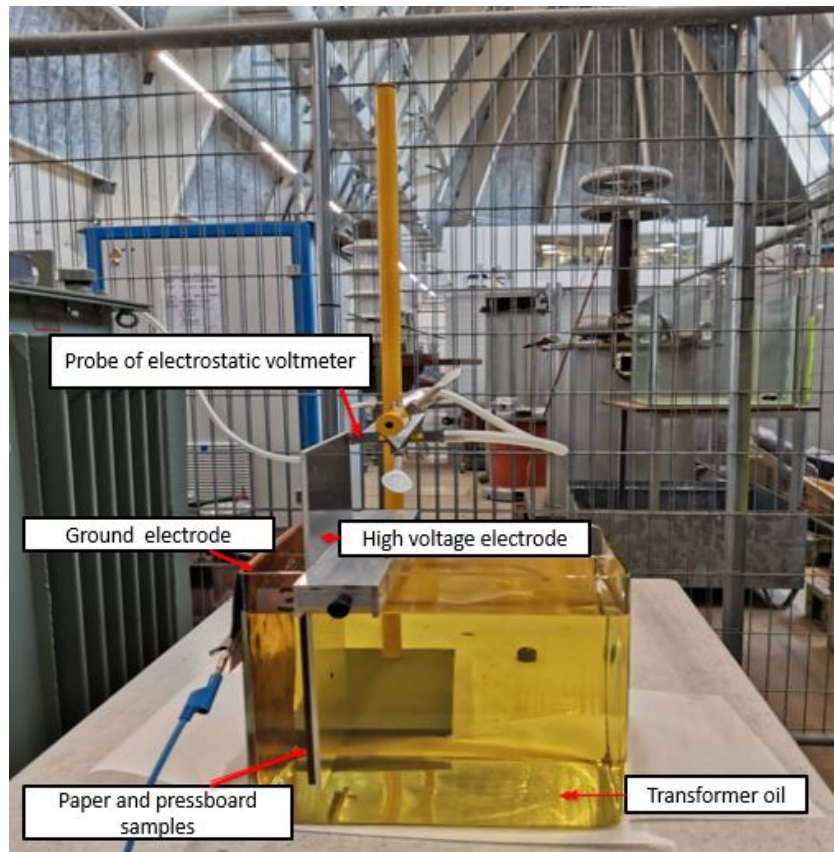


Figure 3.3: Test set up with sample

### 3.2.2. Proposed model for discharge voltage measurement

The proposed test set up for the discharge voltage measurement is described in this section. The test aquarium was filled with transformer oil (Nynas NITRO). The test samples of paper and pressboard were screwed on the HV electrode. The test samples were dried and vacuum treated prior to the measurements.

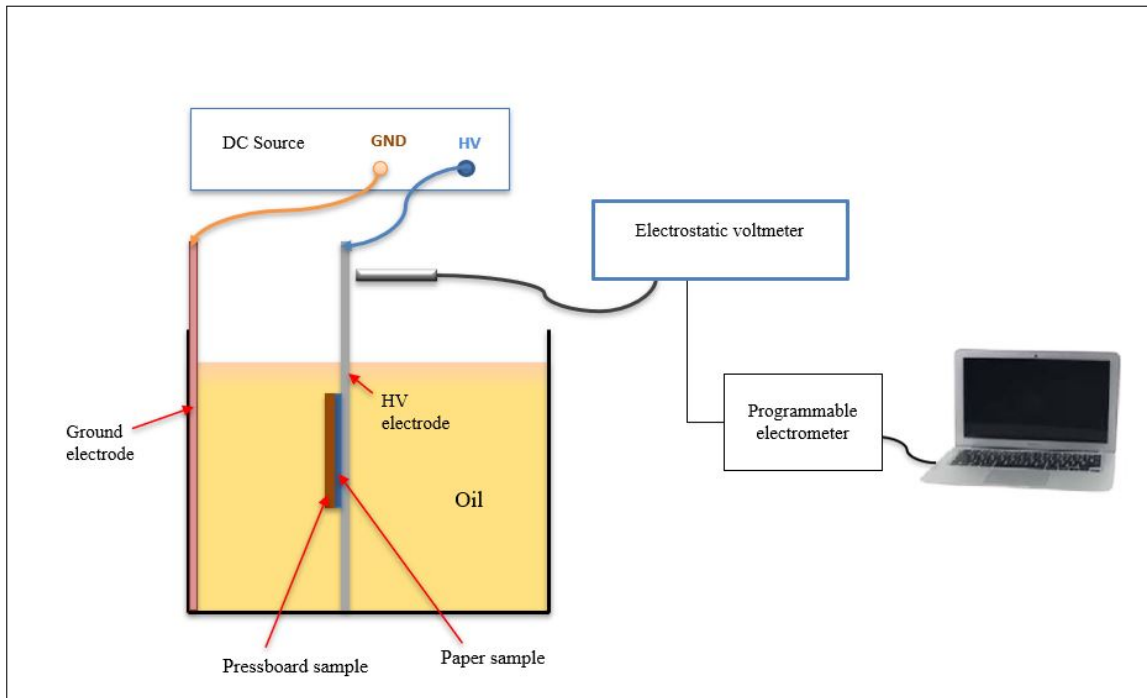


Figure 3.4: Schematic diagram of the test aquarium with samples and the measurement set-up

A DC voltage of 2 kV was applied to the HV electrode for a set charging time  $t_c$  and then removed. The electrostatic voltmeter, with its non-contacting probe, was used to measure the decaying voltage with respect to time. With the help of the programmable electrometer, which acted as an interface, the measurement data was displayed and recorded in LabVIEW environment [figure 3.4].

### 3.2.3. Equipment used for measurements

The following table 3.1 presents the equipment used for administering the measurements of discharge voltage.

<b>DC source</b>	<b>12.5 kV/ 0-2.5 mA</b>
<b>Electrostatic voltmeter</b>	<b>20 kV , Trek Model 341B</b>
<b>Programmable Electrometer</b>	<b>Keithley 617</b>

Table 3.1: Equipment used for measurement of discharge voltage

### 3.2.4. Electrostatic voltmeter for discharge voltage measurement

An electrostatic voltmeter measures voltage with virtually no charge transfer, therefore, does not modify and influence the real value of voltage being measured. These instruments use non-contacting sensors with a high voltage amplifier to drive the sensing probe to the same potential as that of the test object. Electrostatic voltmeters typically can measure over the range from millivolts to several thousand volts [50].

The conventional voltmeters cannot accurately take very high impedance ( $> 10^{10} \Omega$ ) voltage measurements without the charge transfer into the voltmeter. While using such a voltmeter for measuring voltage distribution on a dielectric surface, any small amount of charge transfer may affect the actual value of the potential to be determined. In such types of applications, an electrostatic voltmeter can be effectively used.

The non-contacting electrostatic voltmeter employs an electrostatic voltage monitoring probe, which is placed in close proximity (at a distance of 3 mm) to the surface to be measured. The potential of the probe body is brought to the same potential as the unknown surface. Therefore highly accurate measurement of the surface potential is possible using the electrostatic voltmeter without any physical contact [50].

**3.2.5. Preparation of the test samples**

The pressboard sample with the paper sample in between was screwed on the aluminium electrode [figure 3.5]. The test aquarium with the samples of pressboard and paper was then dried in a vacuum oven at a temperature of 65 ° C for 24 hours.



Figure 3.5: Test set with sample paper-pressboard is kept in vacuum oven



Figure 3.6: Vacuum Oven used for vacuum treatment of pressboard and paper

The oil was dried and vacuum treated in a separate oven at the temperature of 80 ° C for 24 hours. Afterwards, it was filled into the test aquarium containing the pressboard and paper samples. The impregnation of solid test samples with the transformer oil in the vacuum oven was carried out at a temperature of 65°C for a

duration of 24 hours. Lastly, the test aquarium with the test samples was placed in vacuum at ambient temperature for another 24 hours [figure 3.7].



Figure 3.7: Vacuum oven used for degassing and vacuum treatment of oil

### 3.2.6. Procedure

The discharge voltage measurements were conducted on composite test samples of oil, paper and press-board. The pressboard and paper samples were screwed on the aluminium electrode (HV electrode), as seen in figure 3.3. Another parallel plate acted as the ground electrode. The sample insulation was charged with a DC voltage of 2 kV for different charging times  $t_c$ . After the DC source was removed, the corresponding decaying voltage measurements were taken with the electrostatic voltmeter. The electrostatic voltmeter was connected to Keithley 617 programmable electrometer which acted as an interface to display and record the measured data in the LabVIEW programming environment.

The discharge voltage measurements were divided into three test cases with respect to different test conditions as presented in Tables 3.2, 3.3 and 3.4.

- Test case -I

The distance between HV aluminium electrode and the ground electrode was varied and kept as 3.2 cm and 6.4 cm respectively. The measurement of discharge voltage vs time was conducted immediately after the test aquarium with the test samples were taken out from the oven. The temperature of oil in the test aquarium was measured as  $T = 39^\circ\text{C}$ . The charging time  $t_c$  was taken as given in the Table 3.2.

Test sample	Distance between the electrodes $d$	Charging time $t_c$
<b>Oil</b> + <b>Paper</b> ( 0.25 mm thickness ) + <b>Pressboard</b> ( 3 mm thickness )	3.2 cm	1 min
		5 min
	6.4 cm	1 min
		5 min

Table 3.2: Test case-I: Measurement of discharge voltage taken at  $T= 39^\circ\text{C}$

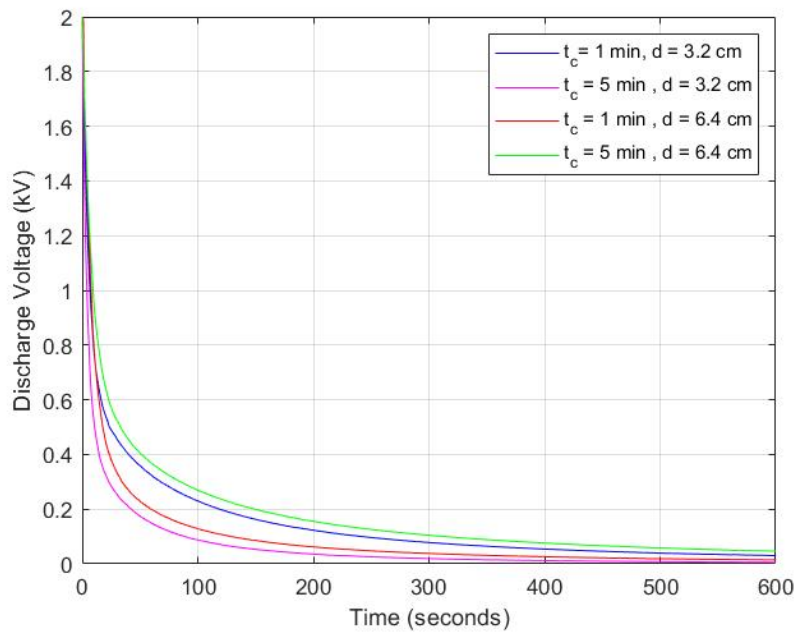


Figure 3.8: Discharge voltage vs time obtained at  $T=39^\circ\text{C}$

- Test case -II

The distance between the electrodes was kept as 3.2 cm. The temperature of the oil in the test aquarium was measured as  $T = 22^\circ\text{C}$  and the measurement of discharge voltage vs time was carried out. The charging time  $t_c$  was taken as given in the Table 3.3.

Test Sample	Distance between the electrodes $d$	Charging time $t_c$
<b>Oil</b> + <b>Paper</b> (0.25 mm thickness) + <b>Pressboard</b> (3 mm thickness)	3.2 cm	50 sec
		1 min
		100 sec
		10 min

Table 3.3: Time constants obtained at  $T=22^\circ\text{C}$  for different charging times  $t_c$ ;  $d=3.2$  cm

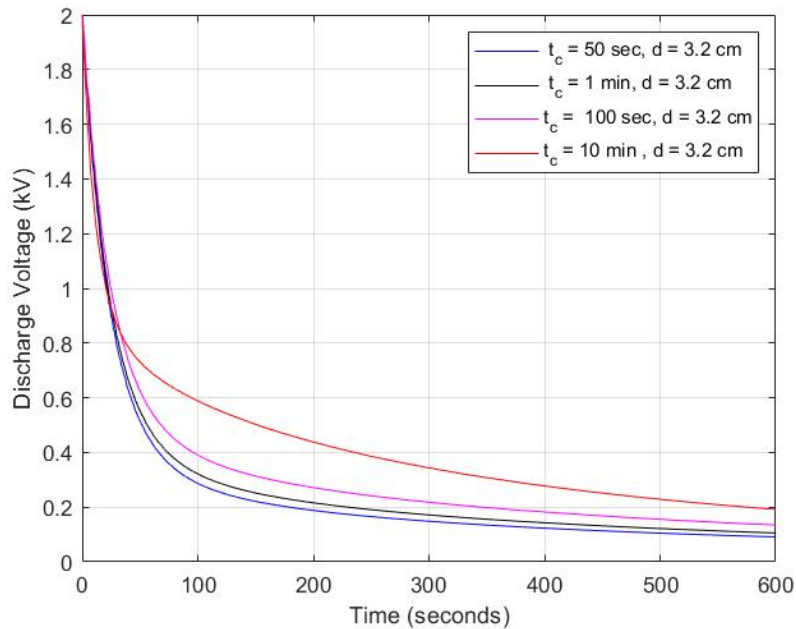


Figure 3.9: Discharge voltage vs time at  $T=22^\circ\text{C}$ ;  $d=3.2$  cm

- Test case -III

The distance between the electrodes was kept as 3.2 cm. The test aquarium was kept uncovered and exposed to air humidity for 4 days. Afterwards, the measurement of discharge voltage vs time was conducted. The temperature of the oil in the test aquarium was measured as  $T = 22^\circ\text{C}$ . The charging time  $t_c$  was taken as given in the Table 3.4.

Test sample	Distance between the electrodes $d$	Charging time $t_c$
<b>Oil</b> + <b>Paper</b> ( 0.25 mm thickness ) + <b>Pressboard</b> ( 3 mm thickness )	3.2 cm	1 sec
		5 sec
		10 sec
		20 sec
		50 sec
		100 sec

Table 3.4: Test case-III: Measurement of discharge voltage taken at  $T= 22^\circ$ , after the test aquarium with samples was kept open and exposed to ambient air for 4 days ;  $d= 3.2$  cm

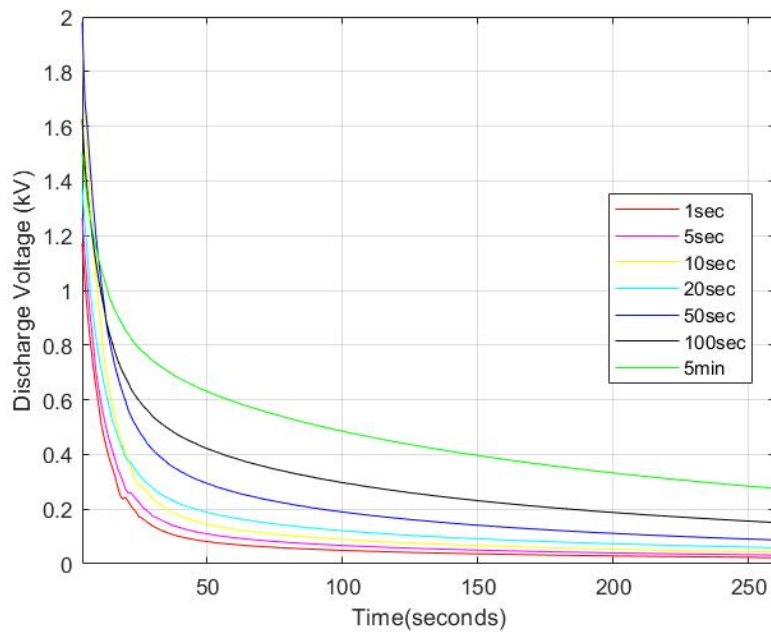


Figure 3.10: Discharge voltage vs time at  $T= 22^\circ$ , after the test aquarium with samples was kept open and exposed to ambient air for 4 days ;  $d= 3.2$  cm

### 3.3. Estimation of the time constants of the discharge voltage curve

The following section describes the estimation of the time constants of the discharge voltage curves varying over time. The plot of discharge voltage vs time [figure 3.11] obtained from the test case given in Table 3.2 is used as an example to show how the time constants were computed using the curve fitting tool in MATLAB [figure 3.12].

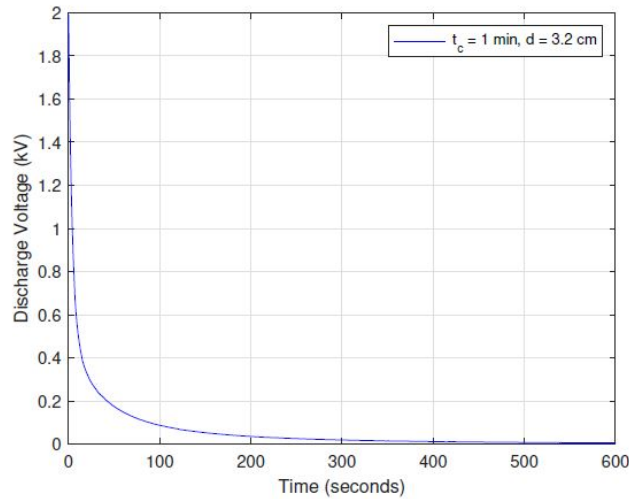


Figure 3.11: Discharge voltage vs Time ; Distance between the electrodes 'd'= 3.2 cm ; T= 39°C

- The general equation of exponential decay can be written as:

$$V(t) = V * e^{-t/\tau} \quad (3.1)$$

where  $\tau = RC$  which is equal to the time constant of decay .

- The figure 3.12 represents the discharge of voltage versus time when the DC voltage was removed from the HV electrode. The curve fitting tool in MATLAB was employed to realise the time constants of the exponential curve. By doing so , the dominant depolarisation processes involved in the decaying voltage with respect to time could be studied. Using the curve fitting tool , an exponential fit was fitted on the plot of discharge voltage [figure 3.12].

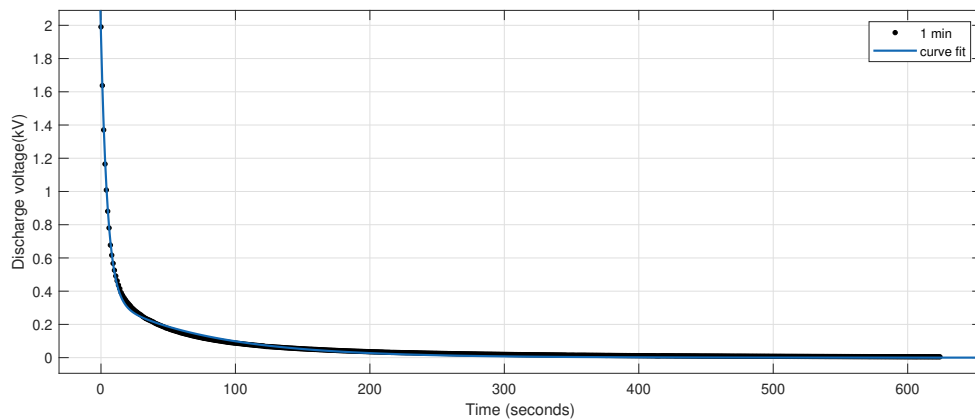


Figure 3.12: Exponential curve fit is used on the plot of discharge voltage curve varying with time

The exponential curve which was fitted on the discharge voltage curve is characterised by a general model equation defined by a function  $F(x)$  i.e.

$$F(x) = a * e^{bx} + c * e^{dx} \quad (3.2)$$

where the values of coefficients are automatically computed by curve fitting tool as  $a = 1.588$ ,  $b = -0.2058$ ,  $c = 0.3539$  and  $d = -0.0128$

- Comparing the above equation 3.2 with the general equation of exponential decay [equation 3.1], the time constants of the discharge voltage curve [figure 3.12] is estimated as  $\tau_1 = 5$  seconds and  $\tau_2 = 78$  seconds respectively.
- $\tau_1$  and  $\tau_2$  represents the time constants of decay of the two polarisation processes influencing the discharge voltage with respect to time. It can be concluded that there are majorly two dominant polarisation processes happening characterised by two time constants of exponential decay  $\tau_1$  and  $\tau_2$ . From the estimated value for  $\tau_2$ , it can be interpreted that the second polarisation takes longer time to depolarise and fall back to zero.

### 3.3.1. Estimated values of time constants of the discharge voltage curve

The time constants of the measured discharge voltage curves as given in the Table 3.2, 3.3 and 3.4 were computed with the help of the curve fitting tool as described in the above section 3.3. The comparison of the exponential curve fit with the plot of discharge voltage is provided in the Appendix [A]

The R-square value can be used to confirm the accuracy of the exponential curve fit on the discharge voltage curve. It is a statistical tool that describes how close the measured data is to the adjusted regression model. For example, a R-square value of 0.7 reveals that 70% of the data fit the regression model. The higher the R-square value, the better will be the exponential fit and more accurate will be the values of the estimated time constants. It was also observed that by increasing the number of exponential coefficients in the model function of  $F(x)$  [equation 3.2] resulted in lower R-square values for the curve fit. Hence the model equation with two exponential terms was adopted for the estimation of time constants of the discharge voltage curves.

The R-square values obtained from the exponential curve fits on the discharge voltage curves showed very high values ( $\geq 0.9$ ). Therefore the computation of time constants of discharge voltage using the curve fitting tool in MATLAB can be justified.

- Test case -I

Test sample	Distance between the electrodes $d$	Charging time $t_c$	Time constant values (seconds)	R square value
<b>Oil</b> +	3.2 cm	1 min	$\tau_1 = 5, \tau_2 = 78$	0.9957
		5 min	$\tau_1 = 7, \tau_2 = 171$	0.9919
<b>Paper</b> (0.25 thickness) +	6.4 cm	1 min	$\tau_1 = 9, \tau_2 = 132$	0.9958
		5 min	$\tau_1 = 11, \tau_2 = 233$	0.993
<b>Pressboard</b> (3 mm thickness)				

Table 3.5: Time constants obtained at  $T=39^\circ C$  for different charging times  $t_c$ ; Distance between the electrodes ' $d$ ' = 3.2 cm

- Test case -II

Test sample	Distance between the electrodes $d$	Charging time $t_c$	Time constant values (seconds)	R square value
<b>Oil</b> + <b>Paper</b> (0.25 mm thickness) + <b>Pressboard</b> (3 mm thickness)	3.2 cm	50 sec	$\tau_1 = 26, \tau_2 = 560$	0.9940
		1 min	$\tau_1 = 27, \tau_2 = 574$	0.994
		100 sec	$\tau_1 = 29, \tau_2 = 588$	0.9934
		10 min	$\tau_1 = 22, \tau_2 = 489$	0.9197

Table 3.6: Time constants and R-square values obtained at  $T=22^\circ C$  for different charging times  $t_c$ . Distance between the electrodes ' $d$ '= 3.2 cm

- Test case -III

Test sample	Distance between the electrodes $d$	Charging time $t_c$	Time constant values (seconds)	R square value
<b>Oil</b> + Paper (0.25 mm thickness) + <b>Pressboard</b> (3 mm thickness)	3.2 cm	1 sec	$\tau_1 = 7, \tau_2 = 122$	0.9973
		5 sec	$\tau_1 = 8, \tau_2 = 162$	0.9989
		10 sec	$\tau_1 = 9, \tau_2 = 169$	0.9835
		20 sec	$\tau_1 = 9, \tau_2 = 222$	0.9963
		50 sec	$\tau_1 = 12, \tau_2 = 240$	0.9910
		100 sec	$\tau_1 = 12, \tau_2 = 288$	0.9916

Table 3.7: Time constants and R-square values obtained at room temperature of  $T = 22^\circ C$  after the test aquarium with samples was kept open and exposed to ambient air for 4 days; Distance between the electrodes ' $d$ '= 3.2 cm

### 3.4. Observations and Discussions

From the discharge voltage measurements conducted on the composite test sample of oil, paper and press-board following the procedure described under subsection 3.2.6, it was estimated that there were two dominant time constants of decay for the discharge voltage curves. The time constants of decay were obtained

using the curve fitting tool in MATLAB. This section addresses some of the observations made from the estimated values of time constants of decay for the discharge voltage curves on the basis of oil-gap distance, temperature and moisture content.

### 3.4.1. Effect of the oil-gap distance on the time constant values

A DC voltage of 2 kV was applied on the HV aluminium electrode for the charging time  $t_c$  and then removed. The distance ' $d$ ' between the HV electrode and the ground electrode was varied and taken as 3.2 cm and 6.4 cm respectively [Table 3.5]. The discharging voltage was recorded and the time constants were obtained from the plot of the discharge voltage vs time using the curve fitting tool in MATLAB.

Charging time ( $t_c$ )	Time constant values (seconds) $d = 3.2$ cm	Time constants values (seconds) $d = 6.4$ cm
1 min	$\tau_1 = 5$ $\tau_2 = 78$	$\tau_1 = 9$ $\tau_2 = 132$
5 min	$\tau_1 = 7$ $\tau_2 = 171$	$\tau_1 = 11$ $\tau_2 = 233$

Table 3.8: Time constants obtained at Temperature of  $T = 39^\circ\text{C}$  for charging time  $t_c = 1$  min and 5 min.

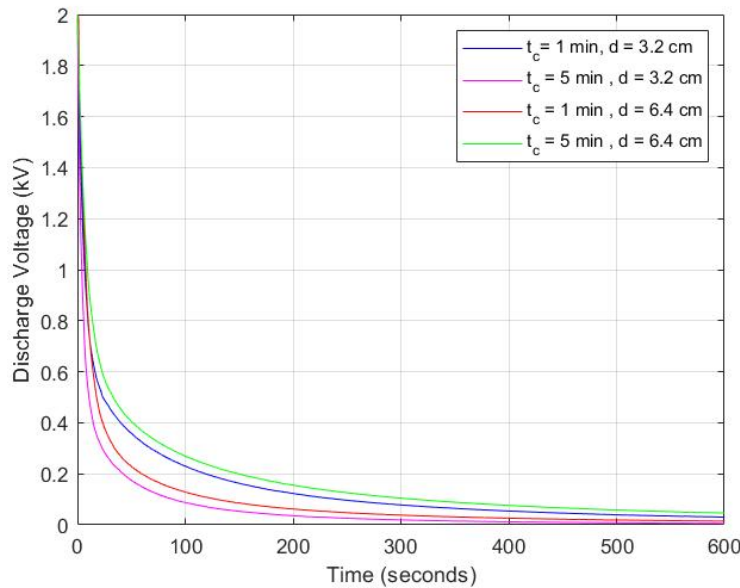


Figure 3.13: Comparison of plots of discharge voltage vs time to study the effect of oil-gap

With an increase in the distance, it takes a longer time for the charge carriers to migrate and participate in the polarisation process. Charge accumulation and charge trapping are predominant in composite insulation due to difference in the  $\epsilon/\sigma$  values. After detrapping, the charges take longer time to migrate and contribute to the depolarisation current. This may be the reason for comparatively higher values of time constants obtained for discharge voltage curves when the distance between the electrodes was doubled [figure 3.13].

For both discharge voltage measurements [Table 3.8], the temperature of the oil was measured at  $T = 39^\circ\text{C}$ . With an increase in temperature, the conductivity of oil will be more. It can be assumed that an increase in

oil conductivity due to a temperature rise will not affect the comparison of the estimated time constants as both the discharge voltage measurements were conducted at the same temperature.

### 3.4.2. Effect of the temperature on the time constant values

For the analysis of the effect of the temperature on time constant values, the estimated time constants of discharge voltage curves given by the Test cases [Tables 3.5 and 3.6] were employed.

Distance between the electrodes $d$	Charging time $t_c$	Temperature	Time constant values (seconds)
3.2 cm	1 min	(a) $T=39^{\circ}\text{C}$	$\tau_1 = 5, \tau_2 = 78$
		(b) $T=22^{\circ}\text{C}$	$\tau_1 = 27, \tau_2 = 574$

Table 3.9: Time constants obtained at  $T=22^{\circ}\text{C}$ ;  $d = 3.2\text{ cm}$

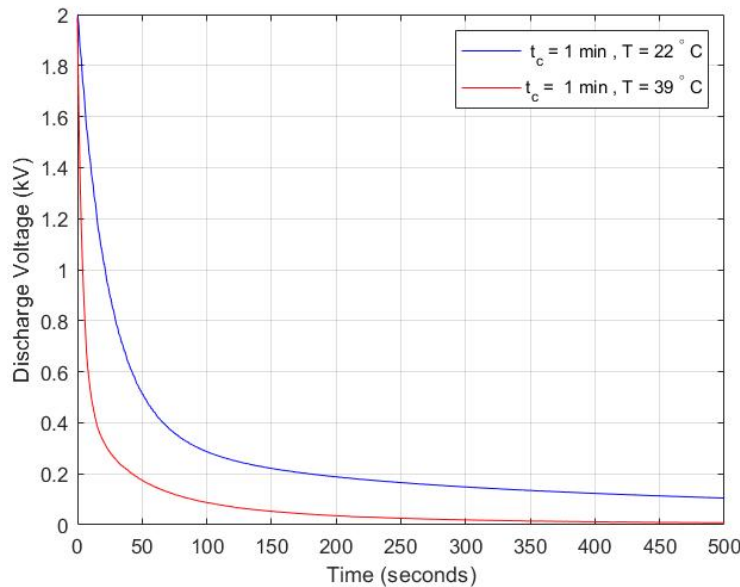


Figure 3.14: Discharge voltage vs time obtained at  $T=39^{\circ}\text{C}$  and  $T=22^{\circ}\text{C}$

Under the influence of an electric field, the mismatch of  $\epsilon/\sigma$  values for the different dielectrics in the insulation causes the charges to accumulate on the interfacial region. There would be enhanced localised polarisation in this region due to charge trapping and hopping of charge carriers between localised charge trap centers.

The effect of the temperature on the values of the time constants could be very crucial as the mobility of charge carriers in oil increases with temperature. With the increase in the mobility of the charge carriers, the conductivity of oil also increases [6]. With enhanced oil conductivity, there is a faster migration of the interfacial and trapped charges. This results in an easier dipole formation during polarisation and faster relaxation of the dipoles during depolarisation [10], [53]. The magnitude of the depolarisation current decays at a faster rate at a temperature of  $T=39^{\circ}\text{C}$  than at  $T=22^{\circ}\text{C}$  [figure 3.14]. This could be understood from the smaller values of time constants obtained at a temperature of  $T=39^{\circ}\text{C}$  when compared with the values of time constants obtained for  $T=22^{\circ}\text{C}$  [Table 3.9].

### 3.4.3. Effect of the moisture content on the time constant values

For the analysis of the effect of the moisture content on time constant values, the estimated time constants of discharge voltage curves given by the Test cases [Tables 3.6 and 3.7] were applied :

- (a) In the first case, the temperature of oil before discharge voltage measurement was measured as  $T = 22^{\circ}\text{C}$ .
- (b) In the second case, the test aquarium with the test samples was left open (exposed to ambient air) for four days. The temperature of oil in the test aquarium before discharge voltage measurements was taken and measured as  $T = 22^{\circ}\text{C}$ . The discharge voltage measurement was then conducted following the same procedure as in the previous tests and the discharge voltage curves varying over time were obtained [ figure 3.15]

In the above measurements, the distance between the HV electrode and the ground electrode was kept as 3.2 cm [ Table 3.10]. The time constants were obtained using the curve fitting tool in MATLAB [section 3.3].

Distance between the electrodes $d$	Temperature	Charging time $t_c$	Time constant values (seconds)
3.2 cm	(a) $T=22^{\circ}\text{C}$	50 sec	$\tau_1 = 26, \tau_2 = 560$
		100 sec	$\tau_1 = 29, \tau_2 = 588$
	(b) $T=22^{\circ}\text{C}$ (Test samples are exposed to moisture)	50 sec	$\tau_1 = 12, \tau_2 = 240$
		100 sec	$\tau_1 = 12, \tau_2 = 288$

Table 3.10: Time constants obtained at  $T=22^{\circ}\text{C}$  (Same oil temperature but in the second case the test samples were exposed to moisture for four days). Distance between the electrodes ' $d$ '= 3.2 cm

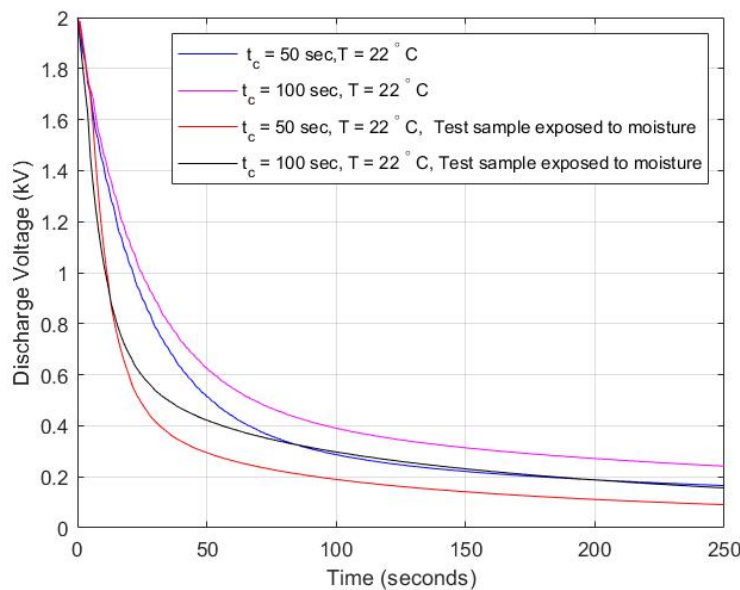


Figure 3.15: Comparison of plots of discharge voltage vs time to study the effect of moisture in the composite test sample

The presence of moisture could be the factor responsible for the comparatively lower time constant values of the discharge voltage curves of the test samples kept exposed to air [41].

Due to the moisture content in the sample, the conductivity of oil was increased. As a result, the polarisation increases due to the faster migration of the charge carriers. Subsequently, the depolarisation is also quicker due to faster relaxation of the charge carriers, which in turn would result in lower values of time constants of decay [10].

All the above observations on the effects of oil-gap, temperature and moisture content are based on the discharge voltage measurements performed on the composite test sample of oil, paper and pressboard. Though the estimated time constants in each of the cases [Table 3.8, 3.9 and 3.10] could be justified by theoretical analysis of many researchers [34], [10], [57], more testing and practical results are needed to confirm the results and understand the effects of oil-gap, temperature and moisture content on the dielectric response of the composite insulation of oil, paper and pressboard.

### 3.5. Summary

- In this chapter, the dielectric behaviour of the transformer insulation was studied with the help of discharge voltage measurements on the composite test sample of oil, paper and pressboard. A DC voltage of 2 kV was applied on the composite test sample and then removed. The discharging voltage was measured using an electrostatic voltmeter.
- The time constants of the discharge voltage curves varying with time were estimated using the curve fitting tool in MATLAB. It was found that each discharge curve was governed by two dominant time constants of decay, one representing the faster polarisation process and the other representing the slower polarisation process.
- An attempt was made to analyse the time constants of decay obtained from discharge voltage measurements based on oil-gap distance, temperature and moisture content in the test samples.
- For the discharge voltage measurements where the oil-gap distance in the test aquarium was increased, the corresponding time constants of decay were comparatively higher. It was also found that when the temperature of oil in the test sample was higher, the time constant values of the discharge voltage curves became comparatively smaller. Similarly, the higher moisture content in the test samples due to the exposure to air resulted in smaller values for the time constant of decay for the discharge voltage curves.

### 3.6. Conclusion

In composite insulation, the liquid dielectric polarises much earlier than solid insulation due to its easy polarisability. The polarisation in the solid insulation occurs much later. Hence for accurate estimation of the time dependency of the slower polarisation phenomena in the composite oil-paper-pressboard insulation under DC voltage, a longer charging duration needed. Also, longer charging time is crucial to realise the individual relaxation behaviour of the constituent dielectrics and the effect of interfacial polarisation in complex multi-layered insulation. However, a very long measurement duration is not always feasible due to time constraints.

Hence, although the measurement of discharge voltage varying over time is helpful to understand the dielectric behaviour of the composite insulation of oil, paper and pressboard, this method is not ideal for determining the behaviour of the slower polarisation processes occurring within the transformer insulation. Also, it is not possible to separate and apprehend the response of the constituent dielectrics in the composite insulation to the applied electric field using this measurement technique.

# 4

## Simplified R-C model

A linear dielectric model efficiently describes the measured dielectric responses of power transformers. It is essential to apprehend the dielectric responses of oil, paper and pressboard separately from the total dielectric behaviour of the transformer insulation system.

A description of the simplified equivalent circuit of test sample representing a multi-dielectric insulation system is presented in the first section. Furthermore, an attempt has been made to deduce the equivalent RC circuit of the test sample to an analytical solution. Lastly, the basic relations of polarisation and depolarisation currents according to the linear dielectric response theory has been explained.

### 4.1. R-C equivalent model of transformer insulation

The main constituents of transformer insulation are oil, paper and pressboard. The transformer oil acts a good insulator and assists in heat dissipation. The paper is employed in the form of strips of insulation between winding layers and also for winding the wires. The use of pressboard barriers helps to prevent particle-induced breakdown, whereas the pressboard spacers provide separation and mechanical support to the windings [12], [33].

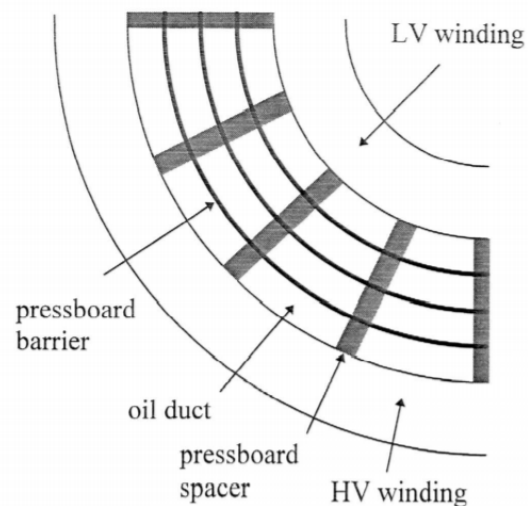


Figure 4.1: Cross-section of the transformer insulation between low and high voltage windings [12]

The simplified R-C circuit was built based on the 'X-model' of the transformer insulation. In the X model, the two components - oil and pressboard are kept in series in order to analyse the dielectric behaviour of transformer insulation [28]. For the study of dielectric response for this thesis, the test sample was composed of complex insulation of three dielectrics - oil, paper and pressboard [figure 4.2]. Hence the equivalent circuit of the test insulation consisted of a series arrangement of three parallel R-C circuits with each parallel connection of resistor and capacitor representing the constituent dielectric in the insulation, i.e. oil, paper and pressboard.

#### 4.1.1. Modelling of simplified R-C equivalent circuit

From the test results of discharge voltage versus time detailed in Chapter 3 , it could be concluded that for each charging time  $t_c$ , there is a discharge curve governed by the depolarisation current having two dominant time constants. The time constants were obtained using the curve fitting tool in MATLAB. A simplified equivalent circuit of the test sample consisting of oil, paper and pressboard is constructed to verify this result analytically. By solving the equivalent RC circuit representing the test sample , an analytical solution is derived which gives an idea about the number of polarisation processes occurring in the composite test sample that represents the transformer insulation system.

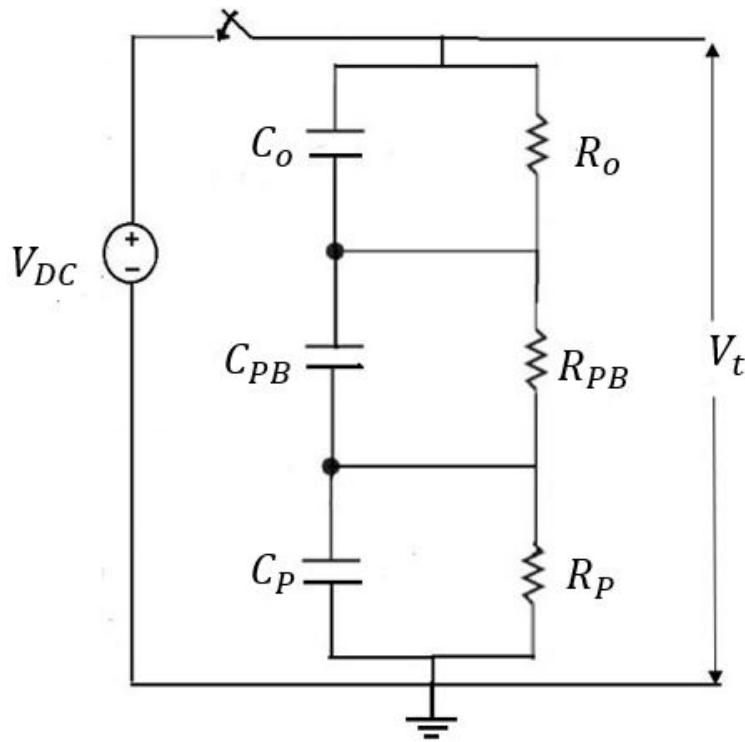


Figure 4.2: R-C equivalent circuit of sample in time domain

- The test sample representing transformer insulation was modelled into series connection of three parallel R-C circuit with each parallel R-C network representing the dielectric material present in the sample i.e. oil, paper and pressboard as seen in figure 4.2. The resistors  $R_O$ ,  $R_{PB}$  and  $R_P$  denotes the respective resistances of oil, pressboard and paper. The capacitors  $C_O$ ,  $C_{PB}$  and  $C_P$  denotes the capacitances of oil, pressboard and paper respectively.

On applying a DC voltage  $V_{DC}$  on the test sample, the capacitors  $C_O$ ,  $C_{PB}$  and  $C_P$  start to charge. After a specific charging duration, the applied voltage  $V_{DC}$  was removed, and the test sample was shorted. The capacitors  $C_O$ ,  $C_{PB}$  and  $C_P$  now begin to discharge, with voltages  $V_{01}$ ,  $V_{02}$  and  $V_{03}$  respectively. The equivalent circuit of capacitor discharge in s-domain is presented in figure 4.3.

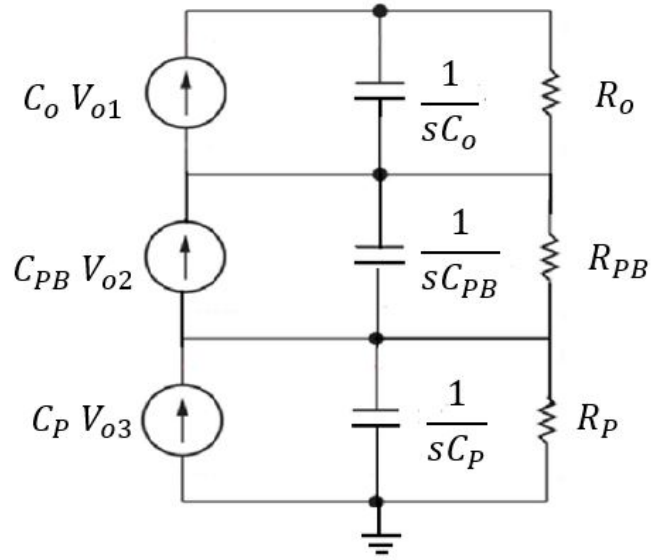


Figure 4.3: R-C equivalent circuit of sample in s-domain

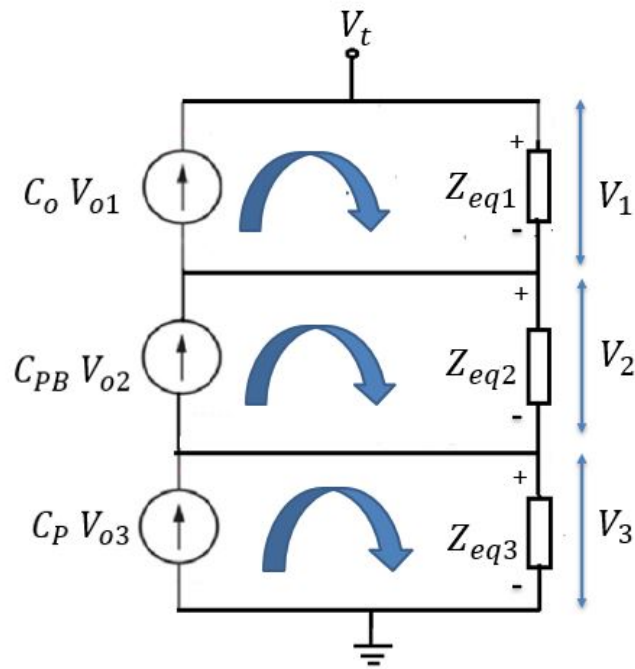


Figure 4.4: Simplified R-C equivalent circuit of sample in s-domain

- In the circuit 4.3, the impedances  $Z_{eq1}$ ,  $Z_{eq2}$  and  $Z_{eq3}$  can be solved as

$$Z_{eq1} = \frac{R_o}{1 + R_o s C_o} \quad (4.1)$$

$$Z_{eq2} = \frac{R_{PB}}{1 + R_{PB} s C_{PB}} \quad (4.2)$$

$$Z_{eq3} = \frac{R_P}{1 + R_P s C_P} \quad (4.3)$$

where  $Z_{eq1}$ ,  $Z_{eq2}$  and  $Z_{eq3}$  are the equivalent impedance of oil, pressboard and paper respectively.

$$V_1 = C_o V_{01} Z_{eq1} = \frac{R_0 C_0 V_{01}}{1 + R_0 s C_0} \quad (4.4)$$

$$V_2 = C_{PB} V_{02} Z_{eq2} = \frac{R_{PB} C_{PB} V_{02}}{1 + R_{PB} s C_{PB}} \quad (4.5)$$

$$V_3 = C_P V_{03} Z_{eq3} = \frac{R_P C_P V_{03}}{1 + R_P s C_P} \quad (4.6)$$

- The output voltage  $V(s)$  can be written as

$$\boxed{V(s) = V_1 + V_2 + V_3} \quad (4.7)$$

- Substituting for  $V_1$ ,  $V_2$  and  $V_3$  and converting back to t-domain, the output discharge voltage  $V_t$  can be derived as

$$V_t = V_{01} e^{-\frac{t}{R_0 C_0}} + V_{02} e^{-\frac{t}{R_{PB} C_{PB}}} + V_{03} e^{-\frac{t}{R_P C_P}} \quad (4.8)$$

$$= V_{01} e^{-\frac{t}{\tau_1}} + V_{02} e^{-\frac{t}{\tau_2}} + V_{03} e^{-\frac{t}{\tau_3}} \quad (4.9)$$

where  $V_t$  is the discharge voltage in the time domain.  $\tau_1$ ,  $\tau_2$  and  $\tau_3$  represents the time constants of decay of oil, paper and pressboard respectively

- The analytical solution evidently shows that the total output discharge voltage is the sum of the discharge voltages appearing across each dielectric in the composite insulation viz. oil, paper and pressboard. The time dependency of the discharge voltage was governed by dielectric time constants of oil, paper and pressboard [ equation 4.8 ]. Contrary to the results obtained from the discharge voltage tests where two time constants of decay governs each discharge curve, the analytical equation of the output discharge voltage is influenced by three time constants of decay  $\tau_1$ ,  $\tau_2$  and  $\tau_3$ .

#### 4.1.2. Analysis of the simplified R-C model

For the analysis of the contribution of individual dielectrics namely transformer oil, paper and pressboard, the time constant of decay corresponding to each insulating material can be found by their dielectric time constant. The dielectric time constant of an insulation can be expressed as the product of the insulation resistance  $R$  and geometrical capacitance  $C$  of the material [48].

$$\tau = R C \quad (4.10)$$

For a parallel circuit of  $R$  and  $C$ , after introducing the characteristic material parameters to get rid of the actual geometric dimensions, the dielectric time constant ' $\tau$ ' can be rewritten as [47]:

$$\tau = \frac{\epsilon_0 \epsilon_r}{\sigma} \quad (4.11)$$

where  $\epsilon_0$  is the permittivity of vacuum,  $\epsilon_r$  is the permittivity of the dielectric material and  $\sigma$  is the electrical conductivity of the dielectric material. The Table 4.1 provides the time constants computed from

the equation 4.11. The values of relative permittivity  $\epsilon_r$  and conductivity  $\sigma$  of oil, paper and pressboard were taken in reference to [30] , [54] , [33].

Dielectric	Permittivity $\epsilon_r$	Conductivity $\sigma$ (S/m)	Time constant $\tau$ (seconds)
Oil	2.3	$10^{-12}$	20
Paper	2.7	$10^{-13}$	239
Pressboard	4.3	$10^{-13} - 10^{-16}$	380-38000

Table 4.1: Dielectric time constants of the oil, paper and pressboard

The results from the simplified RC model could be summarised as follows:

- The DC measurements of discharge voltage versus time conducted on the combined insulation of oil, paper and press board gives the conclusion that the discharge voltage curves has prominently two time constants of decay. Hence it could be inferred that there may be two dominant polarisation processes occurring in the test sample.
- On the contrary, the analytical solution of the simplified R-C model indicates that there are in fact three polarisation processes occurring within the test sample , each having a characteristic time constant .
- The time constant calculated from the analytical formula due the polarisation process in oil is found to be of least value at  $\tau = 20$  seconds. The time constant values calculated using the analytical formula for paper and pressboard is presented in the Table 4.1. Similar time constant values were estimated from the measured discharge voltage curves using the curve fitting tool in MATLAB [Table 3.7] .
- The simulated plots of the discharge voltage over time were obtained from simplified R-C model of the test sample built in PSPICE. The measurements of discharge voltage given under Table 3.2 were compared with the results obtained from simulated models.

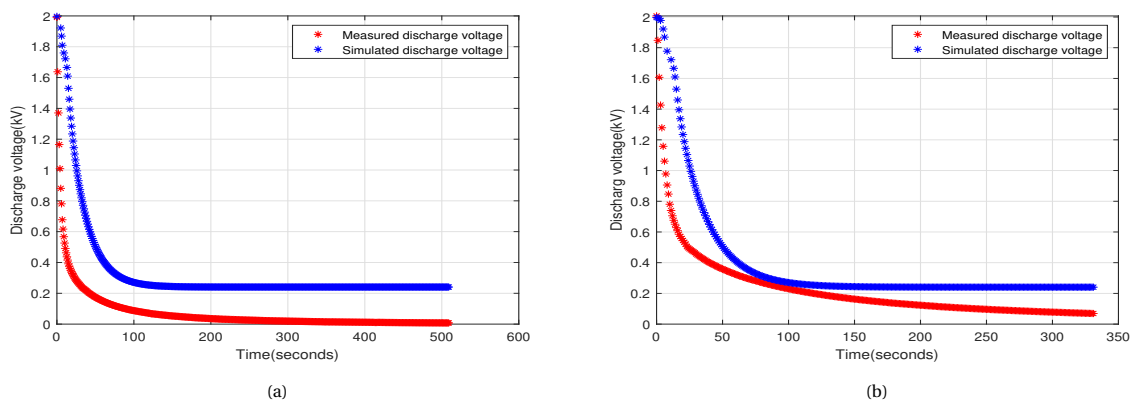


Figure 4.5: Comparison between measured discharge voltage plot and the simulated discharge voltage plot

- On comparing the plots of the measured discharge voltage and the simulated plots of discharge voltage [figure 4.5], there is an evident difference in the decaying trend of the two voltages. The simplified

R-C model only considers the contributions due to the circuit parameters of insulation resistance  $R_0$  and geometric capacitance  $C_0$  of the constituent dielectrics of the test sample. The model does not take into account the time dependency of the polarisation processes occurring within the constituent dielectrics of the test sample, i.e. oil, paper and pressboard.

Table 4.1 shows that paper and pressboard have dielectric time constant values higher than that of oil. From the analysis of the time constants obtained using the equation 4.11, it can be concluded that the slower polarisation processes having longer relaxation time could be in the solid insulation of paper and pressboard.

## 4.2. Modified equivalent R-C model of the insulation system

This section presents the modified equivalent R-C model of the insulation system given by the test sample consisting of oil, paper and pressboard. This is an extended circuit model which also mitigates some of the imperfections of the simplified equivalent R-C circuit given above. The simplified equivalent R-C model [figure 4.2] of the sample does not clearly describe many of the polarisation processes that are occurring inherently within each dielectric of the composite insulation system. It is also difficult to explain the individual dielectric behaviour of the component dielectrics and to quantify interfacial polarisation using this model. Additionally, the simplified equivalent model cannot explicitly explain the phenomenon of 'return voltage' that appears after removing the short circuit at the electrodes [60], [44].

On these grounds, the simplified R-C circuit of the insulation system was extended and represented by a model consisting of three linear dielectric circuits of oil, pressboard and paper in series. The modified equivalent model helps to investigate the dielectric behaviour of a complex insulation system from the properties of the linear dielectric model of the constituent dielectrics [ figure 4.7 ]. The following section 4.2.1 details the basic theory behind the model of a linear dielectric.

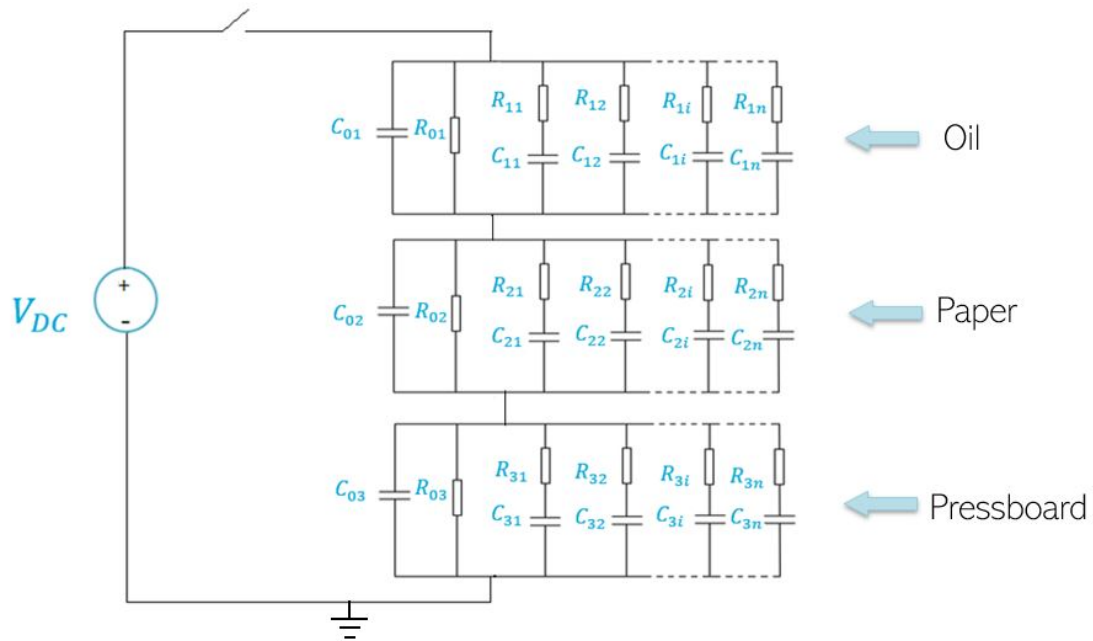


Figure 4.6: Modified R-C equivalent circuit of the insulation system

$C_{01}$ ,  $C_{02}$  and  $C_{03}$  are the respective geometrical capacitance of oil, paper and pressboard in the extended equivalent model;  $R_{01}$ ,  $R_{02}$  and  $R_{03}$  are the respective insulation resistance of oil, paper and pressboard in the extended equivalent model, the individual branches  $R_{1i}-C_{1i}$ ,  $R_{2i}-C_{2i}$  and  $R_{3i}-C_{3i}$  represent the various polarisation processes in oil, paper and pressboard respectively, when DC voltage is applied.

### 4.2.1. Basic relations of the linear dielectric response theory

In the presence of an electric field, the dipoles align themselves in the direction of the field which causes a polarisation current to flow. On the removal of the field, the dipoles relax and return back to the original state. In a linear dielectric, there may be more than one occurrence of such polarisation processes. Henceforth, the response time of each polarisation process after the application of an electric field may differ from one to another. These processes can be modelled as a parallel arrangement of branches, each containing a series connection of resistors and capacitors represented as  $R_i$  and  $C_i$ . The associated time constants of relaxation are given by  $\tau_i = R_i C_i$  [47], [29].

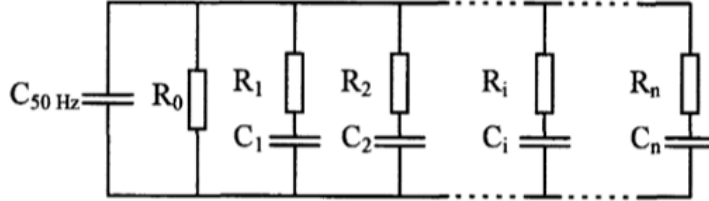


Figure 4.7: Equivalent circuit of the linear dielectric [12]

Accordingly, any oil-paper insulation system can be adequately described by means of the basic relations of linear dielectric response theory. The dielectric response investigations on multi-layer samples clearly show that the total dielectric response of such test samples depends on the dielectric response of the constituent insulating materials - oil and impregnated paper-pressboard and their volume ratio.

### 4.3. Identification of the circuit parameters of the equivalent R-C model

This section presents how various model parameters of the modified equivalent model could be identified. Most of the circuit parameters of the modified R-C model can be derived from the measurements of polarisation currents  $i_{pol}$  of individual dielectrics - oil, paper and pressboard using IDAX 300.

1. The capacitance  $C_0$  is determined by measurement of geometrical capacitance of the test sample at power frequency using IDAX 300.
2. The insulation resistance  $R_0$  can be obtained from the DC measurements on the test sample using IDAX 300.
3. Under the influence of applied DC voltage  $U_0$ , the polarisation currents appearing in the dielectric is due to the various polarisation processes occurring within the insulation.

$$i_{pol}(t) = \frac{U_0}{R_0} + \sum_{i=1}^n \frac{U_0}{R_i} \exp \frac{-t}{\tau_i} \quad (4.12)$$

where n is the number of parallel R-C branches ;  $\tau_i = R_i C_i$ .

4. The corresponding parameters  $R_i$  and  $C_i$  of the branches of the linear dielectric model [4.7] could be predicted and fitted in the model.
5. After assigning the values to all circuit parameters of the linear dielectric model of individual test samples of oil, paper and pressboard, the corresponding R-C circuit was built in PSPICE simulation platform.

## 4.4. Dielectric response in time domain

This section discusses about the dielectric response in the time domain and its relations with polarisation currents and depolarisation currents. The dielectric response of a material can be defined as its response to an electric field within it. This response of the dielectric can be analysed employing the polarisation currents and the depolarisation currents appearing in the dielectric under the influence of an electric field. The dielectric response analysis can also be used to study the dielectric response function  $f(t)$ , which is the characteristic of the slower polarisation processes occurring in the dielectric [60], [44], [41].

When a dielectric kept between two plane electrodes is subjected to a high DC field, the capacitance will rapidly be charged. After that, a relatively small current is detectable, which is caused by the DC conductivity of the dielectric material and by polarisation phenomena. Due to polarisation processes, there would be a displacement of the positive and negative charge carriers, initially cancelling each other. Hence, after a specific duration, a dipole moment is established. The process of depolarisation of the charge carriers occurs when the DC source is disconnected, and the electrodes of the test sample are short-circuited. As the return of the charge carriers to its origin follows after a certain time lag, a so-called return voltage is measurable between the electrodes of the test sample after removing the short circuit [44].

### 4.4.1. Relation between polarisation current and the dielectric response function $f(t)$

In this section, the relationship between the polarisation current and the dielectric response function  $f(t)$  is addressed. For this, the essential relations of linear dielectric response theory are discussed first.

- Assuming a homogeneous electric field  $E(t)$  is applied over a dielectric between two electrodes arrangement, the resulting current density  $J(t)$  in the material can be expressed as summation of the conductive component and the displacement component [60], [44].

$$J(t) = \sigma E(t) + \frac{dD(t)}{dt} \quad (4.13)$$

- The electric displacement  $D(t)$  can be represented as

$$D(t) = \epsilon_0 \epsilon_r E(t) + P(t) \quad (4.14)$$

where  $\epsilon_0$  is the vacuum permittivity and  $\epsilon_r$  is the relative permittivity of the dielectric,  $\sigma$  is the DC conductivity.

- The term  $P(t)$  in the equation 4.14 represents the polarisation and can be expressed in terms of the dielectric response function  $f(t)$  as follows :

$$P(t) = \epsilon_0 (\epsilon_\infty - 1) E(t) + \epsilon_0 \int_{-\infty}^t f(t - \tau) E(\tau) d\tau \quad (4.15)$$

where  $\epsilon_\infty$  is the permittivity of the dielectric at optical frequency.

- The response function  $f(t)$  is defined in the time domain as the polarisation  $P(t)$  developed in the dielectric in response to a step-function charging field. Hence it characterises the polarisation property of the dielectric material.
- Two terms characterise the electrical polarisation  $P(t)$ . The first term represents the faster polarisation processes, and the second term represents the slower polarisation processes [ equation 4.15].

- From equation 4.15, it could be seen that the faster polarisation follows the applied electric field  $E(t)$ , whereas slower polarisation is built up from a convolution integral between the applied electric field  $E(t)$  and the dielectric response function  $f(t)$ . Substituting equation (4.15) in equation (4.14) ,

$$D(t) = \epsilon_0 \epsilon_r E(t) + \epsilon_0 (\epsilon_\infty - 1) E(t) + \epsilon_0 \int_0^t f(t-\tau) E(\tau) d\tau \quad (4.16)$$

- The current density  $J(t)$  in the dielectric given by the equation 4.13 can be rewritten as

$$J(t) = \sigma_0 E(t) + \epsilon_0 \epsilon_\infty \frac{dE(t)}{dt} + \epsilon_0 \frac{d}{dt} \int_0^t f(t-\tau) \cdot E(\tau) d\tau \quad (4.17)$$

- According to the theory of dielectric response, the total current  $i(t)$  appearing in an isotropic dielectric material under the influence of external voltage  $U(t)$  can be derived using the above equation 4.17

$$i(t) = C_0 \left[ \frac{\sigma_0}{\epsilon_0} U(t) + \epsilon_\infty \frac{dU(t)}{dt} + \frac{d}{dt} \int_0^t f(t-\tau) \cdot U(\tau) d\tau \right] \quad (4.18)$$

where  $\sigma_0$  is the DC conductivity,  $U(t)$  is the applied voltage,  $C_0$  is the geometry capacitance of the dielectric.

- The polarisation current  $i_{pol}(t)$  flowing through the dielectric when a step DC voltage  $U_0$  is suddenly applied to the dielectric test sample can be written as:

$$i_{pol}(t) = U_0 C_0 \left[ \frac{\sigma_0}{\epsilon_0} + \epsilon_\infty \delta(t) + f(t) \right] \quad (4.19)$$

where  $\delta(t)$  is the delta function arising from the suddenly applied step voltage at  $t=0$ .

- From the above equation (4.20) , it can be observed that the polarisation current  $i_{pol}(t)$  consists of three parts:

1. The first term is related to the inherent conductivity of the test object and is independent of any polarisation process.
2. The middle part with the delta function  $\delta(t)$  is difficult to be recorded in practice and is always ignored in the calculation due to the large dynamic range of current amplitudes arising from extremely fast polarisation processes occurring for very short period of time.
3. The third term  $f(t)$  relates to slow polarisation phenomena and can be seen as the memory of the material [37].

Neglecting the middle term in the equation of  $i_{pol}$  [4.20] , the final equation defining the relation between the polarisation current  $i_{pol}$  and the dielectric response function  $f(t)$  is given by

$$i_{pol}(t) = U_0 C_0 \left[ \frac{\sigma_0}{\epsilon_0} + f(t) \right] \quad (4.20)$$

#### 4.4.2. Estimation of depolarisation current and its relation with dielectric response function $f(t)$

This section presents the relation between the depolarisation current  $i_{depol}(t)$  and the dielectric response function  $f(t)$ . After charging time  $t_c$ , the charging voltage  $U_0$  is removed and the test dielectric is short-circuited, the depolarisation current  $i_{depol}$  can be measured.

$$i_{depol}(t) = -U_0 C_0 [f(t) - f(t + t_c)] \quad (4.21)$$

When the charged time  $t_c$  is long enough for all polarisation processes to complete, then the depolarisation current  $i_{depol}(t)$  is proportional to dielectric response function  $f(t)$  and can be simplified as:

$$i_{depol}(t) = -U_0 C_0 f(t) \quad (4.22)$$

In other words, the dielectric response function  $f(t)$  could be determined from the depolarisation currents obtained after a long charging duration.

$$f(t) = \frac{-i_{depol}(t)}{U_0 C_0} \quad (4.23)$$

Henceforth by estimating the dielectric response function  $f(t)$ , the time dependency and the behaviour of slower polarisation processes occurring in the test sample can be analysed .

#### 4.5. Dielectric response of multi-layered insulation

To investigate the overall dielectric response behaviour of the multi layered insulation from the linear dielectric model, it is essential to identify analytically the individual dielectric response of each of its constituent materials under an applied voltage  $U(t)$ . In a series arrangement of equivalent circuits of 'm' materials, the relation between the total voltage  $U(t)$  and the local voltages  $u_k(t)$  across each individual equivalent circuit is given by [12]:

$$U(t) = \sum_{k=1}^m u_k(t) \quad (4.24)$$

The relation between the total current  $i(t)$  and the local voltages  $i_k(t)$  across each individual equivalent circuit is given by

$$i(t) = i_k(t) = i_1(t) = i_2(t) = i_m(t) \quad (4.25)$$

where  $i_k(t)$  denotes the local currents in dielectric  $k = 1 \dots m$ .

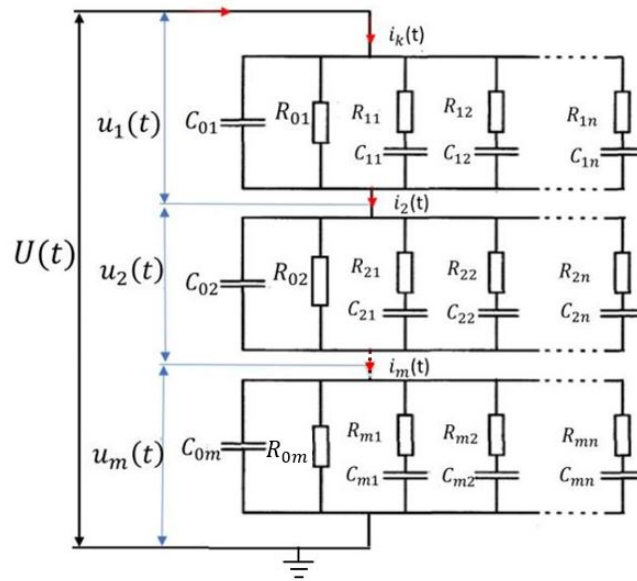


Figure 4.8: Extended model of linear multi-layer dielectric

For the multi-layered insulation represented by a series arrangement of 'm' equivalent circuits, the equation of the total current  $i(t)$  for the linear dielectric model [ equation 4.18] can be modified to represent the relationship between the current  $i_k(t)$  and the voltage  $u_k(t)$  .

$$i_k(t) = C_{0k} \left[ \frac{\sigma_{0k}}{\epsilon_0} u_k(t) + \epsilon_{rk} \frac{du_k(t)}{dt} + \frac{d}{dt} \int_0^t f_k(t-\tau) \cdot u_k(\tau) d\tau \right] \quad (4.26)$$

for  $k= 1 \dots m$ ,

where  $C_{0k}$  is the geometric capacitance of material k ;  $\epsilon_{rk}$  is the individual relative permittivity,  $\sigma_{0k}$  is the conductivity of the dielectric and  $f(t)$  represent the dielectric response function of material k [12].

#### 4.5.1. Polarisation current through multi-layered insulation of oil, paper and pressboard

When a DC voltage  $U_0$  is applied to a series arrangement of equivalent circuits of oil, paper and pressboard, by the condition of continuity of currents the generated polarisation current  $i_{pol}(t)$  is equal to the local currents flowing through each of the individual equivalent circuits of oil, paper and pressboard.

$$i_{pol}(t) = i_1(t) = i_2(t) = i_3(t) \quad (4.27)$$

where  $i_1(t)$  ,  $i_2(t)$  and  $i_3(t)$  are the local currents flowing through individual equivalent circuits of oil, paper and pressboard respectively [figure 4.9].

Accordingly, the polarisation current  $i_{pol}(t)$  through the extended circuit under the influence of the applied DC voltage  $U_0$  is given by:

$$i_{pol}(t) = i_1(t) = \frac{U_1}{R_{01}} + \sum_{i=1}^n \frac{U_1}{R_{1i}} \exp \frac{-t}{\tau_{1i}} \quad (4.28)$$

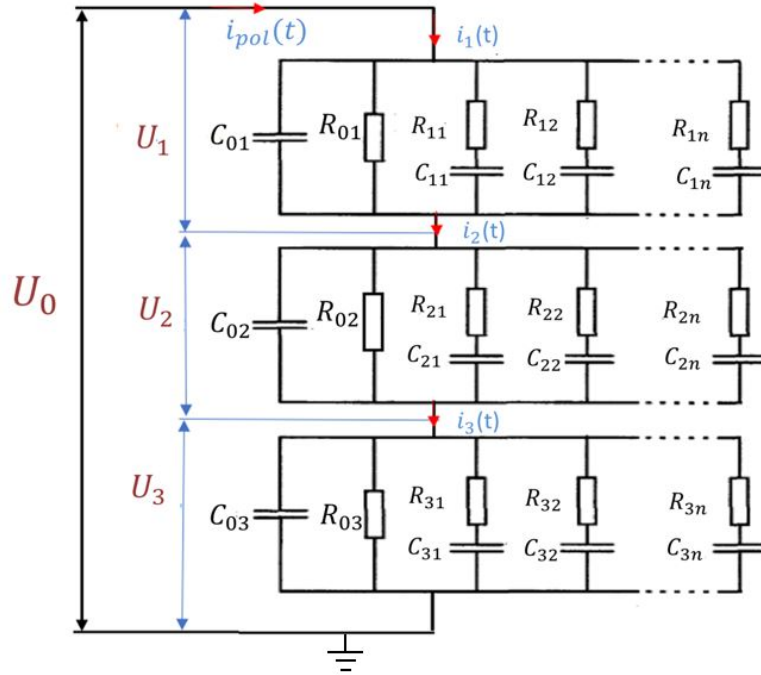


Figure 4.9: Extended circuit of the multi-layered dielectric

where  $n$  is the number of parallel branches with series connection of a resistor  $R_i$  and capacitor  $C_i$  ;  
 $\tau_{1i} = R_{1i} C_{1i}$  [21].

## 4.6. Summary

The test sample representing the transformer insulation can be modelled into a series connection of three parallel R-C circuits with each parallel R-C network describing the dielectric material present in the sample, i.e. oil, paper and pressboard. The simplified R-C circuit of the test sample was solved to get the analytical output equation of discharge voltage in the time domain. To improve the shortcomings of the simplified R-C circuit of the test sample, a modified and extended R-C equivalent circuit was suggested where each insulating material was expressed as a linear dielectric model. The branches of the linear dielectric model represent the different activated polarisation processes with corresponding time constants occurring within the individual dielectric of the test sample. The essential relations of the polarisation currents and depolarisation currents with the dielectric response function  $f(t)$  were explained with the help of the linear dielectric model. By understanding the behaviour of the dielectric response function  $f(t)$  of the test dielectrics, the time dependency of the depolarisation current of the composite transformer insulation could be analysed. For this, the DC measurements of the polarisation currents of the individual test samples of oil, paper and pressboard and the composite test samples consisting of a combination of oil, paper and pressboard were performed using the dielectric spectroscopy instrument IDAX 300. The test procedure and results will be presented in Chapter 5.

# 5

## DC measurements of polarisation currents

The chapter presents an outline of the polarisation current measurements performed on the individual samples of oil, paper and pressboard and also, on the composite insulation consisting of oil, paper and pressboard in the High voltage laboratory of Delft University of Technology under the supervision of Ing. Paul Van Nes and Dr Luis Carlos. The tests were conducted on the sample dielectrics with the dielectric spectroscopy instrument IDAX 300 under DC voltage at ambient temperature.

The first section provides the details about the test sample and the test cells used for measuring the individual samples of oil, paper and pressboard. The section also presents the measured polarisation curves of the test samples and the values of measured resistance  $R_m$  and measured capacitance  $C_m$  of the individual test samples. The next section provides a description of the optimal charging time  $t_c$  for measurements on the composite test samples. Finally, the chapter concludes with the section giving an overview of the polarisation current measurements of the composite test samples consisting of oil, paper and pressboard.

### 5.1. Dielectric measurements using IDAX 300

IDAX 300 is a diagnostic instrument which provides precise and reliable condition assessment of insulation in transformers, bushings, generators and cables. The state-of-the-art software enables easier and faster measurements of moisture content and oil conductivity of transformer insulation in approximately 22 minutes (20° C). Using IDAX 300, the capacitance and dissipation factor values could be measured over a wide range of frequencies (0.1 mHz-1 kHz). It measures the moisture content, oil conductivity and  $\tan \delta$  values of the test object by advanced fitting to the reference material model already defined in IDAX 300 [1].

By using VAX020 -a high-voltage amplifier, the test voltage can be extended from 200 V up to 2 kV. This allows the instrument to measure test samples of very low capacitance accurately. For the measurements taken using IDAX 300 for this research, the test mode was taken as 'Ungrounded Specimen Test (UST)'. The analysis by IDAX 300 is automatic, and the only input to be entered is the value of the ambient temperature. The time-domain dielectric measurements the test sample were conducted at power frequency, and the polarisation current in the test sample was measured over time.



Figure 5.1: IDAX 300 [1]

The following Tables 5.1 and 5.2 provides the measurement specifications of IDAX 300.

Measurement	Range
Voltage	0-200 V peak
Current	0-50 mA peak
Capacitance	10 pF - 100 $\mu$ F
Dissipation factor range (% DF)	0-10

Table 5.1: Measurement specifications of IDAX 300

Specifications for Time domain current measurements (PDC)	
Range	$\pm 20$ mA
Resolution	0.1 pA
Inaccuracy	0.5 % $\pm 1$ pA
Input resistance (DC mode)	$\leq 10$ kOhm* * 10 kOhm is the input impedance in worst case situation

Table 5.2: Specifications of PDC measurements using IDAX 300

## 5.2. Overview of the dielectric measurements on individual test samples

For the dielectric tests on paper and pressboard samples, the charging voltage was taken as 200 V and the charging time was taken as  $t_c=1000$  seconds. The samples of pressboard and kraft paper used for the measurements were obtained from Royal Smit Transformers. The test samples were subjected to vacuum treatment for 24 hours at 65 °C to avoid the effects of moisture on the measurements. In order to eliminate edge effect and to ensure a homogeneous field up to the measuring area, the test samples were measured using test cells with guard electrode to minimise the influence of leakage currents on the measured values.

The transformer oil Nynas NYTRO was used as the liquid insulation. The oil was dried and vacuum treated for 24 hours at 80 °C. Later, it filled in the oil test cell [figure 5.4]. The oil test cell is then placed in the vacuum until the measurements were taken. The oil was tested in an oil test cell by applying a voltage of  $U_0=500$  V for a charging duration of  $t_c = 10,000$  seconds. The details regarding the test samples, test voltage, charging time  $t_c$  and the measured parameters are provided in Table 5.3.

Test sample	Applied Voltage (V)	Charging time $t_c$	Measured parameters
Transformer oil (Nynas NITRO)	500	10000	$i_{pol}, R_m, C_m$
Paper (0.25 mm thickness)	200	1000	$i_{pol}, R_m, C_m$
Pressboard (1 mm thickness)	200	1000	$i_{pol}, R_m, C_m$
Pressboard (2 mm thickness)	200	1000	$i_{pol}, R_m, C_m$

Table 5.3: Test samples and measured parameters obtained from IDAX 300

For each measurement, the charging voltage is applied until a stable, steady DC conduction current was obtained. By administering the DC measurements on the test samples using IDAX 300, the values of polarisation currents varying over time, the insulation resistance  $R_m$  and the capacitance  $C_m$  of the test samples at 50 Hz were measured [Table:5.5].

### 5.2.1. Test cells used for the measuring test samples of oil, paper and pressboard

DC measurements were conducted on the samples of oil, paper and pressboard with dielectric spectroscopic instrument IDAX 300. After testing, the corresponding geometric parameters of insulation resistance  $R_m$ , capacitance  $C_m$  and the polarisation current  $i_{pol}(t)$  of the samples were obtained.

1. The test samples of paper and pressboard were measured with the Tettex 2914 test cell for solid insulants [2]. The test cell has a shielded measuring electrode equipped with guard ring which has a diameter of 49.5 mm. The base plate of the test cell has sockets for test voltage, temperature control and measuring bridge. The high voltage electrode is mounted on the insulated base plate [figure 5.2]. The whole test cell is protected with a bell jar. Before taking measurements, the test cell is evacuated with a vacuum pump and is filled with dry air. The pressure inside the the test cell could be controlled from outside and is kept at ambient pressure.

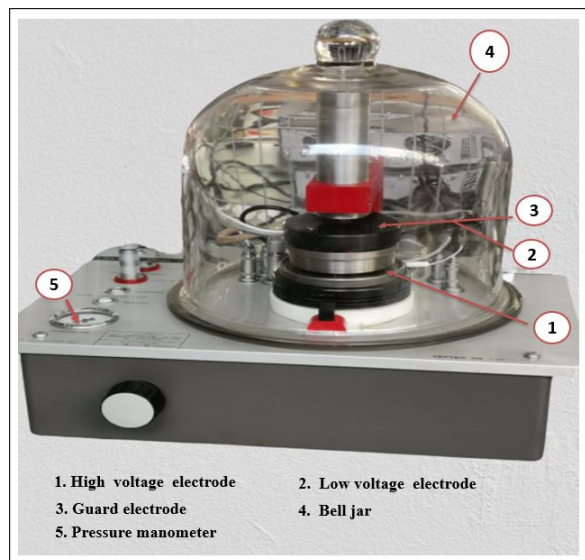


Figure 5.2: 2914 Tettex test cell for solid insulants

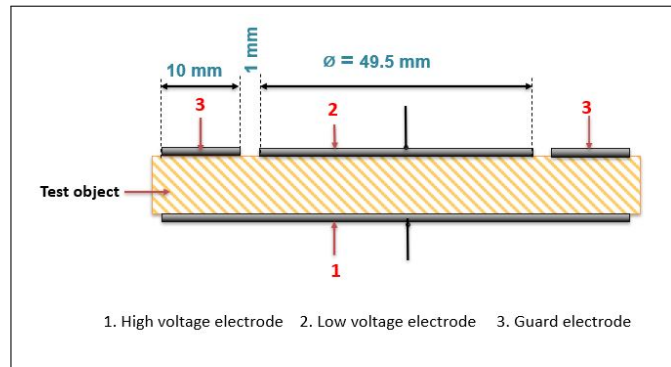


Figure 5.3: Schematic diagram of test object and guarded measuring electrode

- By using the guard electrode [figure 5.3], the leakage current due to stray capacitances can be eliminated and the in-homogeneity of the field on the edge of the high voltage electrode can be reduced. Therefore it enables accurate dielectric measurements, especially while conducting tests for small samples of insulating material.
2. The transformer oil was tested with the oil test cell having an inbuilt guard electrode. The test cell was designed at the High voltage laboratory, TU Delft. The test cell was first appropriately cleaned to avoid the presence of contaminants and embedded oil particles from previous tests.
- The test cell has two electrodes- a high voltage (HV) electrode and a low voltage (LV) electrode. Both electrodes are made of stainless steel. The top cover of the LV electrode is made of epoxy and has a potential guard built inside it. The guard ring is connected to the shield of the coaxial cable. The guard ring helps to avoid the influence of stray leakage currents on the dielectric measurements. The small hole at the side of the LV electrode and the junction pipe at the side of the HV electrode ensure that there is no air trapped inside the test cell after being filled with the oil sample.
  - Firstly, the capacitance  $C_{t.c}$  of the empty test cell was measured using IDAX. Similarly, the capacitance  $C_m$  of the oil was obtained by measuring the capacitance of test cell filled with transformer oil. From the values of capacitances  $C_{t.c}$  and  $C_m$ , the value of permittivity  $\epsilon_r$  of oil is obtained.

$$\epsilon_r = \frac{C_m}{C_{t.c}} \quad (5.1)$$

$$= 3.1$$

where  $C_m = 430.3 \text{ pF}$ ;  $C_{t.c} = 135.2 \text{ pF}$ .

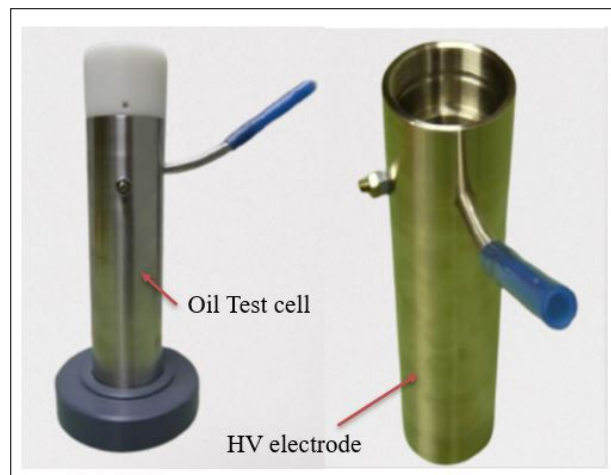


Figure 5.4: Oil test cell

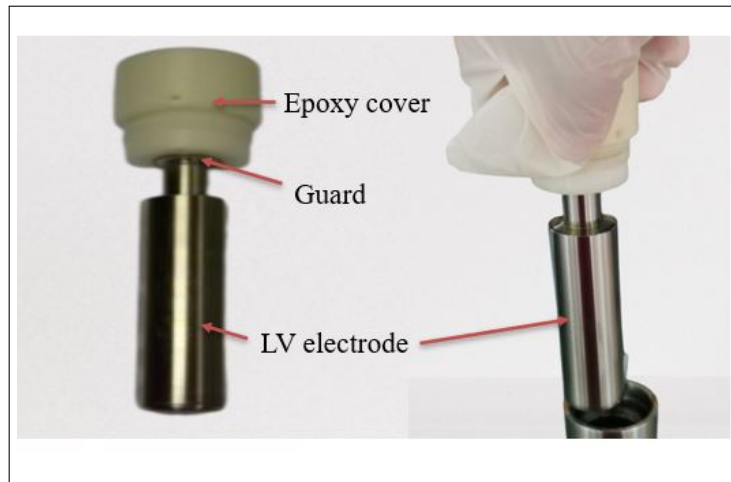


Figure 5.5: Low voltage electrode of oil test cell

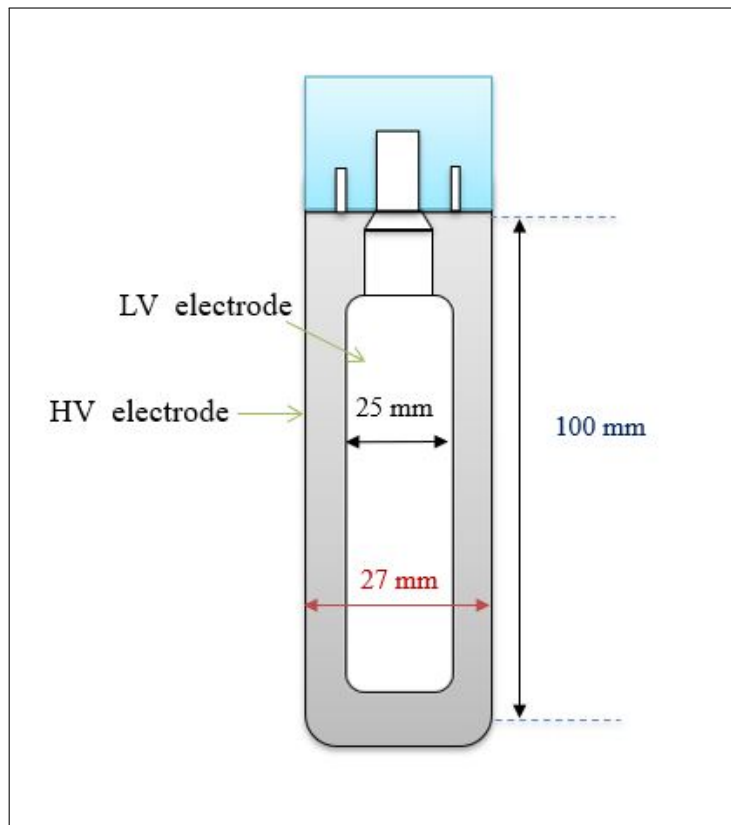


Figure 5.6: Oil test cell dimensions

### 5.2.2. Test Conditions

The following Table 5.4 details the values of ambient temperature ( $^{\circ}\text{C}$ ), ambient relative humidity (RH %) and ambient pressure (mbar) under which measurements were conducted on individual test samples of oil, paper and pressboard.

<b>Test sample</b>	Ambient temperature °C	Ambient RH %	Ambient pressure mbar
<b>Oil</b>	20	55	1020
<b>Paper</b> ( 0.25 mm thickness )	22	55	1021
<b>Pressboard</b> ( 1 mm thickness )	23	55	1035
<b>Pressboard</b> ( 2mm thickness )	22	55	1021

Table 5.4: Ambient test conditions for individual samples

### 5.2.3. IDAX test results of individual samples of oil, paper and pressboard

In this section, the measured parameters of individual dielectrics of oil, paper and pressboard along with the plots of the polarisation currents varying over time have been presented. The following Table 5.5 presents the values of the measured insulation resistances  $R_m$  and measured capacitances  $C_m$  of the individual test samples. The  $\tan \delta$  values and the estimated moisture content in the individual test samples of oil, paper and pressboard have been provided in Appendix B for reference. The time-domain current measurements (PDC) using IDAX 300 have measurement resolution of 1 pA and has a very low measurement inaccuracy of 0.5 % .

<b>Test Sample</b>	<b>Measured parameters</b>	
	$R_m$	$C_m$
<b>Transformer Oil</b>	14.29 G $\Omega$	430.3 pF
<b>Paper</b> ( 0.25 mm thickness )	12.95 G $\Omega$	230 pF
<b>Pressboard</b> ( 1 mm thickness )	1388 G $\Omega$	60.2 pF
<b>Pressboard</b> ( 2 mm thickness )	292 G $\Omega$	37.86 pF

Table 5.5: Measured values of capacitance  $C_m$  and insulation resistance  $R_m$  obtained from IDAX 300

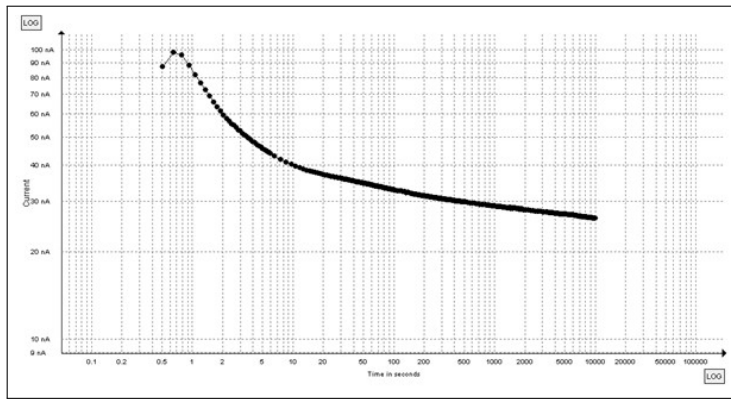


Figure 5.7: Polarisation current vs Time plot for oil

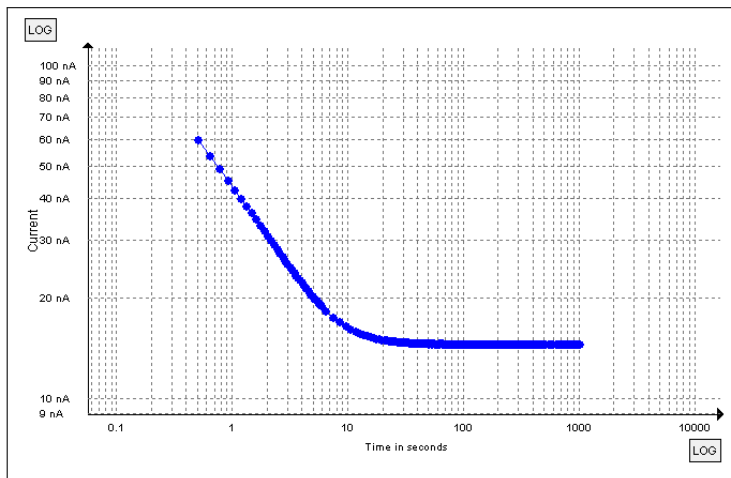


Figure 5.8: Polarisation current vs Time plot for paper sample of thickness 0.25 mm

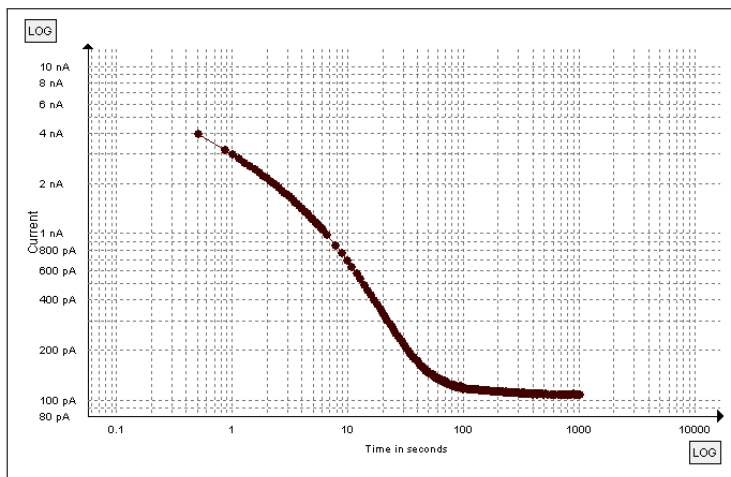


Figure 5.9: Polarisation current vs Time for pressboard sample of thickness 1 mm

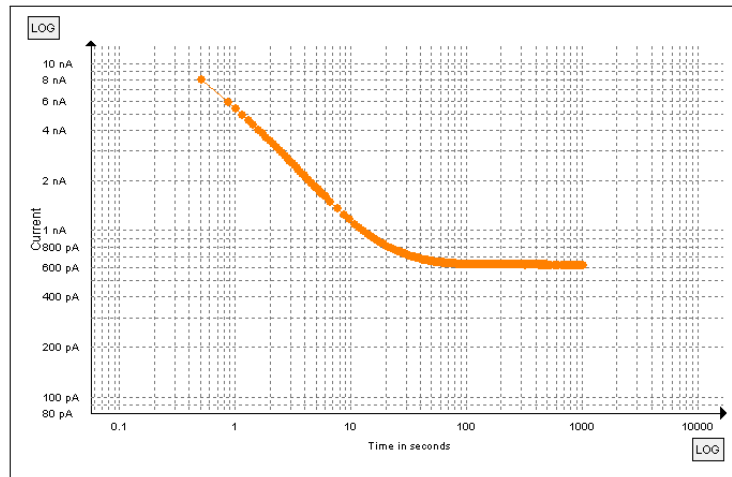


Figure 5.10: Polarisation current vs Time for pressboard sample of thickness 2 mm

- As can be seen from the plot of the polarisation current vs time [figure 5.7], the polarisation current  $i_{pol}(t)$  increases in the first few seconds. This increase may be an indication of very fast polarisation processes happening in a very short span of time. Also, as defined in the equation of polarisation current [equation 4.20], transients may be observed at the peak of the polarisation curve due to the inclusion of the delta function  $\delta(t)$  arising from the voltage being applied immediately following  $t = 0$  [10].
- On a comparison between the plots of  $i_{pol}(t)$  of pressboard samples of 1 mm and 2 mm thickness, an evident change in the slope of the polarisation current can be seen. Referring to Table 5.5, the insulation  $R_m$  resistance of pressboard test sample of 2 mm thickness is lower than that of pressboard sample of 1 mm thickness at power frequency. The slope of the polarisation  $i_{pol}(t)$  of pressboard sample of 2 mm thickness also indicates faster decay than the pressboard sample of 1 mm thickness.

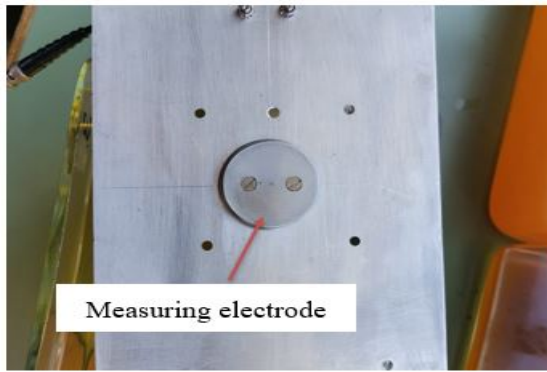
The polarisation current flowing through the test sample under the influence of applied voltage is a combination of displacement current and conduction current. The nature of this displacement current is dependent on the polarisation process occurring in the dielectric material, which in turn depends on the condition of the test dielectric under consideration [10].

- The  $\tan \delta$  values of paper and the pressboard sample of thickness 2 mm are much higher as presented in Table 6.4. A dissipation factor ( $\tan \delta$ ) greater than '1' is an indicator of a high level of moisture content in the test sample. This, in turn, would mean that the tested samples of the paper and pressboard (of thickness of 2 mm) have higher conductivity values due to the presence of moisture in the samples. Hence, the plots of polarisation current vs time of paper and pressboard samples show lower insulation resistance values in the initial stages of measurements.

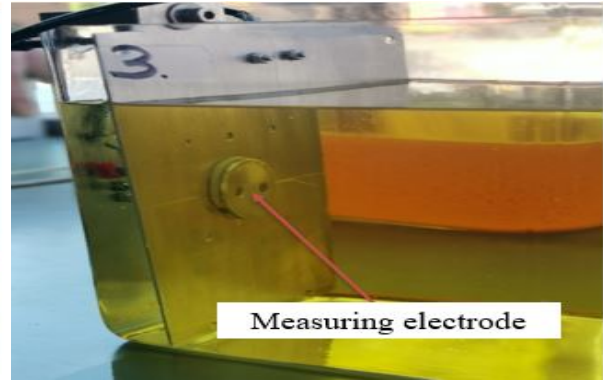
### 5.3. Overview of the tests performed on the composite test samples

The measurements of the polarisation currents for the composite insulation of oil, paper and pressboard were carried out by applying a voltage of  $U_0 = 500$  V for a charging duration ranging between  $t_c = 1000$  to 10000 seconds until a steady-state conduction current was obtained.

A circular electrode of diameter 45.5 mm was used to measure the dielectric response of the composite test samples [figure 5.11a]. In all the three sets of measurements the distance between the electrodes were varied [Table: 5.10, 5.11, 5.12].



(a) Measuring Electrode



(b) Measuring electrode screwed to metallic plate

Figure 5.11: Test aquarium with measuring electrode

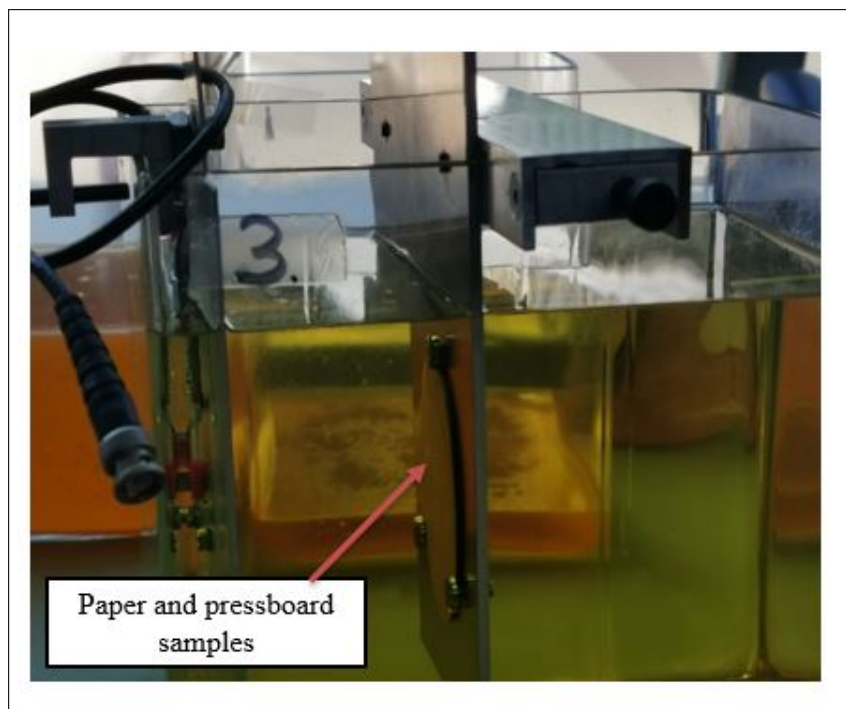


Figure 5.12: Paper and pressboard samples screwed to the metallic parallel plate

The measuring electrode was screwed to a metallic parallel plate. The parallel plate (LV plate) was separated from the metal electrode by a support insulator. The support insulator is used to electrically separate the LV plate from the measuring electrode. The circular measuring electrode was connected to the inner conductor of the coaxial cable and the LV connection was given to the shield of the coaxial cable. The test samples were screwed on to a metallic parallel plate to which the HV connection is given.

In the test set up [figure 5.13], both the LV plate and the measuring electrode were maintained at the same potential. The arrangement ensures that the electric field lines near the edge of the measuring electrode remain perpendicular to the measuring electrode as well as the second parallel plate. This guarantees a homogeneous electric field distribution up to the edge of the measuring area. Thus the measuring volume can be accurately determined by the area of the measuring electrode, and the electrode separation ' $d$ '. For taking measurements, the HV connection was connected to the output of IDAX 300, and the measuring electrode was connected to the input of the instrument (IDAX 300).

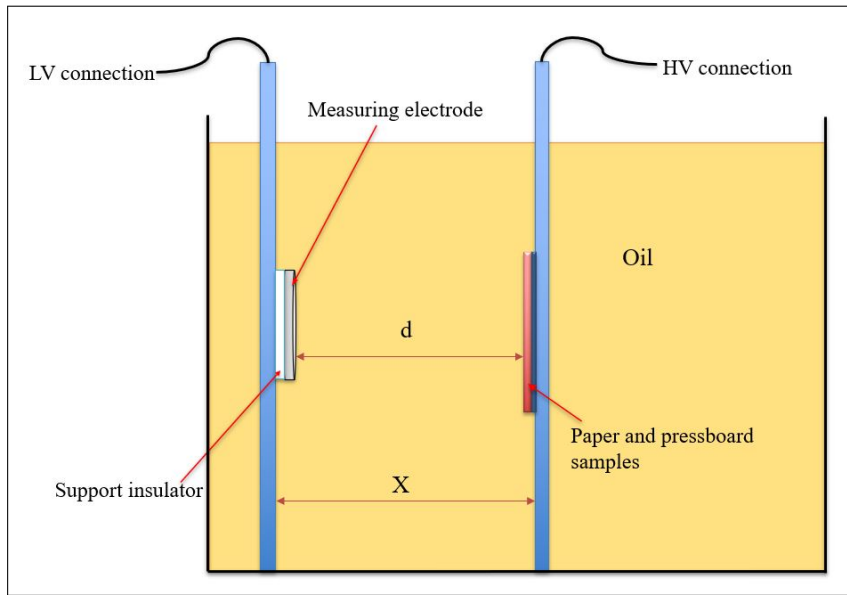


Figure 5.13: Test aquarium with test dielectrics

In the figure 5.13, the 'X' stands for the distance between the metallic plates. The distance between the electrodes 'd' calculated as follows:

$$X = 5.5 \text{ mm} + d$$

$$d = d_{oil} + d_{pap} + d_{pb}$$

where  $d_{oil}$ ,  $d_{pap}$  and  $d_{pb}$  represents oil gap, thickness of paper and pressboard in the composite test sample.

As seen in the figure 5.13, a support insulator is placed between the measuring electrode and the metallic plate (LV plate). The additional 5.5 mm is the distance between the metallic plate and the measuring electrode and is accounted for in the calculation of 'd' [5.3]. The following Table presents an overview about the calculation of the distance between electrodes 'd' as given in figure 5.13.

Test sample	Distance between the parallel plates X	Distance between the electrodes d	Oil gap $d_{oil}$	Thickness of paper $d_{pap}$	Thickness of pressboard sample $d_{pb}$	Oil to paper-pressboard ratio
<b>Oil</b>	15 mm	9.5 mm	8.25 mm	0.25 mm	1 mm	6
<b>+ Paper</b> (0.25 mm thickness)	20 mm	14.5 mm	13.25 mm	0.25 mm	1 mm	10
<b>+ Pressboard</b> (1 mm thickness)	25 mm	19.5mm	18.25 mm	0.25 mm	1 mm	14

Table 5.6: Computed parameters of distance between electrodes 'd', oil-gap and oil-solid insulation ratio); Thickness of pressboard in composite insulation = 1 mm

The calculations for the distance between the electrodes 'd' in the test set up for the remaining test cases are provided in the Appendix B

### 5.3.1. Test conditions

The following Tables 5.7, 5.8, 5.9 present the values of ambient temperature (°C), ambient relative humidity (RH %) and ambient pressure (mbar) under which measurements were conducted on composite test samples of oil, paper and pressboard.

Test sample	Distance between the electrodes $d$	Ambient temperature °C	Ambient RH %	Ambient pressure mbar
<b>Oil</b> + <b>Paper</b> ( 0.25 mm thickness ) + <b>Pressboard</b> ( 1 mm thickness )	9.5 mm	22	60	1025
	14.5 mm			
	19.5 mm			

Table 5.7: Ambient test conditions for composite test samples; Thickness of pressboard in the sample = 1 mm

Test sample	Distance between the electrodes $d$	Ambient temperature °C	Ambient RH %	Ambient pressure mbar
<b>Oil</b> + <b>Paper</b> ( 0.25 mm thickness ) + <b>Pressboard</b> ( 2 mm thickness )	15.5 mm	25	55	1017
	20.5 mm			
	25.5 mm			

Table 5.8: Ambient test conditions for composite test samples; Thickness of pressboard in the sample = 2 mm

Test sample	Distance between the electrodes $d$	Ambient temperature °C	Ambient RH %	Ambient pressure mbar
<b>Oil</b> + <b>Paper</b> ( 0.25 mm thickness ) + <b>Pressboard</b> ( 5 mm thickness )	12 mm	22	55	1023
	17 mm			
	22 mm			

Table 5.9: Ambient test conditions for composite test samples; Thickness of pressboard in the sample = 5 mm

### 5.3.2. Optimal charging time $t_c$

In a complex multi-layered dielectric, there would be charge accumulation at the interface where there is a difference in the conductivity and permittivity values. Therefore, for a perfect PDC measurement, proper charging and discharging time must be given for all the interfacial polarisation processes to relax.

From the polarisation-depolarisation current (PDC) measurements on the composite test samples consisting of oil-paper/pressboard, many researchers [35], [26], [17] have concluded that while the initial part of the PDC dielectric response curves relates to the oil conductivity, the final part of the response curves evidently is influenced by the conductivity of the solid insulation. It is possible to determine the conductivity of oil from a smaller duration of PDC measurements on the test samples, but the same is not true for the estimation of the conductivity of solid insulation of paper and pressboard [51].

The estimation of conductivity of solid insulation requires the value of steady-state DC current, obtained after the completion of all the polarisation processes. The longer the charging time taken for PDC measurements, the more stable value of DC is attained and hence leading to better accuracy in the measured values. Test duration of 10,000 seconds of charging and 10,000 seconds of discharging is considered optimal for PDC measurements of power transformer insulation [52], [51]. Nevertheless, such a long measurement time is not always feasible due to time constraints in the laboratory. Hence a charging time  $t_c$  between 1000-5000 seconds is chosen, and the measurement of polarisation currents is continued until a steady-state DC current is established [52], [55].

### 5.3.3. IDAX test results of composite insulation of oil, paper and pressboard

In this section, the measured parameters of insulation resistance  $R_m$  and geometric capacitance  $C_m$  of composite oil- paper and pressboard insulation are presented. The thickness of pressboard in the test sample is varied in each of the test cases. The corresponding plots of the polarisation currents varying over time are also given. The  $\tan \delta$  values and the estimated moisture content in the composite test samples have been provided in Appendix B for reference. The time domain current measurements (PDC) using IDAX 300 have measurement resolution of 1 pA and measurement inaccuracy of 0.5 %.

The following test case [Table 5.10] presents the values of the insulation resistances  $R_m$  and the capacitances  $C_m$  of the composite test samples measured for different values of distance between the electrodes 'd'. The pressboard thickness in the composite insulation was taken as 1 mm.

#### Test case: 1

Test Sample	Applied Voltage	Distance between the electrodes $d$	Charging time $t_c$ (seconds)	Measured Capacitance (pF)	Measured Resistance ( $G\Omega$ )
Oil + Paper (0.25 mm thickness) + Pressboard (1 mm thickness)	500 V	9.5 mm	2000	4.729	2830
		14.5 mm	10000	3.213	3545
		19.5 mm	6000	2.44	3292

Table 5.10: Test case:1 Measured parameters from IDAX ; Thickness of pressboard in composite insulation = 1 mm

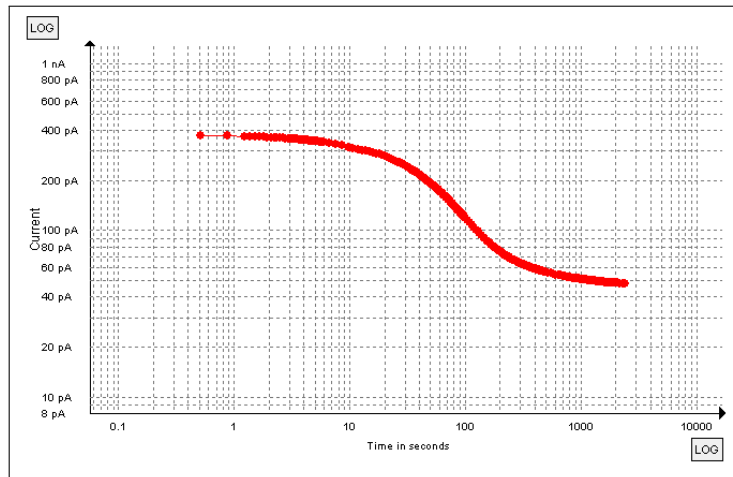


Figure 5.14: Polarisation current vs Time for composite insulation of oil, paper and pressboard sample ;  $d = 9.5$  mm

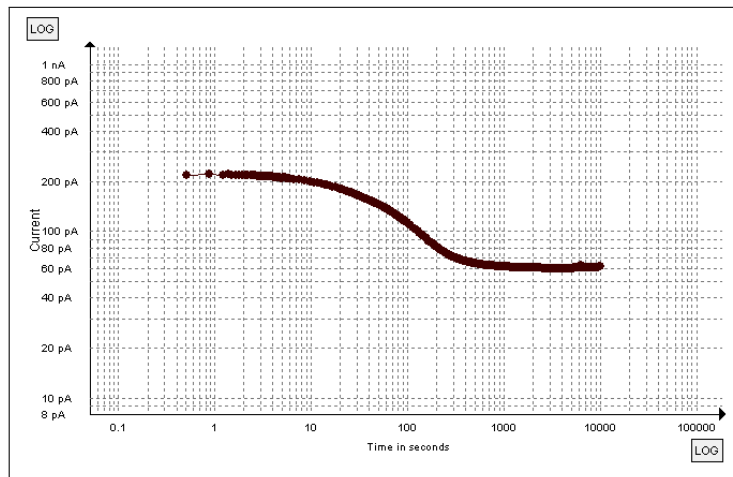


Figure 5.15: Polarisation current vs Time for composite insulation of oil, paper and pressboard sample ;  $d = 14.5$  mm

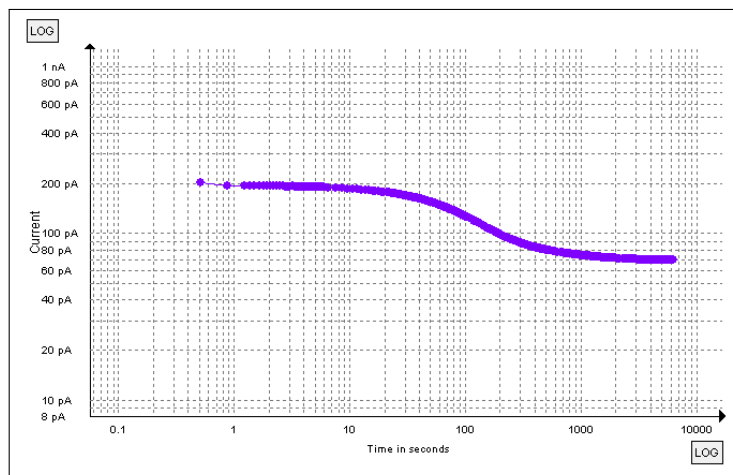


Figure 5.16: Polarisation current vs Time for composite insulation of oil, paper and pressboard sample ;  $d = 19.5$  mm

Test case: 2

Test case: 2 displays the values of the insulation resistances  $R_m$  and the capacitances  $C_m$  of the composite test samples measured for varying distances between the electrodes [Table 5.11]. The pressboard thickness in the composite insulation was taken as 2 mm.

Test Sample	Applied Voltage	Distance between the electrodes $d$	Charging time $t_c$ (seconds)	Measured Capacitance (pF)	Measured Resistance ( $G\Omega$ )
Oil + Paper (0.25 mm thickness) + Pressboard (2 mm thickness)	500 V	15.5 mm	5000	3.412	2343
		20.5 mm	4000	2.217	3387
		25.5 mm	4000	2.008	3069

Table 5.11: Measured parameters from IDAX ; Thickness of pressboard in composite insulation = 2 mm

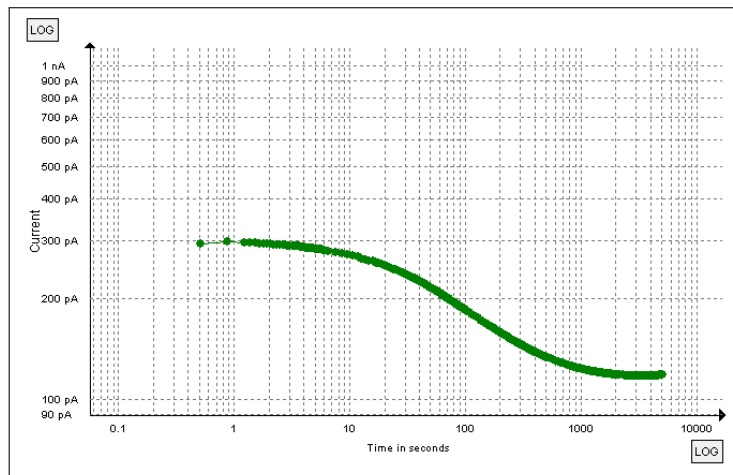


Figure 5.17: Polarisation current vs Time for composite insulation of oil, paper and pressboard sample ;  $d= 15.5$  mm

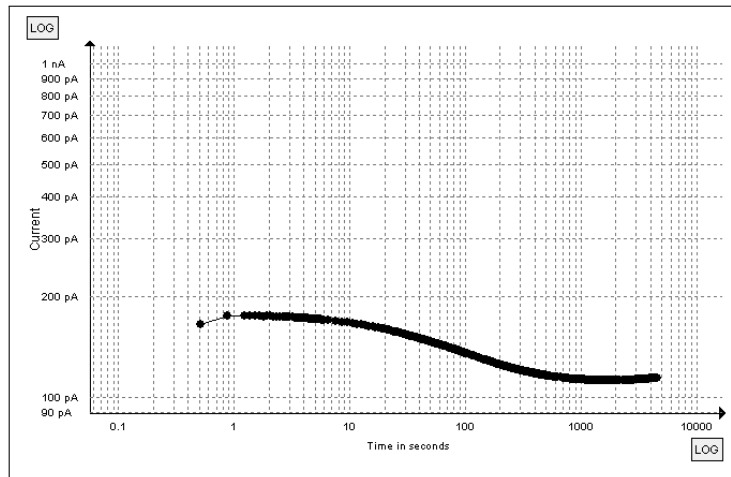


Figure 5.18: Polarisation current vs Time for composite insulation of oil, paper and pressboard sample ;  $d = 20.5$  mm

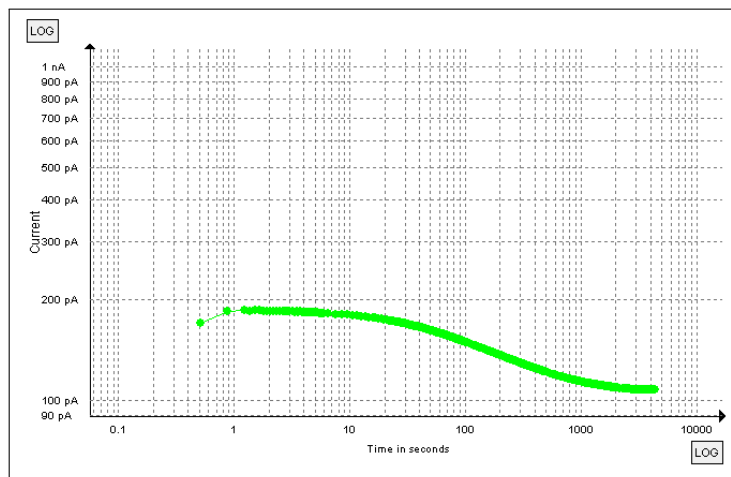


Figure 5.19: Polarisation current vs Time for composite insulation of oil, paper and pressboard sample ;  $d = 25.5$  mm

### Test case: 3

Test case: 3 displays the values of the insulation resistances  $R_m$  and the capacitances  $C_m$  of the composite test samples measured for varying distances between the electrodes [table 5.12]. The pressboard thickness in the composite insulation was taken as 5 mm.

Test Sample	Applied Voltage	Distance between the electrodes $d$	Charging time $t_c$ (seconds)	Measured Capacitance (pF)	Measured Resistance ( $G\Omega$ )
Oil + Paper (0.25 mm thickness) + Pressboard (5 mm thickness)	300 V	12 mm	1000	19.72	371.5
		17 mm	1000	13.44	511.4
		22 mm	1000	10.79	601.8

Table 5.12: Measured parameters from IDAX; Thickness of pressboard in composite insulation = 5 mm

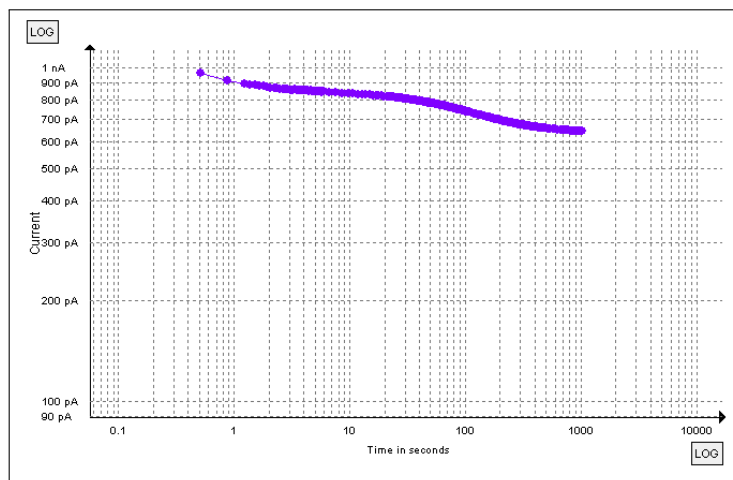


Figure 5.20: Polarisation current vs Time for composite insulation of oil, paper and pressboard sample ;  $d = 12$  mm

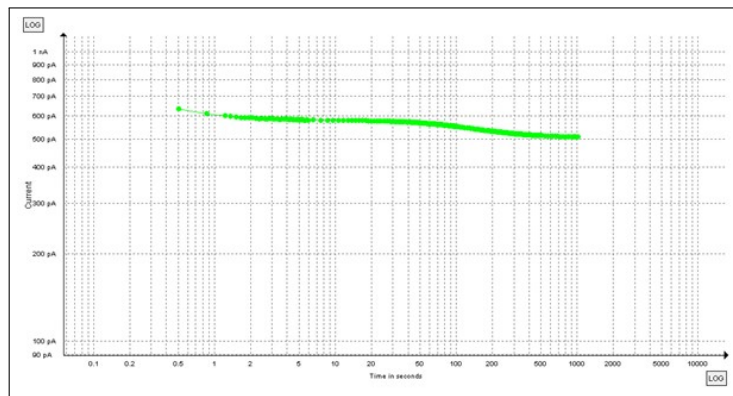


Figure 5.21: Polarisation current vs Time for composite insulation of oil, paper and pressboard sample ;  $d = 17$  mm

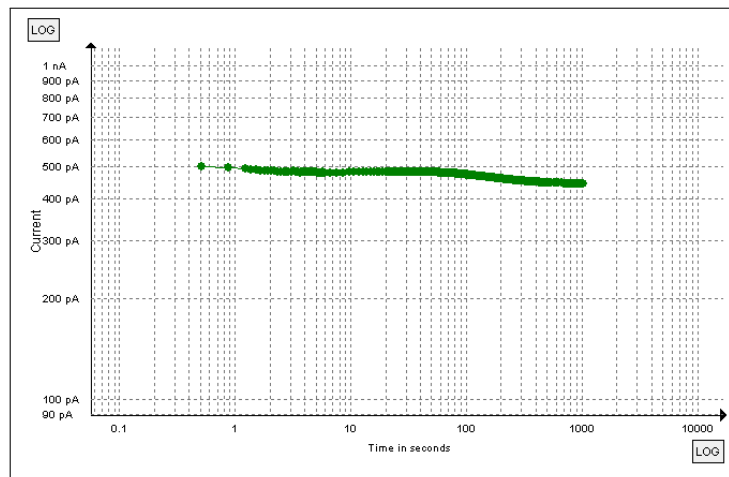


Figure 5.22: Polarisation current vs Time for composite insulation of oil, paper and pressboard sample ;  $d = 22$  mm

In the measurements of the polarisation current  $i_{pol}(t)$  given by the test cases, it can be seen that as the distance between the electrodes ' $d$ ' was increased, the peak magnitude of polarisation current  $i_{pol}(t)$  decreases. This may be due to delayed polarisation process as the charges have to migrate longer distance to participate in the polarisation. As the charging time  $t_c$  taken is different in various test cases, it is not easy to compare and analyse the influence of the thickness of pressboard on the polarisation current  $i_{pol}(t)$  curves. With the R-C models of the composite test samples built in PSPICE simulation platform, the analysis of the polarisation currents  $i_{pol}(t)$  can be conducted at uniform charging times  $t_c$  for all composite test samples. In this way, it would be possible to have a reasonable comparison of the test results.

## 5.4. Summary

This chapter provides the summary of the DC measurements of the individual and composite dielectrics consisting of oil, paper and pressboard conducted in the High voltage laboratory, TU Delft. Chapter 5 stages as a bridge between the theoretical background of the extended R-C equivalent circuit of the test sample given in Chapter 4 and actual implementation of the dielectric response model of the test sample using PSPICE simulation software presented in Chapter 6.

- The time domain current measurements (PDC) of individual test samples of oil, paper and pressboard and composite test samples consisting of oil, paper and pressboard were carried out using IDAX 300. The test samples were subjected to vacuum treatment and drying prior to measurements.
- The solid insulation of paper and pressboard samples were tested with Tettex 2914 test cell [ figure 5.2]. The transformer oil Nynas NITRO was tested in an oil test cell [ figure 5.4]. Both these test cells were equipped with a guard electrode to eliminate the influence of stray capacitances on the measured values.
- The test samples of paper and pressboard (of 2 mm thickness) were found to have high  $\tan \delta$  values. This indicated the presence of moisture content greater than the threshold limit of 0.3-0.5 % in the test samples, [34].
- For taking dielectric measurements of the composite test samples of oil, paper and pressboard, a test set up was developed [figure 5.13] in High Voltage laboratory, TU Delft. The test aquarium was equipped with a guard electrode to ensure homogeneity of field distribution on the measuring electrode and to eliminate the leakage currents due to stray capacitances.
- The dielectric testing of composite test samples showed that as the distance between the electrodes ' $d$ ' decreases, there is an overall uplift of the polarisation curves as seen from the figures [ 5.20-5.22].

# 6

## Simulation of the modified R-C model

A model of the transformer main insulation system, which describes its dielectric behaviour, has been presented in this chapter. The values of the parameters of the equivalent model have been obtained from DC measurements of polarisation currents using the dielectric spectroscopic instrument IDAX 300. Once the extended R-C model was parameterized, dielectric responses such as the polarisation and depolarisation currents were simulated using the electronic simulation PSPICE software.

### 6.1. Introduction

The experimental platform was set up in the high voltage laboratory to measure the polarisation currents of the test samples in the time domain. After obtaining the measurements of polarisation currents  $i_{pol}(t)$  of the test sample, an equivalent R-C circuit model based on the time-domain dielectric response was established with PSPICE simulation software. The following figure 6.1 represents the analysis flowchart describing the steps followed to obtain the final R-C model of the composite transformer insulation.

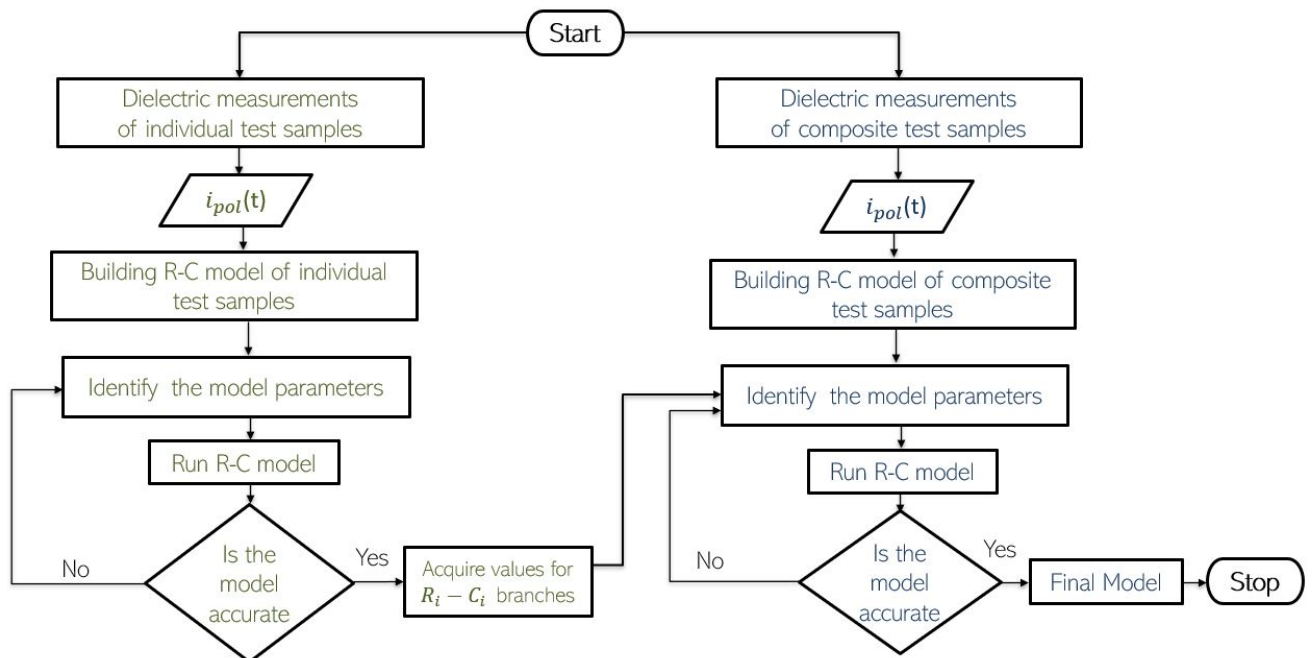


Figure 6.1: Analysis flowchart

With the simulation model, not only the polarisation currents but also the depolarisation currents of the samples could be replicated for different charging and discharging durations. This investigation allowed the

study of polarisation-depolarisation (PDC) measurements of the test samples of oil, paper and pressboard and also an arrangement of oil, paper and pressboard representing composite transformer insulation. The test results and the simulated polarisation current values from the dielectric samples were compared regularly. In this way, the models simulated in PSPICE are optimised to obtain similar results to the measured values of  $i_{pol}(t)$  from IDAX 300. The comparison of the maximum and minimum values of the simulated polarisation currents with the time-domain polarisation currents obtained from dielectric testing demonstrated that relative errors of  $i_{pol}(t)$  values were limited to a maximum of 8 % as seen in Tables 6.2 and Tables 6.6 - 6.11.

## 6.2. Building the linear dielectric model for oil, paper and pressboard samples using PSPICE

This section outlines the approach of building the individual equivalent R-C model for linear dielectrics-oil, paper and pressboard in PSPICE simulation software. The first subsection 6.2.1 discusses the iterative method adopted to identify all the model parameters of the PSPICE model. The succeeding subsection 6.2.2 confers to the modelling the individual R-C circuit of oil, paper and pressboard in PSPICE. In the subsequent section 6.3, the plots of polarisation currents obtained from dielectric testing using IDAX 300 were compared with the simulated waveforms of polarisation currents obtained from PSPICE and error bars between the maximum and minimum polarisation current values are given. The final subsections 6.3.1 and 6.3.2 gives an overview of the analysis of the depolarisation currents and dielectric response function  $f(t)$  obtained from PSPICE models of oil, paper and pressboard.

### 6.2.1. Identifying the model parameters of individual dielectric model

For building the linear model for oil, paper and pressboard, all circuit parameters specifically the geometric resistance  $R_0$ , geometric capacitance  $C_0$ , the resistances and capacitance of individual branches  $R_i-C_i$  have their origin from the IDAX measurements of individual samples of the dielectric [ Table 5.5].

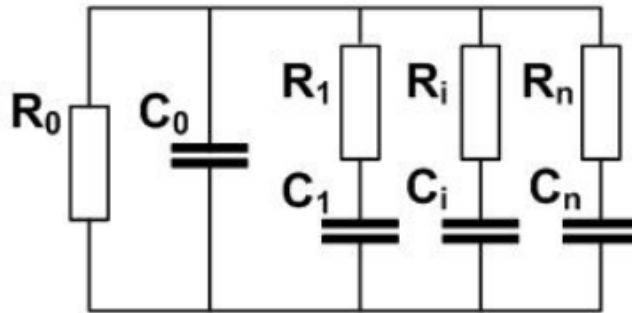


Figure 6.2: Linear dielectric model

- To extract the values of the resistances and capacitance of individual branches  $R_i-C_i$ , the analytical equation of the polarisation current was solved in MATLAB by inserting arbitrary values for  $R_i$  and  $C_i$  parameters for each branch of the linear dielectric model [figure 6.2]. The analytical equation for the polarisation current flowing through the dielectric when applied with a charging voltage  $U$  is given by:

$$i_{pol}(t) = \frac{U}{R_0} + C_0 \frac{dU}{dt} + \sum_{i=1}^n \frac{U}{R_i} \exp \frac{-t}{\tau_i} \quad (6.1)$$

where  $n$ = number of parallel branches with series connection of a resistor  $R_i$  and capacitor  $C_i$  ;

$$\tau_i = R_i C_i$$

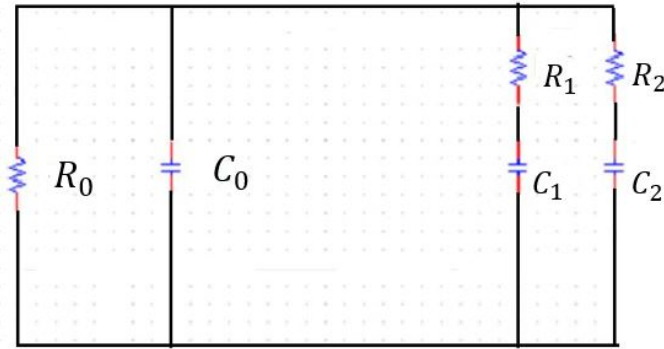


Figure 6.3: Linear dielectric model for individual test samples of oil, paper and pressboard

- When DC voltage  $U_0$  is applied on test dielectric, the above equation 6.1 can be rewritten after neglecting the second term as:

$$i_{pol}(t) = \frac{U_0}{R_0} + \sum_{i=1}^n \frac{U_0}{R_i} \exp\left(-\frac{t}{\tau_i}\right) \quad (6.2)$$

$$= \frac{U_0}{R_0} + \frac{U_0}{R_1} \exp\left(-\frac{t}{R_1 C_1}\right) + \frac{U_0}{R_2} \exp\left(-\frac{t}{R_2 C_2}\right)$$

where,  $U_0$  = Applied DC voltage ;

The two-branches  $R_1$ - $C_1$  and  $R_2$ - $C_2$  represent the two major polarisation processes within the dielectric.

- The model parameters  $R_1$  ,  $C_1$  ,  $R_2$  and  $C_2$  parameters were assigned values best suited to match the  $i_{pol}(t)$  from the PSPICE model with the  $i_{pol}(t)$  obtained from the dielectric test of the individual samples of oil, paper and pressboard. A good fit was obtained after several iterations, and the PSPICE model for linear dielectric was simulated with final iterated values of  $R_i$  and  $C_i$  for each branch [Table 6.1]
- The geometric capacitance  $C_0$  of the individual dielectrics is the the measured capacitance at 50 Hz obtained from IDAX 300 [12].
- The insulation resistance  $R_0$  of the dielectric under test was estimated from the steady state value of the polarisation current  $I_{DC}$  of the test sample measured using IDAX 300.

$$R_0 = \frac{U_0}{I_{DC}} \quad (6.3)$$

- The final circuit parameters  $R_0$ ,  $C_0$ ,  $R_i$  and  $C_i$  of the linear dielectric model [figure 6.3] for the individual dielectrics- oil, paper and pressboard are presented in the Table 6.1.

Circuit Model	Geometric parameters		Branch parameters			
	$R_0$	$C_0$	$R_1$	$C_1$	$R_2$	$C_2$
<b>Oil</b>	17.9 G $\Omega$	430.2 pF	8.5 G $\Omega$	1.35 nF	35 G $\Omega$	12 nF
<b>Paper</b> (0.25 mm thickness)	12.95 G $\Omega$	230 pF	8.8 G $\Omega$	0.35 nF	7.8 G $\Omega$	45 nF
<b>Pressboard</b> (1 mm thickness)	1735 G $\Omega$	60.2 pF	165 G $\Omega$	0.048 nF	65 G $\Omega$	5.8 nF
<b>Pressboard</b> (2 mm thickness)	320 G $\Omega$	37.68 pF	25 G $\Omega$	0.032 nF	63 G $\Omega$	6 nF

Table 6.1: Estimated model parameters

### 6.2.2. Modelling the individual R-C circuit of oil, paper and pressboard

With the dielectric models of individual test samples of oil, paper and pressboard built using PSPICE simulation software, the plots of polarisation currents with respect to time were obtained by applying a DC voltage  $U_0$  for a charging time of  $t_c$ . The applied voltage  $U_0$  and the charging times  $t_c$  were matched and kept the same as for the dielectric tests performed on the samples with IDAX 300.

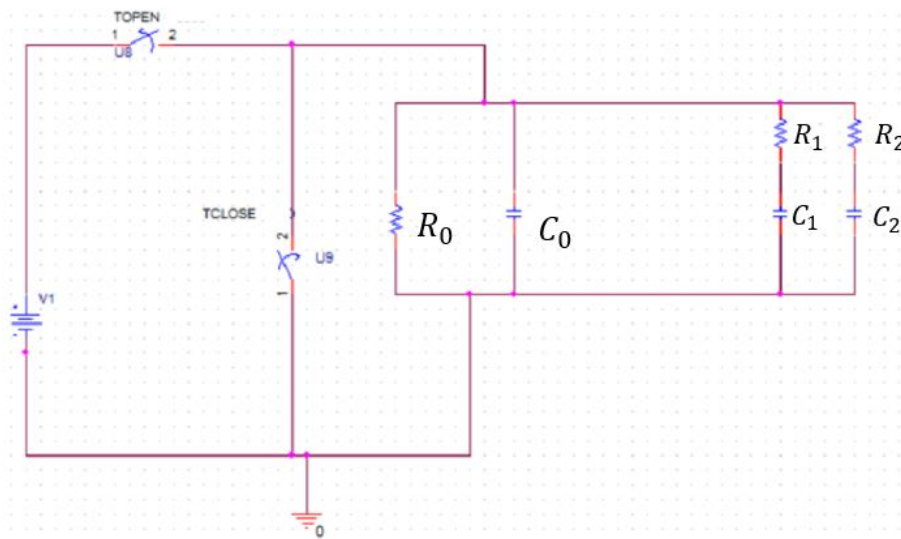


Figure 6.4: PSPICE model of individual dielectric

The switch TOPEN was set to be closed for the charging time  $t_c$  to measure the time-dependent polarisation current  $i_{pol}(t)$  due to charging the capacitances  $C_1$  and  $C_2$ . This current decays exponentially up to a steady-state value of  $i_{DC}$ , which is governed by the DC resistance  $R_0$ . The switch 'TOPEN' was opened at

time  $t = t_c$  as the next step, and at the same instant, the switch 'TCLOSE' was set to be closed. The test sample is disconnected from the DC source [figure 6.4]. Under this condition, the time-dependent depolarisation current  $i_{depol}(t)$  was measurable. Usually, the discharging time  $t_d$  is taken as same as the charging time  $t_c$  [12]. During this discharging stage, a resistive current component is not present due to the short-circuiting of the test object.

### 6.3. Comparison of the polarisation currents obtained from DC tests and the simulated PSPICE models

The following section details the comparison between the polarisation currents  $i_{pol}(t)$  obtained from DC measurements using IDAX 300 and the simulated polarisation currents obtained from PSPICE model of the corresponding test samples. The relative errors between the maximum and minimum  $i_{pol}(t)$  values between the laboratory tested and simulation results of oil, paper and pressboard test samples are given in Table 6.2 and Table 6.3. This helps to understand the level of accuracy obtained for the simulated models of test samples in PSPICE.

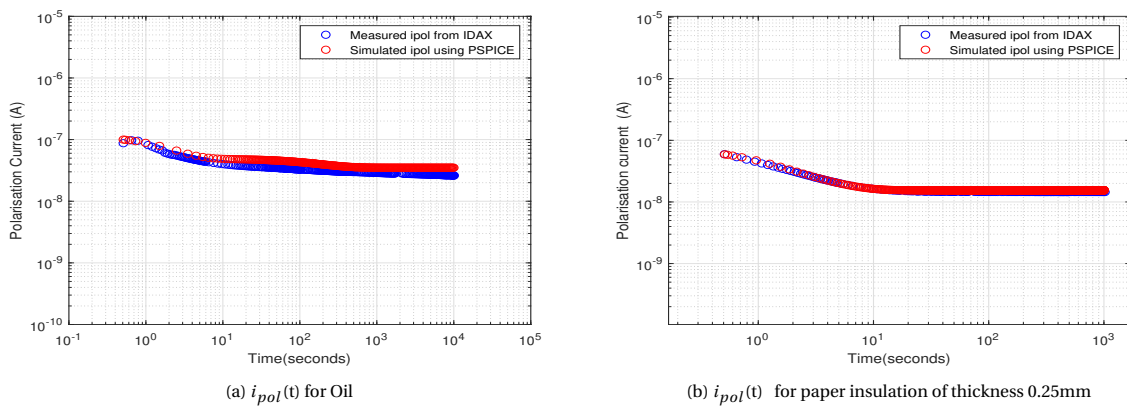


Figure 6.5: Comparison of the polarisation current varying over time obtained from DC tests and the PSPICE models

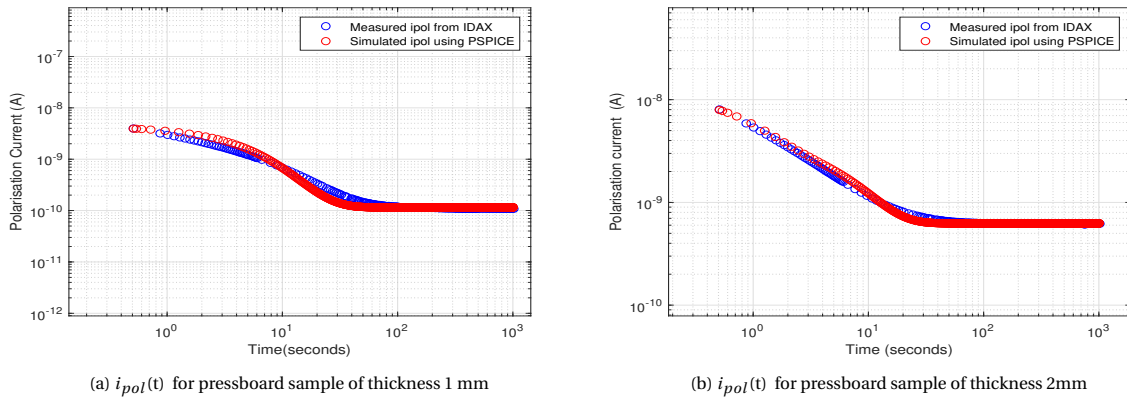


Figure 6.6: Comparison of the polarisation current varying over time obtained from DC tests and the PSPICE models

The error bars between the measured and simulated values of the polarisation currents varying over time are provided in the Table 6.2 and Table 6.3.

Test Sample	Maximum values of polarisation current $i_{pol}(t)$ measured using IDAX 300	Maximum values of polarisation current $i_{pol}(t)$ measured from PSPICE model	Error % for maximum value of the $i_{pol}(t)$
Oil	97.49 nA	98.46 nA	1 %
Paper ( 0.25 mm thickness )	59.52 nA	60.3 nA	1 %
Pressboard ( 1 mm thickness )	3.95 nA	3.93 nA	less than 1 %
Pressboard ( 2mm thickness )	8.03 nA	7.95 nA	less than 1 %

Table 6.2: Relative error % between the maximum values of polarisation currents obtained from IDAX and the simulated PSPICE model

Test Sample	Minimum values of polarisation current $i_{pol}(t)$ measured using IDAX 300	Minimum values of polarisation current $i_{pol}(t)$ measured from PSPICE model	Error % for maximum value of the $i_{pol}(t)$
Oil	26.099 nA	27.9 nA	6 %
Paper ( 0.25 mm thickness )	14.469 nA	15.2 nA	5 %
Pressboard ( 1 mm thickness )	108.4 pA	101 pA	6 %
Pressboard ( 2mm thickness )	619 pA	608 pA	1 %

Table 6.3: Relative error % between the minimum values of polarisation currents obtained from IDAX and the simulated PSPICE model

### 6.3.1. Analysis of the depolarisation currents obtained from PSPICE model

The circuit models were run at the applied voltage of  $U_0 = 500$  V for a charging time of  $t_c = 10,000$  seconds. After removal of applied voltage, the depolarisation currents were measured for a discharging time of  $t_d = 10,000$  seconds. The discharging period started at  $t = 10,000$  seconds and simulation is run until  $t = 20,000$  seconds. The depolarisation current for oil decays to a minimum value of  $6.5 \times 10^{-19}$  A at  $t = 20,000$  seconds. The conductivity of oil was calculated from the values of polarisation and depolarisation currents and is found to be in the order of  $10^{-13}$  S/m [equation 6.4].

$$\sigma_{DC} \approx \frac{\epsilon_0 \epsilon_{oil}}{C_m U_0} (i_p(t) - i_d(t)) \quad (6.4)$$

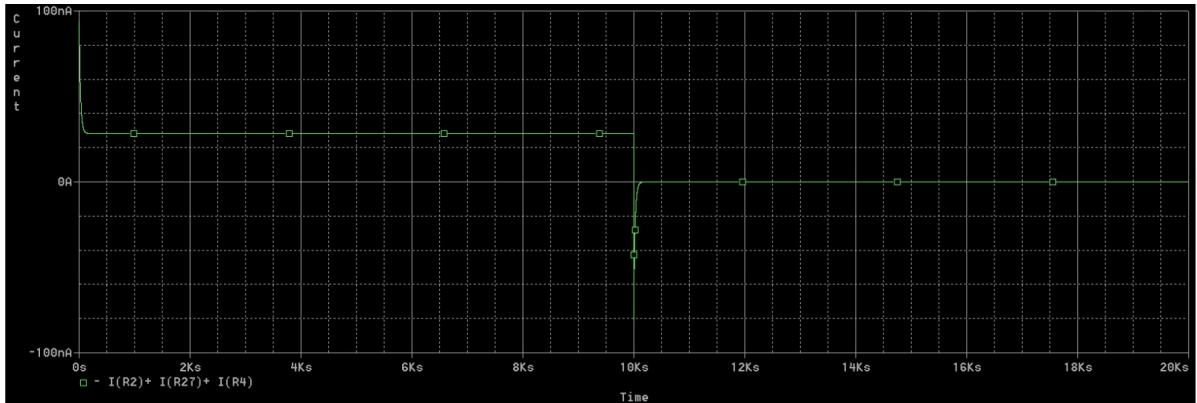


Figure 6.7: Polarisation and depolarisation current varying over time for oil

The depolarisation current for pressboard sample of 1 mm thickness decays to a very low current value of  $2.3 \times 10^{-20}$  A at the end of discharging period of  $t = 20000$  seconds. For both samples of the paper and pressboard (of 2 mm thickness), the depolarisation currents at the end of discharging time  $t = 20000$  seconds, were in the order of  $10^{-20}$  A [Table 6.5].

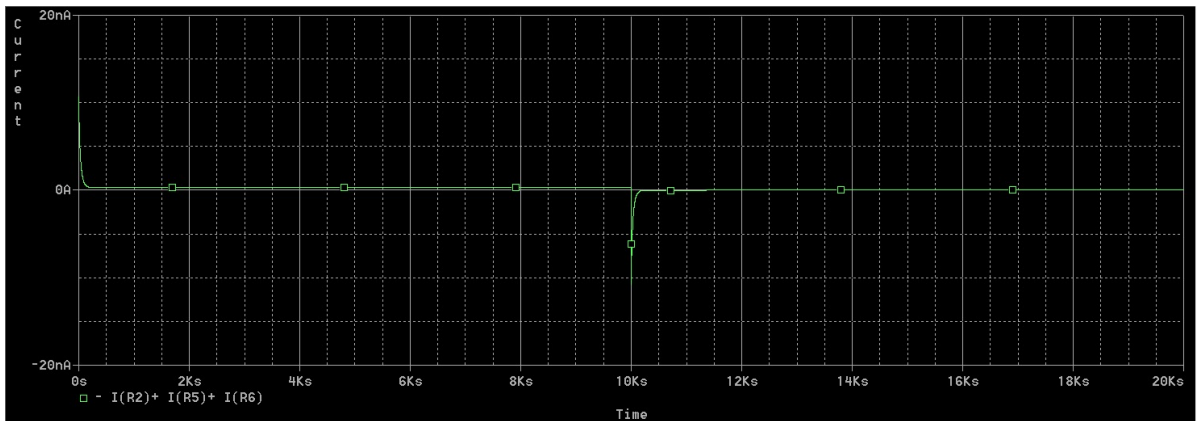


Figure 6.8: Polarisation and depolarisation current varying over time for pressboard sample of 1 mm thickness

The figure 6.9 illustrates the decaying behaviours of depolarisation currents of individual samples of oil, paper and pressboard samples obtained using PSPICE simulation. The depolarisation current plot of pressboard sample of 1 mm thickness clearly depicts a slower decay behaviour. The plots of the depolarisation currents varying with time have been zoomed in to understand the dielectric behaviour of the tested samples. The discharging time started at  $t = 10,000$  seconds and simulation is run until  $t = 20,000$  seconds.

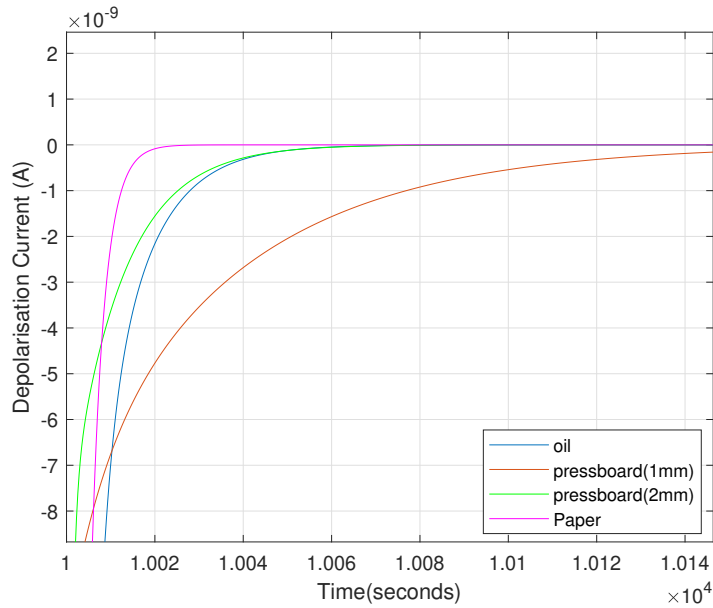


Figure 6.9: Depolarisation current varying over time for individual dielectrics of oil, paper and pressboard

Test Sample	Dissipation factor (%) ( $\tan \delta$ )
Oil	0.13
Paper (0.25 mm thickness)	4.97
Pressboard (1 mm thickness)	1.38
Pressboard (2 mm thickness)	4.32

Table 6.4: Dissipation factor measured at 50 Hz

The depolarisation currents of paper sample and pressboard sample (of 2 mm thickness) in the figure 6.9 clearly show a faster decay to a minimum value. For each of these samples, the respective dissipation factor recorded while testing was very high at 4.32 % and 4.89 % [Table 6.4].

According to the literature [34], the dissipation factor of  $\tan \delta = 1$  is an indication of the moisture content of more than 10 %. Referring to the recorded  $\tan \delta$  values of pressboard sample of 2 mm thickness and paper sample, the water content in the samples was likely to be higher than the allowable threshold value of 0.3-0.5 %. Any amount higher than 0.5% of moisture content will cause an exponential rise in the values of conductivity and dissipation factor. Higher conductivity values would result in lower values for time constants of decay. This could be the reason for the faster fall of the depolarisation currents for the pressboard sample of 2 mm thickness and the paper sample when compared to the depolarisation current of pressboard sample of thickness 1 mm [figure 6.9]. Also, the dielectric strength will be extremely low in such test samples of higher moisture content [34].

The following Table 6.5 provides the values of maximum depolarisation currents for the individual dielectrics of oil, paper and pressboard when applied DC voltage of  $U_0 = 500$  V was applied for charging time

$t_c = 10,000$  seconds and removed. The minimum values of depolarisation currents at the end of the discharging period  $t_d = 10,000$  seconds is given in the same Table 6.5. The values of the depolarisation currents due to the decay of charges at the end of the discharging period of 10,000 seconds is minimal, especially for the solid test samples. The main reason could be the higher conductivities of the test samples due to increased moisture content.

Test Sample	Maximum values of depolarisation current $i_{depol}(t)$ obtained from PSPICE model	Minimum values of depolarisation current $i_{depol}(t)$ obtained from PSPICE model
Oil	73 nA	$6.52 \times 10^{-19}$ A
Paper (0.25 mm thickness)	120 nA	$2.7 \times 10^{-20}$ A
Pressboard (1 mm thickness)	10.7 nA	$2.32 \times 10^{-20}$ A
Pressboard (2 mm thickness)	29.6 nA	$2.5 \times 10^{-20}$ A

Table 6.5: Maximum and minimum values of depolarisation currents of individual test samples

### 6.3.2. Analysis of the dielectric response function $f(t)$ obtained from PSPICE model

The dielectric response function  $f(t)$  is monotonically decreasing function, which provides an insight into the slower polarisation processes occurring within the dielectric. The plots of  $f(t)$  is computed from the depolarisation current plots of individual test samples [figure 6.9] using the equation [4.23]. The following figure 6.10 shows that the behaviour of dielectric response function  $f(t)$  follows a similar trend to that of the depolarisation currents of individual dielectrics of oil, paper and pressboard. The dielectric response function  $f(t)$  for the pressboard sample of 1 mm thickness clearly takes the longest time to decay to a minimum value.

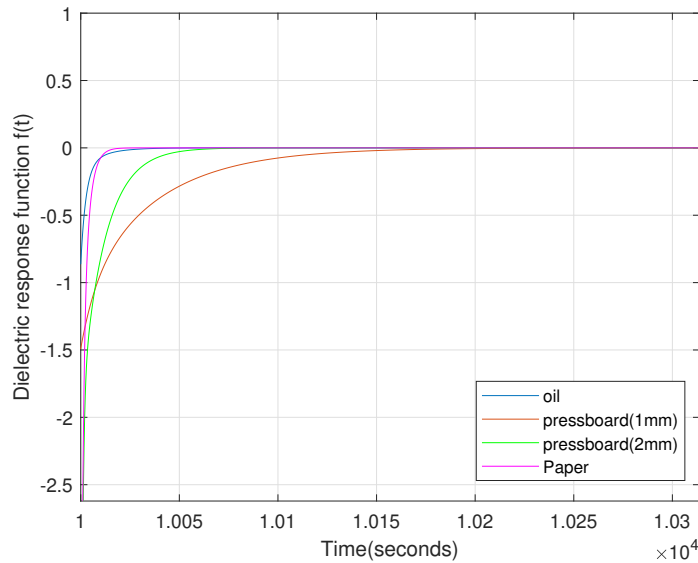


Figure 6.10: Dielectric response function  $f(t)$  for individual dielectrics of oil, paper and pressboard; Plot of  $f(t)$  starts from  $t = 10,000$  seconds.

## 6.4. Building of the PSPICE model of extended R-C circuit of composite insulation of oil, paper and pressboard

This section provides an overview about the modelling of the extended equivalent R-C model for the composite insulation consisting of oil, paper and pressboard in PSPICE simulation software.

The subsection 6.4.1 discusses the identification of the model parameters of extended R-C circuit consisting of oil, paper and pressboard in PSPICE. In the subsection 6.4.2, the polarisation currents  $i_{pol}(t)$  obtained from dielectric measurements of composite test samples were compared with the simulated polarisation currents from the extended R-C models of the composite test samples built in PSPICE. The relative errors between the maximum and minimum polarisation current values are given in the Tables 6.6 - 6.11.

For modelling a composite transformer insulation, a series arrangement of individual R-C circuits of oil, paper and pressboard representing the composite structure of the transformer insulation system has been adopted.

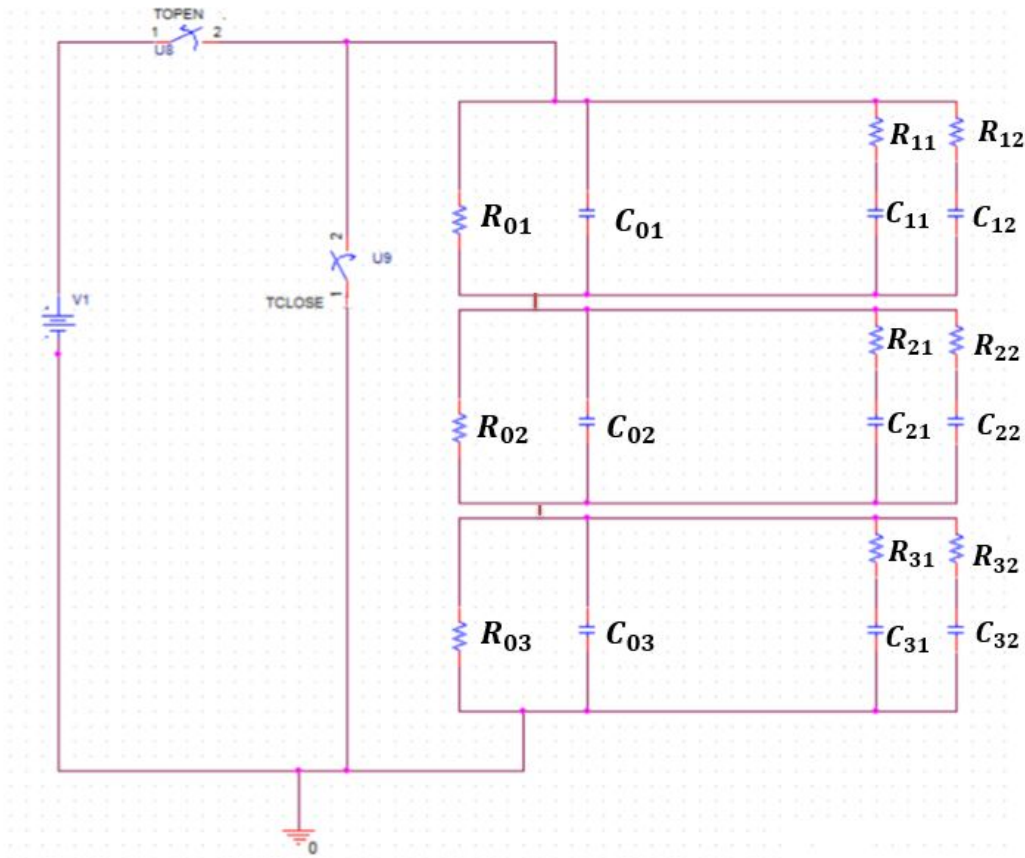


Figure 6.11: Modified extended R-C circuit of composite insulation of oil, paper and pressboard

With the dielectric models of composite test samples built in PSPICE simulation environment, the plots of polarisation currents with respect to time were obtained by applying a DC voltage  $U_0$  for a charging time of  $t_c$ . The applied voltage  $U_0$  and the charging times  $t_c$  were retained from the dielectric measurements of corresponding composite test samples [ Tables 5.10, 5.11, 5.12].

### 6.4.1. Identification the model parameters of extended R-C circuit

In the extended circuit model, the insulation resistances of oil, paper and pressboard is represented by the model parameters  $R_{01}$ ,  $R_{02}$  and  $R_{03}$  respectively. Many research papers [51], [26],[17], [35] have confirmed that the initial parts of the polarisation currents are sensitive to the condition of the oil, whereas it is the condition of the solid insulation that influences the final long-term values of the polarisation currents.

The higher mobility of the charge carriers in the liquid dielectric is responsible for the greater magnitude of the current defining the peak of the polarisation current. This initial response will decline after some time, and the steady-state condition of the conduction current owing to the less mobile charge carriers in the solid insulation becomes predominant. Therefore, the respective model parameters  $R_{01}$  and  $R_{03}$  of oil and pressboard were obtained from initial and final response of the polarisation currents recorded during each of the corresponding dielectric tests.

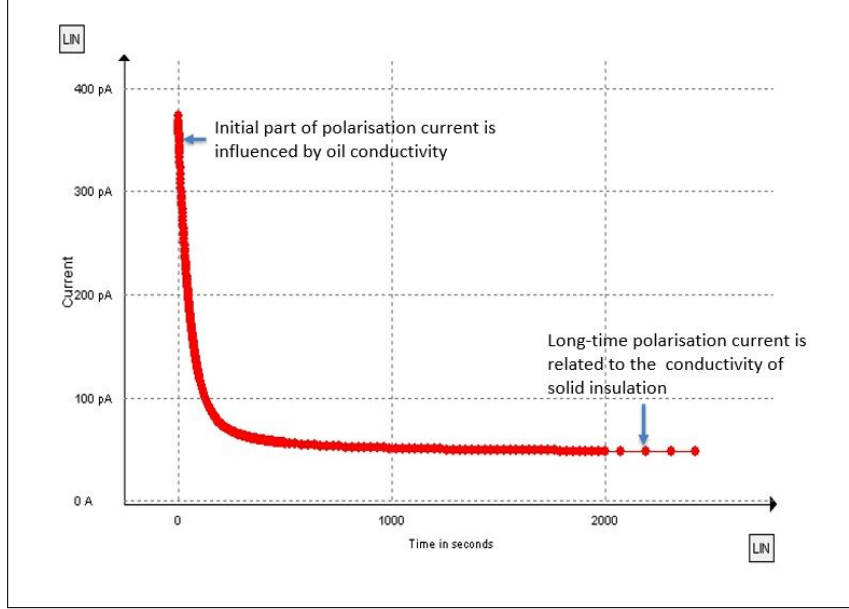


Figure 6.12: Polarisation current in composite insulation of oil, paper and pressboard

1. For identifying the insulation resistance  $R_{01}$ , the oil conductivity was calculated from the initial polarisation current  $i_{pol}(t)$  value obtained from the plot of polarisation current varying over time. The high values of current transients observed at the beginning of the polarisation curve cannot be recorded and hence could be neglected [10],[51]. Generally the value of  $i_{pol}(t)$  after  $t_c=3$  seconds is taken [45].

- When a DC voltage of  $U_0$  is applied on the composite dielectric consisting of oil, paper and pressboard, the initial part of polarisation current can be written as

$$i_p(0+) = C_0 U_0 \frac{\sigma_{oil}}{\epsilon_0 \epsilon_r} \quad (6.5)$$

The above equation 6.5 could be rewritten in terms of conductivity of oil  $\sigma_{oil}$  as:

$$\sigma_{oil} = \frac{\epsilon_0 \epsilon_r}{C_m U_0} i_{pol}(0+) \quad (6.6)$$

where  $\epsilon_0 = 8.854 * 10^{-15}$  F/mm.

For solving the equation 6.6 of oil conductivity  $\sigma_{oil}$ , the corresponding parameters of composite permittivity  $\epsilon_r$ , geometric capacitance  $C_0$  and measured capacitance  $C_m$  were determined.

- The composite relative permittivity  $\epsilon_r$  for test dielectric consisting of oil, paper and pressboard was calculated from the following analytical formula:

$$\epsilon_r = \frac{d_{total} \epsilon_{oil} \epsilon_{pap} \epsilon_{pb}}{(d_{oil} \epsilon_{pap} \epsilon_{pb}) + (d_{pap} \epsilon_{pb} \epsilon_{oil}) + (d_{pb} \epsilon_{pap} \epsilon_{oil})} \quad (6.7)$$

where  $d_{tot}$  = distance between the electrodes ;  $d_{oil}$ ,  $d_{pap}$  and  $d_{pb}$  represents oil gap , thickness of paper and pressboard in the test sample. The individual permittivity of oil, paper and pressboard are given by  $\epsilon_{oil}$ ,  $\epsilon_{pap}$  and  $\epsilon_{pb}$  respectively.

- The permittivity of oil  $\epsilon_{oil}$  can be estimated from the capacitance of oil measured using the oil test cell and the capacitance of the empty test cell [equation 5.1]. Likewise, the relative permittivity  $\epsilon_{pap}$  and  $\epsilon_{pb}$  of the paper and pressboard samples can easily be calculated from their respective geometric configuration as given in Table 5.5. The permittivity of oil, paper and pressboard was calculated as  $\epsilon_{oil} = 3.1$ ,  $\epsilon_{pap} = 3.4$  and  $\epsilon_{pb} = 4.2$ .
- $C_0$  is the geometric capacitance of test sample and be estimated from the measured capacitance  $C_m$  (at or near power frequency) divided by  $\epsilon_r$ .

$$C_0 = \frac{C_m}{\epsilon_r} \quad (6.8)$$

where  $C_m$  the capacitance value measured between two terminals of the insulation system under the test.  $\epsilon_r$  is the composite relative permittivity.

- The values of capacitances  $C_m$  for different distances between the electrodes and for different thickness of pressboard in the composite insulation is given in the previous chapter-5 under section 5.3.
- From the calculated value of conductivity of oil [equation 6.6] , the geometric resistance  $R_{01}$  of the oil was estimated from the analytical formula for dielectric constant.

$$R_{01} = \epsilon_0 \cdot \frac{\epsilon_{oil}}{C_{01} \sigma_{oil}} \quad (6.9)$$

2. The capacitances  $C_{01}$ ,  $C_{02}$  and  $C_{03}$  of the extended model were determined from the geometric capacitance value of the corresponding dielectric and the individual relative permittivity.

$$C_{01} = C_{oil} * \epsilon_{oil} \quad (6.10)$$

$$C_{02} = C_{pap} * \epsilon_{pap} \quad (6.11)$$

$$C_{03} = C_{pb} * \epsilon_{pb} \quad (6.12)$$

- $C_{oil}$  is the geometric capacitance of oil and can be estimated as:

$$C_{oil} = \frac{\epsilon_0 * A}{d_{oil}} \quad (6.13)$$

where  $A$  is the area of cross section of measuring electrode;  $A = 1626 \text{ mm}^2$ ;  
Similarly the values of capacitances of paper  $C_{pap}$  and pressboard  $C_{pb}$  can be evaluated.

3. The geometric dimensions of paper in the composite dielectric was kept exactly same as that of individual test sample of paper [Table 5.5]. Therefore, the value of model parameter  $R_{02}$  of paper could be taken as the value of measured insulation resistance  $R_m$  obtained from the individual dielectric testing of paper.

4. The model parameter  $R_{03}$  can be approximated from the final value of the polarisation current  $i_{pol}(t)$ .

- The effective conductivity  $\sigma_r$  is calculated from the steady state value of the polarisation current  $i_{DC}$ . For this, the final value of  $i_{DC}$  at the end of charging time  $t_c$ .

$$i_{DC} = C_0 U_0 \frac{\sigma_r}{\epsilon_0} \quad (6.14)$$

$$\sigma_r = \frac{i_{DC} \epsilon_0}{C_0 U_0} \quad (6.15)$$

- The conductivity of paper is calculated from the geometrical configuration as given in Table 5.5.

$$\sigma_{pap} = \frac{d_{pap}}{R_{02} * A} \quad (6.16)$$

where  $A$  is the area of cross-section of the measuring electrode;  $A = 1626 \text{ mm}^2$ .

- The relations between effective conductivity  $\sigma_r$  of composite insulation of oil, paper and individual conductivities of oil, paper and pressboard is given by the following equation

$$\frac{d_{tot}}{\sigma_r} = \frac{d_{oil}}{\sigma_{oil}} + \frac{d_{pap}}{\sigma_{pap}} + \frac{d_{pb}}{\sigma_{pb}} \quad (6.17)$$

- From the calculated values of effective conductivity  $\sigma_r$  and the respective conductivities of oil and paper, the conductivity of pressboard  $\sigma_{pb}$  can be calculated.

$$R_{03} = \frac{d_{pb}}{\sigma_{pb} * A} \quad (6.18)$$

5. In the extended R-C circuit model, the parameters  $R_i$  and  $C_i$  branches of the solid insulation- paper and pressboard is kept as same as presented in Table 6.1. The branches  $R_i - C_i$  represent the activated polarisation processes occurring in the individual dielectrics under the influence of the applied DC voltage  $U_0$ .

6. The MATLAB codes for calculating the parameters of linear dielectric models of oil, paper and pressboard in the extended R-C model is described in the Appendix [C].

#### 6.4.2. Comparison of the polarisation currents obtained from DC tests and the simulated PSPICE model

In this section, the polarisation currents  $i_{pol}(t)$  varying over time obtained from DC measurements using IDAX 300 are compared with the simulated polarisation currents obtained from PSPICE model of the corresponding test samples. The relative errors between the maximum and minimum  $i_{pol}(t)$  values have been provided between the laboratory test results and simulation results obtained from test samples to understand the level of accuracy obtained for the simulated models of test samples in PSPICE.

- The figures 6.13, 6.14 and 6.15 presented below, shows the comparison of the polarisation current varying over time obtained from DC tests and the simulated PSPICE models of the test sample consisting of oil, paper (of thickness 0.25 mm), pressboard (of thickness 1 mm). The distance between the electrodes ' $d$ ' was varied and kept at 9.5 mm, 14.5 mm and 19.5 mm respectively. The error bars

between the measured and simulated values of the polarisation currents varying over time is provided in the Tables 6.6 and 6.7.

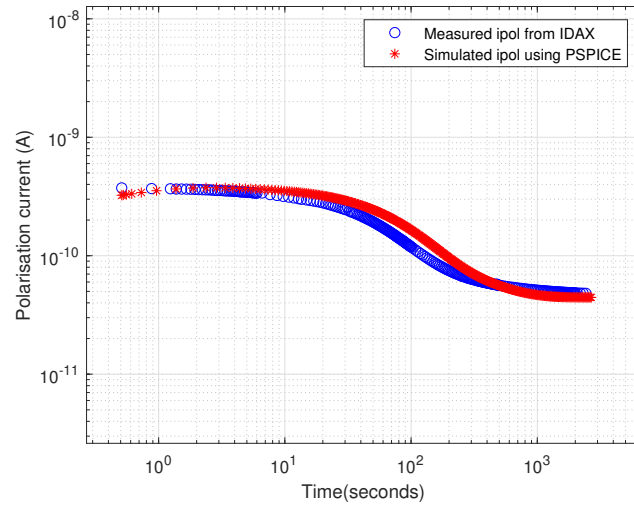


Figure 6.13: Comparison between  $i_{pol}(t)$  values from IDAX and simulated PSPICE model; Distance between the electrodes = 9.5 mm

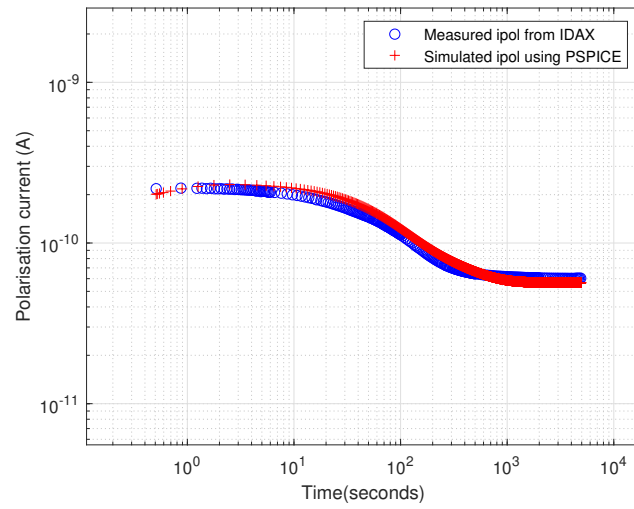


Figure 6.14: Comparison between  $i_{pol}(t)$  values from IDAX and simulated PSPICE model; Distance between the electrodes = 14.5 mm

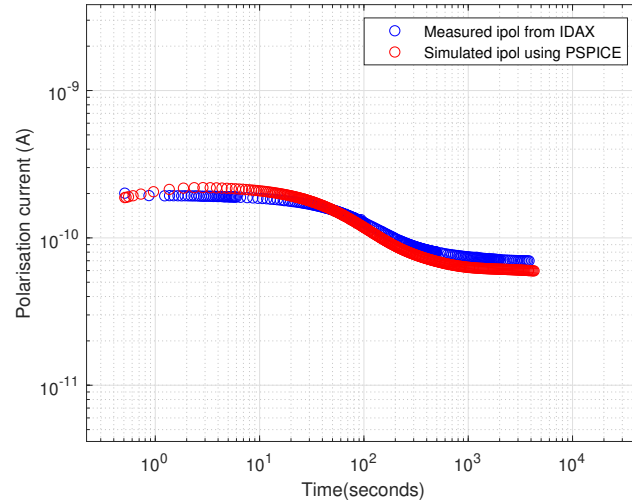


Figure 6.15: Comparison between  $i_{pol}(t)$  values from IDAX and simulated PSPICE model; Distance between the electrodes=19.5 mm

Test Sample	Distance between the electrodes	Maximum values of polarisation current $i_{pol}(t)$ measured using IDAX 300	Maximum values of polarisation current $i_{pol}(t)$ obtained from PSPICE model	Error % for maximum value of the $i_{pol}(t)$
Oil + Paper ( 0.25 mm thickness ) + Pressboard ( 1 mm thickness )	9.5 mm	373.51 pA	344 pA	7 %
	14.5 mm	219.54 pA	205 pA	6 %
	19.5 mm	201.1 pA	193 pA	4 %

Table 6.6: Comparison between measured values of maximum values of polarisation values from IDAX and the simulated model in PSPICE ; Thickness of pressboard in the composite insulation = 1 mm

Test Sample	Distance between the electrodes	Minimum values of polarisation current $i_{pol}(t)$ measured using IDAX 300	Minimum values of polarisation current $i_{pol}(t)$ obtained from PSPICE model	Error % for minimum value for the $i_{pol}(t)$
Oil + Paper ( 0.25 mm thickness ) + Pressboard ( 1 mm thickness )	9.5 mm	48.14 pA	46.08 pA	4 %
	14.5 mm	61.43 pA	56.7 pA	8 %
	19.5 mm	69.86 pA	65.73 pA	5 %

Table 6.7: Comparison between measured values of minimum values of polarisation current from IDAX and the simulated model in PSPICE ; Thickness of pressboard in the composite insulation= 1 mm

- The subsequent figures 6.16, 6.17 and 6.18 shows the comparison of the polarisation currents varying over time obtained from dielectric tests and the simulated PSPICE models of the test sample consisting of oil, paper (of thickness 0.25 mm), pressboard (of thickness 2 mm). The distance between the electrodes ' $d$ ' was varied and kept at 15.5 mm, 20.5 mm and 25.5 mm respectively. The error bars between the measured and simulated values of the polarisation currents varying over time is provided in the Tables 6.8 and Table 6.9.

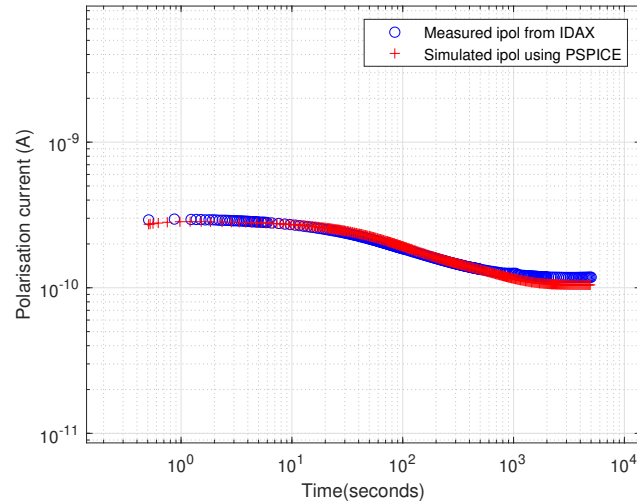


Figure 6.16: Comparison between  $i_{pol}(t)$  values from IDAX and simulated PSPICE model; Distance between the electrodes= 15.5 mm

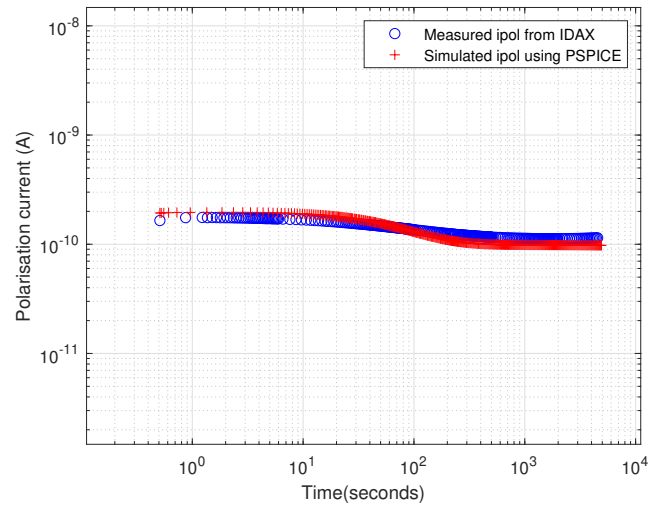


Figure 6.17: Comparison between measured  $i_{pol}(t)$  values from IDAX and simulated PSPICE model; Distance between the electrodes =20.5 mm

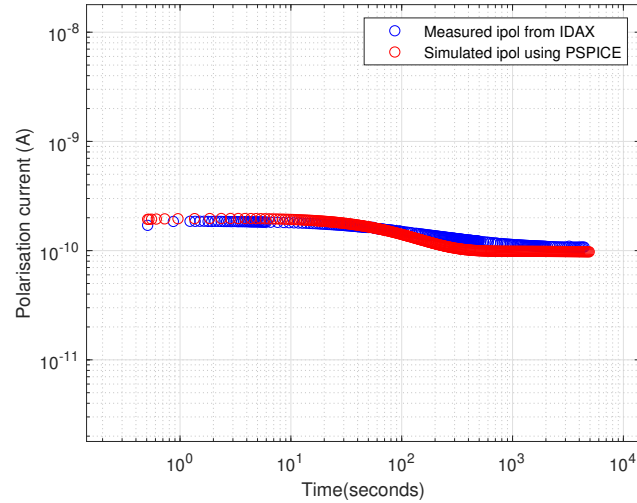


Figure 6.18: Comparison between  $i_{pol}(t)$  values from IDAX and simulated PSPICE model; Distance between the electrodes =25.5 mm

Test Sample	Distance between the electrodes	Maximum values of polarisation current $i_{pol}(t)$ measured using IDAX 300	Maximum values of polarisation current $i_{pol}(t)$ obtained from PSPICE model	Error % for maximum value of the $i_{pol}(t)$ values
Oil + Paper ( 0.25 mm thickness ) + Pressboard ( 2 mm thickness )	15.5 mm	296.12 pA	272 pA	8 %
	20.5 mm	175.72 pA	174 pA	1 %
	25.5 mm	185.79 pA	183.9 pA	1 %

Table 6.8: Comparison between measured values of maximum values of polarisation values from IDAX and the simulated model in PSPICE; Thickness of pressboard in the composite insulation= 2 mm

Test Sample	Distance between the electrodes	Minimum values of polarisation current $i_{pol}(t)$ measured using IDAX 300	Minimum values of polarisation current $i_{pol}(t)$ obtained from PSPICE model	Error % for minimum value for the $i_{pol}(t)$ values
Oil + Paper ( 0.25 mm thickness ) + Pressboard ( 2 mm thickness )	15.5 mm	118.26 pA	115 pA	2 %
	20.5 mm	113.9 pA	121 pA	6 %
	25.5 mm	107.4 pA	98.5 pA	8 %

Table 6.9: Comparison between measured values of minimum values of polarisation current from IDAX and the simulated model in PSPICE; Thickness of pressboard in the composite insulation= 2 mm

- The following figures 6.19, 6.20 and 6.21 shows the comparison of the polarisation currents varying over time obtained from DC tests and the simulated PSPICE models of the test sample consisting of oil, paper (of thickness 0.25 mm), pressboard (of thickness 5 mm). The distance between the electrodes 'd' was varied and kept at 12 mm, 17 mm and 22 mm. The error bars between the measured and simulated values of the polarisation currents varying over time is provided in the Table 6.10 and Table 6.11.

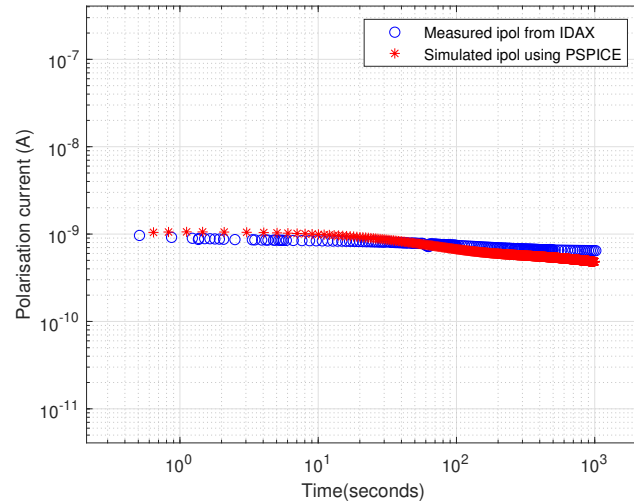


Figure 6.19: Comparison between measured  $i_{pol}(t)$  values from IDAX and simulated PSPICE model; Distance between the electrodes = 12 mm

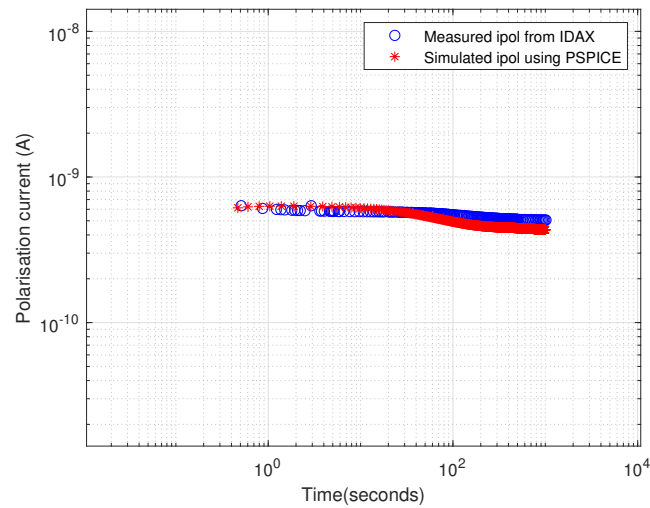


Figure 6.20: Comparison between  $i_{pol}(t)$  values from IDAX and simulated PSPICE model; Distance between the electrodes = 17 mm

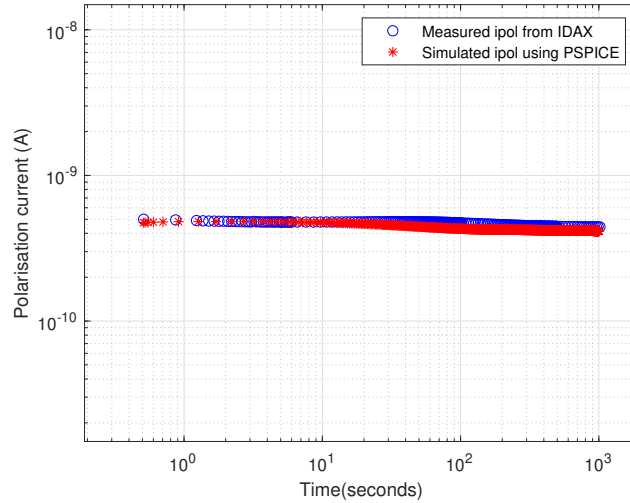


Figure 6.21: Comparison between  $i_{pol}(t)$  values from IDAX and simulated PSPICE model; Distance between the electrodes = 22 mm

Test Sample	Distance between the electrodes	Maximum values of polarisation current $i_{pol}(t)$ measured using IDAX 300	Maximum values of polarisation current $i_{pol}(t)$ obtained from PSPICE model	Error % for maximum value of the $i_{pol}(t)$
Oil + Paper ( 0.25 mm thickness ) + Pressboard ( 5 mm thickness )	12 mm	964 pA	972 pA	1 %
	17 mm	634.8 pA	643 pA	2 %
	22 mm	500.1 pA	517 pA	3 %

Table 6.10: Comparison between measured values of maximum values of polarisation values from IDAX and the simulated model in PSPICE; Thickness of pressboard in the composite insulation= 5 mm

Test Sample	Distance between the electrodes	Minimum values of polarisation current $i_{pol}(t)$ measured using IDAX 300	Minimum values of polarisation current $i_{pol}(t)$ obtained from PSPICE model	Error % for minimum value for the $i_{pol}(t)$
Oil + Paper ( 0.25 mm thickness ) + Pressboard ( 5 mm thickness )	12 mm	645 pA	595 pA	7 %
	17 mm	506.4 pA	472 pA	6 %
	22 mm	443 pA	418 pA	5 %

Table 6.11: Comparison between measured values of minimum values of polarisation current from IDAX and the simulated model in PSPICE ; Thickness of pressboard in the composite insulation= 5 mm

## 6.5. Analysis of the time dependency of depolarisation currents

This section provides the simulated polarisation and depolarisation currents of composite dielectric test samples of oil, paper and pressboard. The polarisation and depolarisation currents of composite dielectric test samples were studied at the applied DC voltages ranging from 500 V to 120 kV. The R-C circuits models of test samples were run for a charging time of  $t_c = 10,000$  seconds and then allowed a discharging time of  $t_d = 10,000$  seconds.

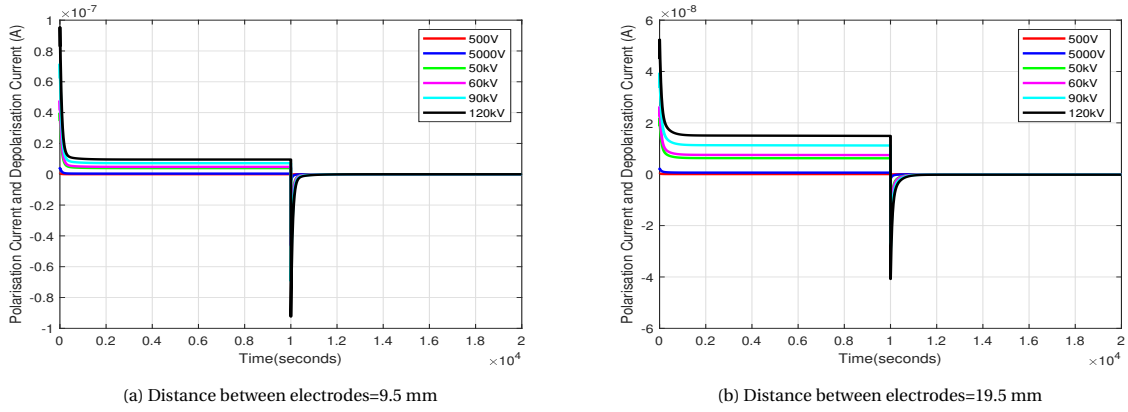


Figure 6.22: Polarisation Currents and Depolarisation Currents; Thickness of pressboard in composite insulation= 1 mm

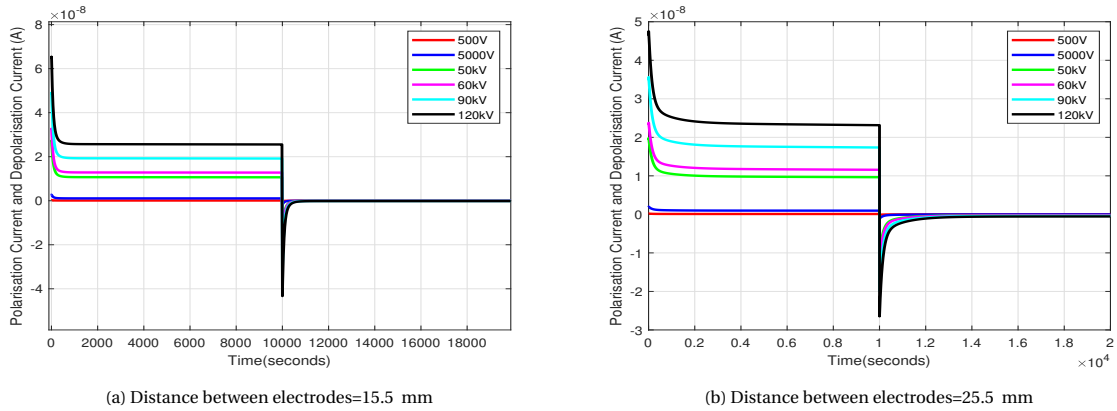


Figure 6.23: Polarisation Currents and Depolarisation Currents; Thickness of pressboard in composite insulation= 2 mm

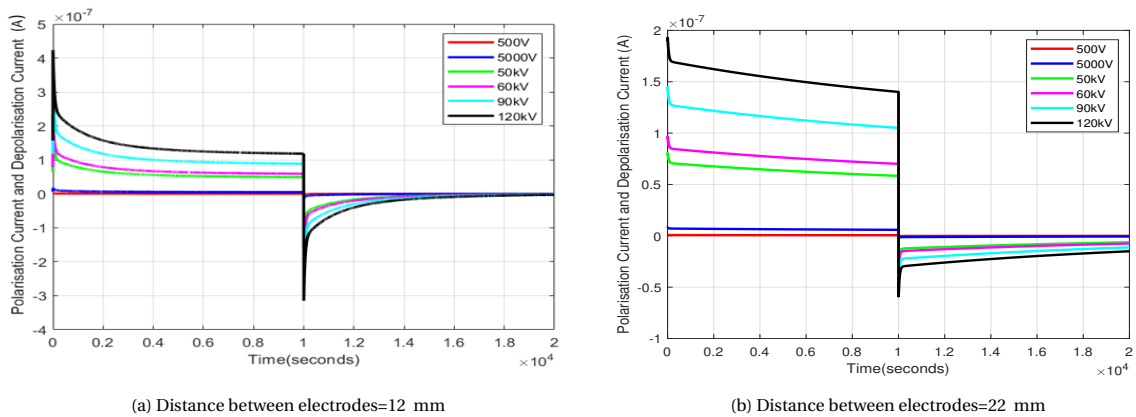


Figure 6.24: Polarisation Currents and Depolarisation Currents; Thickness of pressboard in composite insulation=5 mm

The magnitude of polarisation and depolarisation currents increased as the applied DC voltage was increased from 500 V to 120 kV [ figures 6.22, 6.23 and 6.24].

From the analysis of the depolarisation currents of composite test samples of oil, paper and pressboard, it could be seen that as the distance between the electrodes 'd' increases, the more delayed is the response of the depolarisation currents to fall to a minimum value at the end of discharging duration. The maximum value of depolarisation current at the end of discharging time  $t_d = 10,000$  seconds was obtained in the test sample in which the thickness of pressboard was 5 mm for the applied DC voltage of 120 kV [Table: 6.17] .

Test Sample	Distance between the electrodes	Applied Voltage $U_0$	Maximum values of depolarisation current $i_{depol}(t)$	Minimum values of depolarisation current $i_{depol}(t)$
Oil + Paper (0.25 mm thickness) + Pressboard (1 mm thickness)	9.5 mm	500 V	0.369 nA	0.275 pA
		5 kV	3.71 nA	2.75 pA
		50 kV	36.89 nA	27.5 pA
		60 kV	43.73 nA	33.1 pA
		90 kV	67.1 nA	49.6 pA
		120 kV	87.7 nA	66.1 pA

Table 6.12: Maximum and minimum values of depolarisation currents from PSPICE model; Thickness of pressboard in the sample= 1mm

Test Sample	Distance between the electrodes	Applied Voltage $U_0$	Maximum values of depolarisation current $i_{depol}(t)$	Minimum values of depolarisation current $i_{depol}(t)$
Oil + Paper (0.25 mm thickness) + Pressboard (1 mm thickness)	19.5 mm	500 V	0.172 nA	0.901 pA
		5 kV	1.725 nA	9.01 pA
		50 kV	17.25 nA	90.17 pA
		60 kV	20.81 nA	0.108 nA
		90 kV	31.05 nA	0.1623 nA
		120 kV	41.39 nA	0.216 nA

Table 6.13: Maximum and minimum values of depolarisation currents measured from the PSPICE model; Thickness of pressboard in the sample= 1 mm

Test Sample	Distance between the electrodes	Applied Voltage $U_0$	Maximum values of depolarisation current $i_{depol}(t)$	Minimum values of depolarisation current $i_{depol}(t)$
Oil + Paper (0.25 mm thickness) + Pressboard (2 mm thickness)	15.5 mm	500 V	0.196 nA	1.79 pA
		5 kV	1.96 nA	17.9 pA
		50 kV	19.61 nA	0.179 nA
		60 kV	23.53 nA	0.215 nA
		90 kV	35.3 nA	0.323 nA
		120 kV	47.06 nA	0.43 nA

Table 6.14: Maximum and minimum values of depolarisation currents measured from the PSPICE model; Thickness of pressboard in the sample= 2 mm

Test Sample	Distance between the electrodes	Applied Voltage $U_0$	Maximum values of depolarisation current $i_{depol}(t)$	Minimum values of depolarisation current $i_{depol}(t)$
Oil + Paper (0.25 mm thickness) + Pressboard (2 mm thickness)	25.5 mm	500 V	0.108 nA	2.51 pA
		5 kV	1.08 nA	25.1 pA
		50 kV	10.88 nA	0.251 nA
		60 kV	13.03 nA	0.31 nA
		90 kV	19.56 nA	0.45 nA
		120 kV	26.07 nA	0.603 nA

Table 6.15: Maximum and minimum values of depolarisation currents measured from the PSPICE model; Thickness of pressboard in the sample= 2 mm

Test Sample	Distance between the electrodes	Applied Voltage $U_0$	Maximum values of depolarisation current $i_{depol}(t)$	Minimum values of depolarisation current $i_{depol}(t)$
Oil + Paper (0.25 mm thickness) + Pressboard (5 mm thickness)	12 mm	500 V	1.012 nA	59.4 pA
		5 kV	10.12 nA	0.59 nA
		50 kV	108 nA	5.94 nA
		60 kV	130.6 nA	7.13 nA
		90 kV	196 nA	10.6 nA
		120 kV	253 nA	14.26 nA

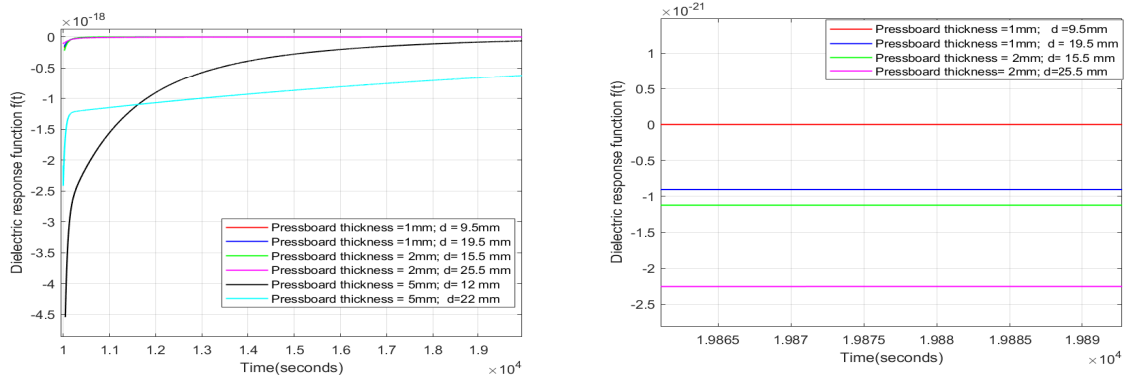
Table 6.16: Maximum and minimum values of depolarisation currents measured from the PSPICE model; Thickness of pressboard in the sample = 5 mm

Test Sample	Distance between the electrodes	Applied Voltage $U_0$	Maximum values of depolarisation current $i_{depol}(t)$	Minimum values of depolarisation current $i_{depol}(t)$
Oil + Paper (0.25 mm thickness) + Pressboard (5 mm thickness)	22 mm	500 V	0.474 nA	75.08 pA
		5 kV	4.74 nA	0.75 nA
		50 kV	47.47 nA	7.51 nA
		60 kV	56.96 nA	9.01 nA
		90 kV	85.45 nA	13.51 nA
		120 kV	118.91 nA	18.01 nA

Table 6.17: Maximum and minimum values of depolarisation currents measured from the PSPICE model; Thickness of pressboard in the sample =5 mm

### 6.5.1. Analysis of the time dependency of dielectric response function $f(t)$ in the composite insulation

The behaviour of dielectric response function  $f(t)$  displays a trend very similar to that of the depolarisation currents of composite insulation of oil, paper and pressboard. The dielectric response function  $f(t)$  for the composite sample with the pressboard of 5 mm thickness evidently takes longer time to decay to a minimum value. The plots of  $f(t)$  was computed from the depolarisation current plots of composite test samples [figures 6.22a- 6.24b] using the equation [4.23]



(a) Dielectric response function  $f(t)$  under applied DC voltage of 500V

(b) Zoomed in plots of dielectric response function  $f(t)$  of composite test samples

Figure 6.25: Estimated  $f(t)$  plots from the depolarisation current plots measured from  $t= 10,000$  to  $20,000$  seconds ; Figure (b) Dielectric function  $f(t)$  of composite test samples was zoomed in for better analysis

The plot of the dielectric response function  $f(t)$  in time domain clearly describes that the  $f(t)$  for the test sample where the electrodes are kept at a distance of 22 mm, is showing a slower decaying trend. The dielectric response  $f(t)$  is still at a significant magnitude at the end of discharging time of  $t_d= 10000$  seconds for this test sample [figure: 6.25a]. Compared to the other test samples, the thickness of pressboard (5 mm) is also more in this test sample.

It could be concluded that as the distance between the electrodes increases, the polarised dipoles will take longer time to reorient and depolarise when the applied electric field was removed. The accumulated charges at the interface also decrease very slowly. Therefore a delayed behaviour of the dielectric response function  $f(t)$  could be justified. The most active decay of  $f(t)$  is seen for the composite sample with the thickness of the pressboard was 1 mm [figure 6.25b].

## 6.6. Analysis of the time dependency of the depolarisation currents in the composite insulation under impulse voltage

In the previous section, the analysis of the time dependency of the depolarisation currents in the composite insulation of oil, paper and pressboard under DC voltages were carried out with the help of extended R-C model of the test samples developed in PSPICE. The following section outlines the analysis of the time dependency of the depolarisation currents in the composite insulation of oil, paper and pressboard under the influence of standard impulse voltage. In the first subsection, the steps followed for the built of one stage Marx generator in PSPICE is given. The next subsection describes the measurements of depolarisation currents of the test samples under the influence of the standard impulse voltage of  $1.2/50 \mu s$ .

### 6.6.1. Building one stage Marx generator in PSPICE

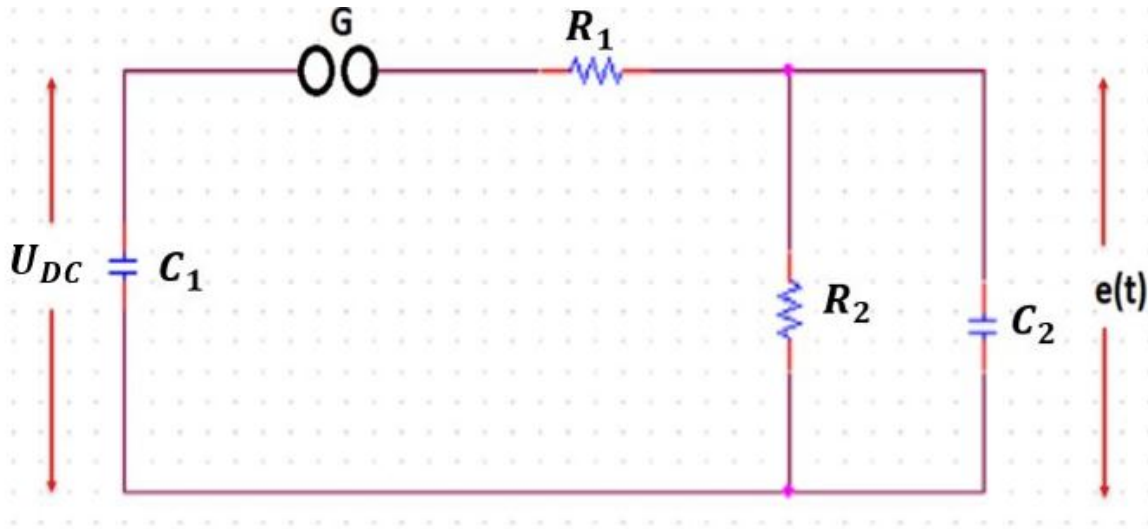


Figure 6.26: One stage Marx generator

Referring to the figure 6.26,  $C_1$  is the stage capacitor;  $C_2$  is the load capacitor;  $R_1$  is the front resistor and  $R_2$  is the tail resistor in the circuit.  $G$  is the sphere gap.

$U_{DC}$  is the applied DC input voltage. From standard waveform  $1.2/50 \mu s$  of Marx generator, the limiting value of  $C_1/C_2$  is 40 [31]. The time constants  $\tau_h$  and  $\tau_f$  bear a relation to the front and half times of the  $1.2/50 \mu s$  standard impulse wave. The relations are  $T_f = 2.96 \tau_f$  and  $T_h = 0.87 \tau_h$ . The calculations of values of  $C_1$ ,  $C_2$ ,  $R_1$  and  $R_2$  are as follows:

$$\frac{T_f}{T_h} = 1.2/50 \mu s$$

$$\tau_f = \frac{T_f}{2.96};$$

$$\therefore \tau_f = 0.4054 \mu s$$

$$\tau_h = \frac{T_h}{0.87};$$

$$\therefore \tau_h = 68.49 \mu s$$

Since maximum value of  $C_1/C_2 = 40$ , let  $C_1 = 0.5 \mu\text{F}$ . This gives  $C_2 = 0.0125 \mu\text{F}$ .

$$\tau_f = R_1 \frac{C_1 C_2}{C_1 + C_2}$$

Solving for  $R_1$ , we get

$$R_1 = 33 \Omega$$

Similarly,  $\tau_h = R_2(C_1 + C_2)$

$$\therefore R_2 \approx 134 \Omega$$

While designing the circuit with PSPICE software, the sphere gap for triggering the lightning was simulated by the use of a switch, as shown in figure 6.27. The output of the generator was also switched, and all switches were closed at the same time. The stage capacitor  $C_1$  was given an initial charge value of  $-20.7 \text{ kV}$  [31].

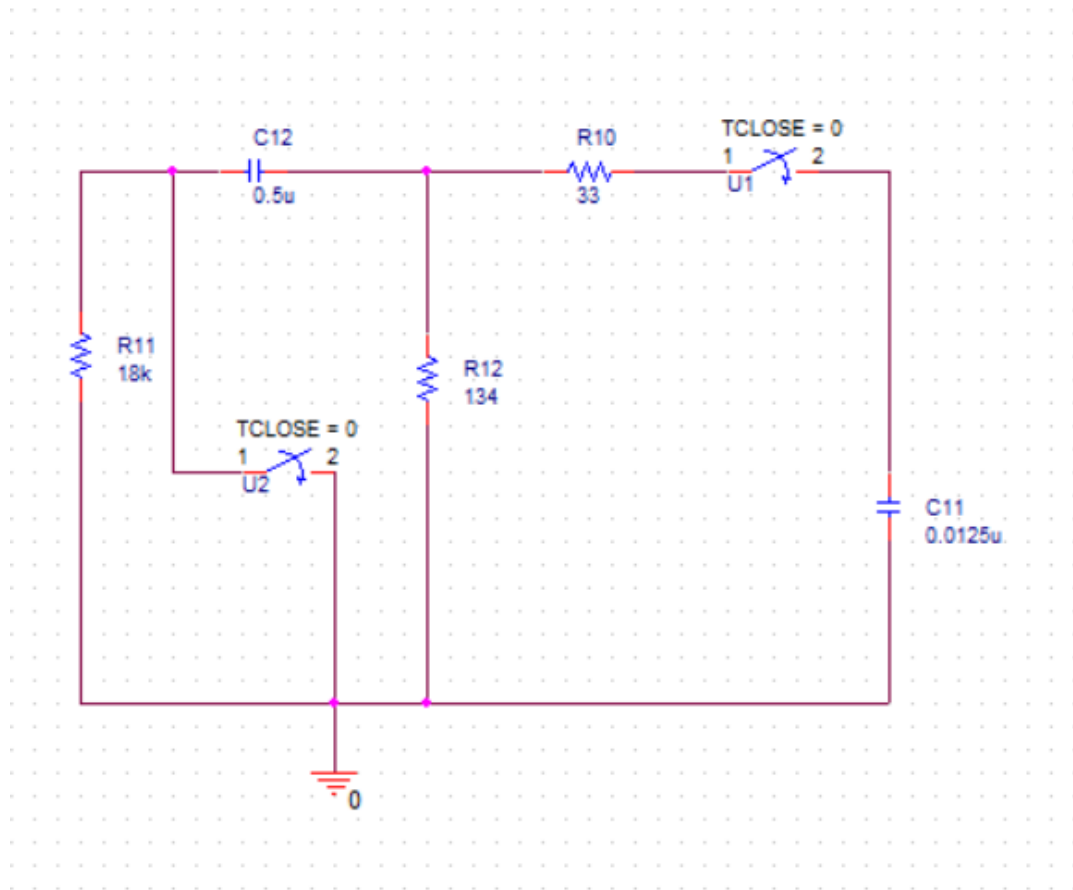


Figure 6.27: Impulse circuit built in PSPICE

### 6.6.2. Measurement of the depolarisation currents under the influence of the 1.2/50 $\mu\text{s}$ impulse voltage

A standard impulse of 1.2/50  $\mu\text{s}$ , with a peak voltage of 20 kV was applied to the R-C model representing the test sample consisting of oil, paper and pressboard to study the dielectric behaviour.

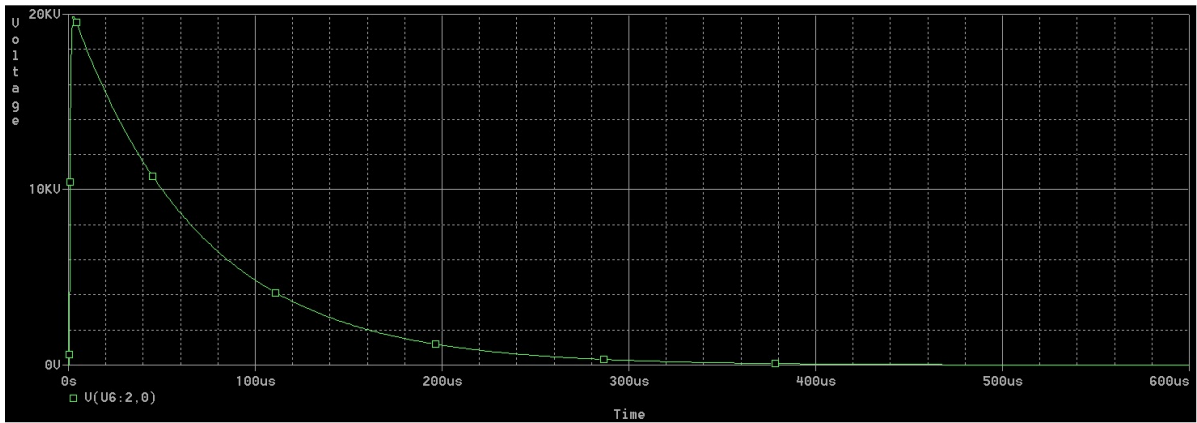


Figure 6.28: 1.2/50 $\mu$ s impulse voltage

The charging time was given as lower values in the range of micro-seconds to see the nature of polarisation and depolarisation currents from the extended R-C circuit clearly. The depolarisation current was measured until a discharge duration  $t_d=500 \mu\text{s}$  for all the test cases [Tables 6.18- 6.23].

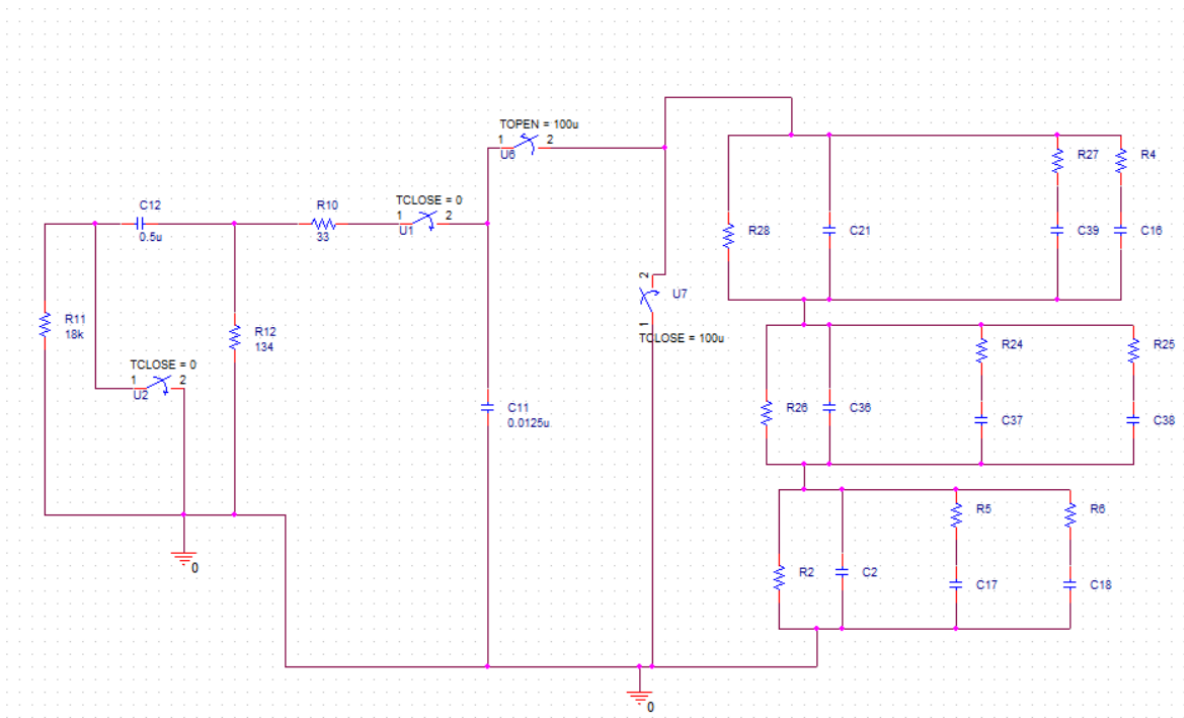


Figure 6.29: Impulse circuit connected to the extended R-C circuit

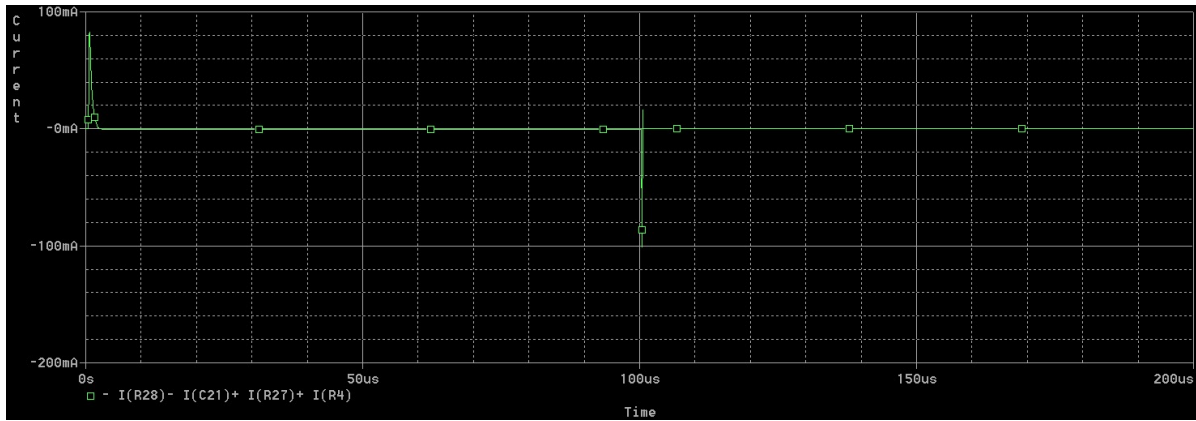


Figure 6.30: Polarisation and Depolarisation current under the influence of the applied impulse voltage

Test Sample	Distance between the electrodes	Charging time $t_c$	Maximum values of depolarisation current $i_{depol}(t)$	Positive values of depolarisation current $i_{depol}(t)$	Minimum values of depolarisation current $i_{depol}(t)$
Oil + Paper (0.25 mm thickness) + Pressboard (1 mm thickness)	9.5 mm	10 $\mu s$	748 mA	126 mA	0.07 pA
		50 $\mu s$	417 mA	70 mA	0.28 pA
		100 $\mu s$	201 mA	34 mA	0.42 pA
		150 $\mu s$	97.47 mA	16.5 mA	0.49 pA
		200 $\mu s$	47 mA	7.9 mA	0.52 pA
		250 $\mu s$	22.75 mA	3.8 mA	0.54 pA

Table 6.18: Test case:1 Maximum and minimum values of depolarisation currents; Thickness of pressboard in the sample = 1 mm

The depolarisation currents observed as a result of the applied impulse voltage was influenced by the charging time  $t_c$  for which the impulse voltage was applied. From the table 6.18, it could be perceived that the higher the charging period for which the impulse voltage was applied, the smaller will be the peak magnitude of the depolarisation current at the end discharge duration  $t_d = 500 \mu s$ . It was also noted that the depolarisation currents show a transition from negative polarity to positive polarity but quickly reverts to the negative polarity in the time frame of less than  $1 \mu s$ . With higher charging durations of  $t_c$  for which the impulse voltage was applied, the lower will be the value of the reversed positive polarity current as observed from the Table 6.18. For charging time  $t_c \geq 1$  second, the transition of depolarisation current from negative to positive polarity and back was no longer observed.

Test Sample	Distance between the electrodes	Charging time $t_c$	Maximum values of depolarisation current $i_{depol}(t)$	Positive values of depolarisation current $i_{depol}(t)$	Minimum values of depolarisation current $i_{depol}(t)$
Oil + Paper (0.25 mm thickness) + Pressboard (1 mm thickness)	19.5 mm	10 $\mu s$	369 mA	59 mA	0.02 pA
		50 $\mu s$	206 mA	33 mA	0.07 pA
		100 $\mu s$	99.5 mA	15.9 mA	0.102 pA
		150 $\mu s$	48.07 mA	7.68 mA	0.12 pA
		200 $\mu s$	23.22 mA	4.19 mA	0.125 pA
		250 $\mu s$	11.2 mA	2.02 mA	0.13 pA

Table 6.19: Test case:2 Maximum and minimum values of depolarisation currents; Thickness of pressboard in the sample = 1 mm

The Tables 6.18 and 6.19 depicts the two test cases in which the thickness of pressboard in the composite insulation was 1 mm, and the distance between electrodes was varied. The distance between the electrodes was kept as ' $d$ ' = 9.5 mm for Test case: 1 and as ' $d$ ' = 14.5 mm for Test case: 2. The comparison of maximum and minimum values of depolarisation currents, provided in Tables 6.18 and 6.19 clearly shows that the magnitude of the depolarisation currents at the end of the discharge time  $t_d$  was more when the distance between the electrodes was taken as ' $d$ ' = 9.5 mm than when kept as ' $d$ ' = 14.5mm. This difference in magnitude of  $i_{depol}(t)$  was negligible with varying ' $d$ ' ( between 9.5 mm and 14.5mm ) for a longer discharging time of  $t_d = 1$  hour.

Test Sample	Distance between the electrodes	Charging time $t_c$	Maximum values of depolarisation current $i_{depol}(t)$	Positive values of depolarisation current $i_{depol}(t)$	Minimum values of depolarisation current $i_{depol}(t)$
Oil + Paper (0.25 mm thickness) + Pressboard (2 mm thickness)	15.5 mm	10 $\mu s$	474 mA	84.5 mA	0.26 pA
		50 $\mu s$	265 mA	47 mA	0.99 pA
		100 $\mu s$	128 mA	22.77 mA	1.48 pA
		150 $\mu s$	61.8 mA	10.9 mA	1.71 pA
		200 $\mu s$	29 mA	5.29mA	1.828 pA
		250 $\mu s$	14.4 mA	2.549 mA	1.88 pA

Table 6.20: Test case:3 Maximum and minimum values of depolarisation currents ; Thickness of pressboard in the sample= 2 mm

Test Sample	Distance between the electrodes	Charging time $t_c$	Maximum values of depolarisation current $i_{depol}(t)$	Positive values of depolarisation current $i_{depol}(t)$	Minimum values of depolarisation current $i_{depol}(t)$
Oil + Paper (0.25 mm thickness) + Pressboard (2 mm thickness)	25.5 mm	10 $\mu s$	284 mA	46.33 mA	0.09 pA
		50 $\mu s$	158 mA	25.87 mA	0.38 pA
		100 $\mu s$	76 mA	12.48 mA	0.56 pA
		150 $\mu s$	37 mA	6 mA	0.65 pA
		200 $\mu s$	17.9 mA	2.9 mA	0.7 pA
		250 $\mu s$	8.64 mA	1.4 mA	0.71 pA

Table 6.21: Test case:4 Maximum and minimum values of depolarisation currents ; Thickness of pressboard in the sample= 2 mm

Test Sample	Distance between the electrodes	Charging time $t_c$	Maximum values of depolarisation current $i_{depol}(t)$	Positive values of depolarisation current $i_{depol}(t)$	Minimum values of depolarisation current $i_{depol}(t)$
Oil + Paper (0.25 mm thickness) + Pressboard (5 mm thickness)	12 mm	10 $\mu s$	4.09 A	250 mA	15.8 pA
		50 $\mu s$	2.289 A	141 mA	63.5 pA
		100 $\mu s$	1.11 A	68 mA	94.7 pA
		150 $\mu s$	533 mA	32.6 mA	109 pA
		200 $\mu s$	257 mA	15.5 mA	117 pA
		250 $\mu s$	124 mA	7.28 mA	120 pA

Table 6.22: Test case:5 Maximum and minimum values of depolarisation currents ; Thickness of pressboard in the sample = 5 mm

Test Sample	Distance between the electrodes	Charging time $t_c$	Maximum values of depolarisation current $i_{depol}(t)$	Positive values of depolarisation current $i_{depol}(t)$	Minimum values of depolarisation current $i_{depol}(t)$
Oil + Paper (0.25 mm thickness) + Pressboard (5 mm thickness)	22 mm	10 $\mu s$	2.309 A	275 mA	5.86 pA
		50 $\mu s$	1.28 A	153 mA	23.5 pA
		100 $\mu s$	623 mA	74 mA	35.1 pA
		150 $\mu s$	300 mA	35.6 mA	40.7 pA
		200 $\mu s$	145 mA	17.09 mA	43.4 pA
		250 $\mu s$	70 mA	8.15 mA	44.7 pA

Table 6.23: Test case:6 Maximum and minimum values of depolarisation currents ; Thickness of pressboard in the sample = 5 mm

After the impulse voltage was applied and removed, the maximum values of the depolarisation currents were observed to be highest for the R-C model representing the test sample where the distance between the electrodes was kept at 12 mm and the thickness of pressboard was 5 mm. From the simulated models of test samples, it could be concluded that the more the thickness of the pressboard in the composite test sample of oil-paper-pressboard, the greater would be the time taken by the depolarisation current to fall to a minimum value. The magnitude of depolarisation current at the end of the discharging period of  $t_d = 3600$  seconds was measured as  $1.28 \times 10^{-16}$  A under the influence of the impulse voltage.

## 6.7. Observations and Discussions

The following section summarises the main observations which were made during the analysis of time dependency of relaxation behaviour of R-C models of individual as well as of composite test samples built with PSPICE simulation software.

1. An accurate evaluation of the dielectric response of the transformer insulation requires the study of the dielectric behaviour of its individual components- transformer oil, pressboard and paper. For this analysis, the polarisation current measurements of the individual test samples of oil, paper and pressboard were carried out.
  - The depolarisation current plot of pressboard sample of 1 mm thickness clearly depicts a slower decaying trend when compared with the depolarisation currents of oil, paper and pressboard of 2 mm thickness [Figure 6.9].
  - The behaviour of dielectric response function  $f(t)$  follows a similar trend to that of the depolarisation currents of individual dielectrics of oil, paper and pressboard. The dielectric response function  $f(t)$  for the pressboard sample of 1 mm thickness clearly takes the longest time to decay to a minimum value [Figure 6.10].
2. Analysis of magnitude of depolarisation currents obtained for composite test samples of oil-paper-pressboard under DC voltages
  - The magnitude of polarisation currents and depolarisation currents increased with the increase in the applied voltage on the composite test samples. This was observed for all the test cases when the applied DC voltage was varied from 50 kV to 120 kV [figures 6.22, 6.23 and 6.24]. Under higher electric fields, there will easier and faster dipole formation during polarisation and therefore subsequent relaxation of the dipoles during depolarisation will also quicker when the field is removed [42].
  - From the R-C models of composite dielectric samples representing the Test cases given by the Tables 5.10, 5.11, 5.12, it was observed that as the distance between the electrodes 'd' increases,

the value of depolarisation current  $i_{depol}(t)$  at the end of the discharging time of  $t_d=10,000$  seconds also increases.

In other words, when the oil-gap  $d_{oil}$  increases for the same thickness of the pressboard sample in the composite insulation, the depolarisation currents show a delayed response to fall to a minimum value at the end of discharging duration of 10,000 seconds. According to the Maxwell-Wagner polarisation law, the charges accumulated at the interface increase with the oil layer thickness when constant electric field is maintained between two electrodes [61]. The accumulated charges decay very slowly as the charge mobility is less in multi-layered dielectrics [16]. This may be the reason for the higher value of depolarisation current  $i_{depol}(t)$  at the end of the discharging time  $t_d=10,000$  seconds for wider oil-gaps.

- After analysis of the Test cases of the composite test samples [ Tables 5.10, 5.11, 5.12 ], the composite test samples with same oil-gaps  $d_{oil}$  with different thickness of pressboard were compared. The test cases of composite samples given in Tables 5.10 and 5.11 were considered for this analysis.

The thickness of solid insulation  $d_{ppb} = \text{Thickness of pressboard} + 0.25 \text{ mm}$  (thickness of paper)

Test sample	Applied voltage $U_0$	Distance between the electrode $d$	Oil gap $d_{oil}$	Thickness of solid insulation in the composite test sample $d_{ppb}$	Minimum value of $i_{depol}(t)$ obtained at the end of discharging time $t_d= 10,000$ seconds
Oil + Paper + Pressboard	500 V	14.5 mm	13.25 mm	1.25 mm	0.597 pA
		15.5 mm	13.25 mm	2.25 mm	1.79 pA

Table 6.24: Comparison of minimum value of depolarisation current obtained from composite test samples with sample oil-gap distance  $d_{oil}$  with different thickness of solid insulation

Test sample	Applied voltage $U_0$	Distance between the electrode $d$	Oil gap $d_{oil}$	Thickness of solid insulation in the composite test sample $d_{ppb}$	Minimum value of $i_{depol}(t)$ obtained at the end of discharging time $t_d= 10,000$ seconds
Oil + Paper + Pressboard	500 V	19.5 mm	18.25 mm	1.25 mm	0.901 pA
		20.5 mm	18.25 mm	2.25 mm	63.8 pA

Table 6.25: Comparison of minimum value of depolarisation current obtained from composite test samples with sample oil-gap with different thickness of solid insulation

- The oil-gap  $d_{oil}$  for both the measurements were kept the same. The thickness of the pressboard sample was taken as 1 mm and 2 mm respectively. As seen from the Table 6.24 and

Table 6.25, with the increase in the thickness of solid insulation in the composite test sample for the same oil-gap, the magnitude of depolarisation current  $i_{depol}(t)$  at the end of the discharging time  $t_d=10,000$  seconds also will be higher [46]. The decay of the charges will be slower in the case of composite samples with thicker solid insulation as in such cases the interfacial region will provide deeper trap sites for the charges. The detrapping of charges will be slower, and this will contribute to the higher value of depolarisation current at the end of the discharging period of  $t_d=10,000$  seconds for composite dielectrics with thicker solid insulation [42].

- The value of depolarisation current  $i_{depol}(t)$  at the end of the discharging time  $t_d=10,000$  seconds was highest for the R-C model of the composite test sample with the oil-gap of  $d_{oil} = 16.75$  mm and with solid insulation thickness of  $d_{ppb} = 5.25$  mm [Table 6.26]. Such a test sample with larger oil-gap and thicker paper-pressboard insulation will have a lower breakdown strength [32].

Test sample	Distance between the electrodes $d$	Thickness of solid insulation $d_{ppb}$	Oil-gap $d_{oil}$	Oil to paper-pressboard ratio (Rounded off to nearest decimal point)	Minimum value of $i_{depol}(t)$ current obtained at the end of discharging time $t_d=10,000$ seconds
Oil + Paper (0.25 mm thickness) + Pressboard (5 mm thickness)	12 mm	5.25 mm	6.75 mm	1	59.4 pA
	17 mm		11.75 mm	2	62.3 pA
	22 mm		16.25 mm	3	75.08 pA

Table 6.26: Depolarisation current values  $i_{depol}(t)$  at the end of discharging time of  $t_d$ ; Applied voltage= 500 V

### 3. Analysis of magnitude of depolarisation currents obtained for composite test samples of oil-paper-pressboard under impulse voltage.

- Under the influence of  $1.2/50 \mu s$  standard impulse voltage, the highest value of the minimum depolarisation current was found for the R-C model representing the composite test sample given in Table 6.22. The thickness of the pressboard in the composite test sample was 5 mm and the distance between the electrodes was 12 mm. The measured minimum value of  $i_{depol}(t)$  was in the order of  $10^{-16}$  A, after allowing a discharging time  $t_d$  of one hour (3600 seconds). At the end of  $t_d$  of 1 hour, the values of depolarisation currents of the composite test samples where the pressboard samples were of thickness 1 mm and 2 mm were in the order of  $10^{-19}$  A and  $10^{-18}$  A respectively.
- From the maximum value of depolarising current at the end of discharging time of one hour measured among the composite test samples, the charge  $Q(t)$  at the end of the discharge time  $t_d=1$  hour could be estimated [11].

$$Q(t) = \int_0^{3600} I_{depol}(t) dt = 1.28 * 10^{-16} * 3600 = 0.46 pC \quad (6.19)$$

The charge density  $\sigma(t)$  is given by:

$$\sigma(t) = \frac{Q(t)}{A} = 2.83 * 10^{-16} C/mm^2 \quad (6.20)$$

where A is the cross-sectional area of the electrode ;  $A=1626 \text{ mm}^2$

The electric field due the charge density is given by:

$$E = \sigma(t)/\epsilon_0 = 32 \text{ mV/mm} \quad (6.21)$$

where  $\epsilon_0= 8.854 \times 10^{-15} \text{ F/mm}$

Hence the calculated value of electric field due to the depolarisation current at the end of the discharge period  $t_d = 1$  hour is small compared to the allowable threshold value of the electric field of 2 kV/mm inside the transformer insulation [22]. Though there is a small field enhancement due to the effect of the charge density at the end of discharging time  $t_d = 1$  hour, this electric field is very small to affect the transformer insulation and furthermore, lower the dielectric strength of the insulation.

- It was also observed that the magnitude of depolarisation current of the composite test sample at the end of the discharging period of 10 minutes and 30 minutes was still in the order of  $10^{-16}$  A. Therefore the electric field at the end of the discharging period of 10 minutes and 30 minutes would not differ drastically from the calculated electric field value at the end of the discharging time of one hour.
- More research is required in this area to have a definite conclusion regarding the effect of field enhancements due to charges remaining at the end of the discharging duration.

## 6.8. Conclusion

This chapter focuses on building an extended R-C equivalent circuit based on the linear dielectric models of oil, paper and pressboard, which forms a significant part of transformer insulation. Using the extended R-C model built-in PSPICE simulation software, the polarisation and depolarisation currents were obtained for the maximum charging and discharging duration of 10,000 seconds.

The magnitude of remnant depolarisation currents at the end of the discharging period  $t_d = 10,000$  seconds were found to be the highest when the distance between the electrodes was kept the farthest at 22 mm, which represents the wider oil gaps. For identical oil-gaps, as the thickness of the pressboard in the composite test sample increases, the magnitude of the depolarisation current at the end of the discharging period ( $t_d = 10,000$  seconds) also increases.

A standard impulse of  $1.2/50\mu\text{s}$  was used to charge the equivalent R-C model of the test sample to study the dielectric behaviour of the test models of the composite insulation. The values of depolarisation current at the end of discharging time of one hour were estimated for all the composite test samples. It was found to be the highest in the order of  $10^{-16}$  A in the test case of composite sample [Table 6.22] where the pressboard thickness was taken as 5 mm. The charge density  $\sigma(t)$  remaining at the end of the discharging period  $t_d=1$  hour in that test case was estimated. The electric field due the charge density was calculated and was found to be below permissible field value of 2 kV/mm inside the transformer insulation.

# 7

## Conclusions and Future Recommendations

This chapter outlines the main conclusions of this thesis project obtained from dielectric testing and also, from modelling of the dielectric response behaviour of transformer oil-paper-pressboard insulation. The final section of the chapter outlines the possible future recommendations in this field of research.

### 7.1. Conclusions

The primary goal of this thesis was to model the relaxation phenomena in transformer oil-paper-pressboard insulation which will help to determine the dielectric response behaviour under DC and impulse voltages. This section summarises the important conclusions made during this thesis in an attempt to answer the research questions formed at the start of the thesis.

1. Analysis of the time dependency of physical processes of polarisation and depolarisation, occurring within the transformer oil-paper-pressboard insulation
  - After a thorough review of the literature available on dielectric response analysis, the time domain diagnostic method of polarisation and depolarisation current measurement (PDC) was found to be most suitable to determine the relaxation time dependencies of oil, paper and pressboard. The study of discharge voltage measurements of the composite test sample consisting of oil, paper and pressboard showed that there are two dominant polarisation processes occurring inside the transformer insulation. The time constants of decay of the discharge voltage curves were estimated using the exponential curve-fit in MATLAB. The accuracy of the fitting was validated by the high R-square values ( $\geq 0.9$ ). The analysis of the time constants helped to ascertain the occurrence of both faster and slower polarisation processes within the transformer insulation.
  - On comparison of the results from the discharge voltage measurements with the analytical solution of the output discharge voltage developed from the simplified R-C model of the transformer insulation, indicated that there could be multiple polarisation processes happening within the complex transformer insulation.
  - The study of the time dependencies of the dielectric response of major constituents of transformer insulation comprising of oil, paper and pressboard is a crucial step to determine the inventory of effects occurring inside transformer insulation. This analysis was successfully realised by studying the simulated polarisation - depolarisation currents obtained from the R-C models of the composite oil-paper-pressboard insulation developed in PSPICE simulation platform.
2. Modified and extended R-C circuit model of transformer insulation
  - Based on the linear dielectric response theory, an extended and modified R-C circuit of the test sample was built to understand the dielectric behaviour of multi-layered dielectric. The extended

model comprised of a series arrangement of equivalent R-C circuits of oil, paper and pressboard. This modified circuit was envisioned and developed in PSPICE simulation environment. The model incorporates the effect of the individual polarisation processes occurring within the constituent dielectrics of the complex transformer insulation. The dielectric properties like conductivity and dielectric response function  $f(t)$  can be estimated accurately with this modified R-C model.

### 3. Verification of the newly developed extended R-C model of transformer insulation

- The model parameters of the linear dielectric model of the individual test samples of oil, paper and pressboard were extracted from the dielectric measurements of corresponding samples. The values of the resistances and capacitance of individual branches  $R_i$ - $C_i$  were identified by inserting arbitrary values for  $R_i$  and  $C_i$  parameters for each branch of the linear dielectric model and solving the analytical equation of the polarisation current. A comparison of the maximum and minimum values of the polarisation currents of the individual test sample obtained from the simulated model and as well as from dielectric testing demonstrated that relative errors between the polarisation current values were  $\leq 6\%$  and the developed R-C models of individual test samples were reasonably accurate.
- The circuit parameters of the extended R-C model can be successfully identified from the dielectric measurements of composite test samples consisting of oil-paper-pressboard. The parallel branches of series resistor and capacitor representing the activated polarisation processes within the constituent dielectrics were obtained from the analysis of dielectric measurements of individual samples of oil, paper and pressboard. After plugging in the values of the circuit parameters in the models built in PSPICE, the simulation of the polarisation currents of the test samples can be obtained. The simulated results were perfected after several iterations and compared with analytical equation of polarisation current derived from the linear dielectric response model. In the final stage, the polarisation current curves obtained from the simulated models were compared with the corresponding time domain polarisation current measurements of test samples. This helped to effectively implement the complex multi-layered model of transformer insulation.
- With the simulation model, not only the polarisation currents but also the depolarisation currents of the test samples can be studied for different charging and discharging durations. The test results and the simulated polarisation current values from the dielectric samples were compared regularly and hence the models of the test samples built in PSPICE were optimised to obtain similar results as the measured values of polarisation currents of the test samples obtained using IDAX 300. The comparison of the maximum and minimum values of the simulated polarisation currents with the time-domain polarisation currents obtained from dielectric testing demonstrated that relative errors of  $i_{pol}(t)$  values were limited to a maximum of 8%.

### 4. Analysis of results derived from the newly developed model

- A precise PDC measurement would take a very long time so to allow the relaxation time for all the interfacial polarisation processes inside the transformer insulation. The PDC measurement duration of 10,000 seconds charging and 10,000 seconds discharging has been regarded as a reasonable trade-off in the context of power transformer insulation. Nevertheless, in a practical situation, it is often not possible to afford such a long measurement time due to economic and time constraints.

Using the modified, extended R-C circuit model of transformer insulation, the dielectric response of the polarisation and depolarisation currents can be studied under the applied voltage  $U_0$  for longer charging and discharging times ( $\geq 10,000$  seconds).

- The analysis of relaxation time characteristics of polarisation and depolarisation currents of transformer insulation system under DC voltages showed that as the distance between the electrodes increases, the magnitude of the depolarisation current at the end of the discharging period ( $t_d =$

10,000 seconds) also increases. For identical oil-gaps, with greater thickness of the pressboard sample in the composite insulation, the magnitude of the depolarisation current at the end of the discharging period ( $t_d = 10,000$  seconds) also increased.

- The study of the depolarisation currents under the influence of impulse voltage obtained from the simulated models of the test samples showed that the charge induced field at the end of the discharging period of one hour does not exceed the permissible threshold electric field of 2 kV/mm inside the transformer insulation.

Efforts were put in to answer the research question of whether a one-hour waiting time is sufficient to allow the decay of charges so that the charge-induced field would not affect the dielectric strength of transformer insulation. The analysis of the depolarisation currents under impulse voltage at the end of the discharging period of one hour, extracted from the simulated models of the test samples helped to determine this research objective partially.

## 7.2. Future Recommendations

- During this research, an attempt was made to derive the total charge and the resultant electric field from the depolarisation current under impulse voltage. However, the analysis of the distribution of charges and charge accumulation inside the transformer insulation require further research and testing. The development of a PEA (Pulse electrode acoustic) system to investigate the space charge accumulation and trapping phenomena when tested with opposite polarity lightning impulses would help to understand the space charges behaviour inside the complex transformer insulation.
- Extensive testing with impulse voltages of opposite polarity with different waiting times ( $\leq 1$  hour) between the impulses will help to identify the 'perfect' waiting time. This waiting time thus obtained would be sufficient enough to allow the decay of charges.

Generally, as an industry standard, a waiting period of one hour is given between the application of opposite polarity LI. Testing with opposite polarity impulses of lower magnitude will serve to determine whether this waiting time could be conveniently reduced.

Administering tests with a sequence of same polarity LI (-/-/-/-) and a sequence of opposite polarity LI (-/+/-/+) and comparison of these results will help gain a better insight about the field enhancement due to the space charge behaviour inside the transformer insulation system under the influence of impulse voltages.

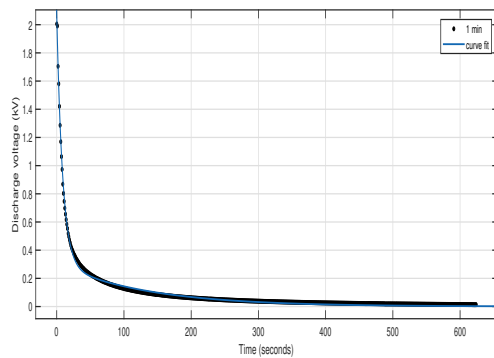
- The modified extended R-C model of transformer insulation was developed based on the time domain dielectric measurements of polarisation currents. The precision of the extended R-C model of the complex oil-paper insulation could be validated by including the measurements of the depolarisation currents to replicate the dielectric response of the test samples more accurately. This would help to improve the accuracy of extended R-C model representing complex transformer insulation (< 8%)
- Future prospects for modification of the model could be applied by the measurements of various dielectric responses concerning the parameters such as moisture content, ageing products, geometrical configuration and temperature. Such measures would serve to check the validity limits of linear dielectric response theory.

# A

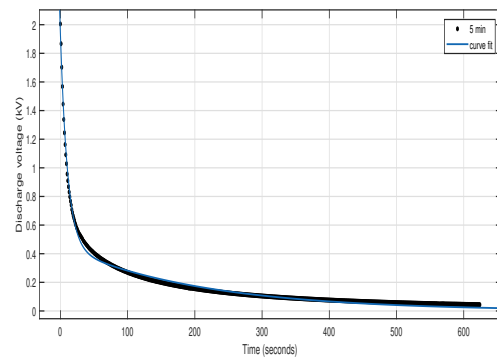
## APPENDIX

### A.1. Exponential curve fitting using curve fitting tool on discharge voltage curves

The following figures present the exponential curve fitting performed on the discharge voltage curves varying over time using the curve fitting tool in MATLAB. The following plots of the discharge voltage corresponds to the measurements given under Table 3.2



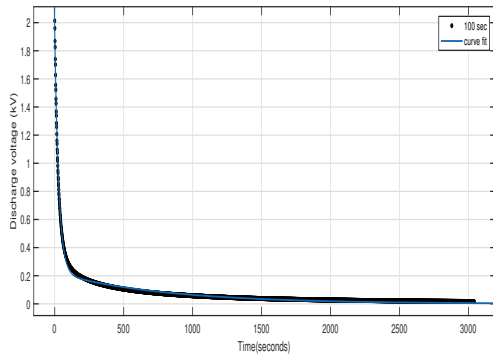
(a) Plot of discharge voltage Vs.time ;  $d = 6.4$  cm ;  $T = 39^\circ\text{C}$  ; Charging time  $t_c = 1$  min



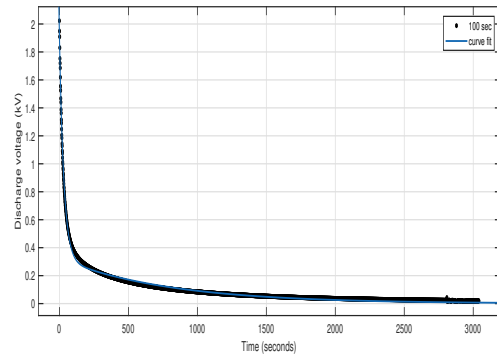
(b) Plot of discharge voltage Vs.time ;  $d = 6.4$  cm ;  $T = 39^\circ\text{C}$  ; Charging time  $t_c = 5$  min

Figure A.1: Exponential curve fitting using curve fitting tool on discharge voltage curve varying over time

The following plot of the discharge voltage corresponds to the measurements given under Table 3.3

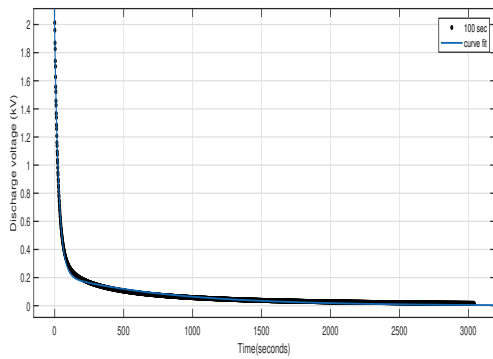


(a) Plot of discharge voltage Vs.time ;  $d = 3.2 \text{ cm}$  ;  $T = 22^\circ\text{C}$  ; Charging time  $t_c = 50 \text{ sec}$

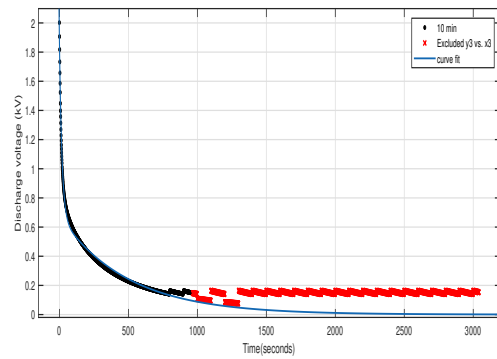


(b) Plot of discharge voltage Vs.time ;  $d = 3.2 \text{ cm}$  ;  $T = 22^\circ\text{C}$  ; Charging time  $t_c = 100 \text{ sec}$

Figure A.2: Exponential curve fitting using curve fitting tool on discharge voltage curve varying over time



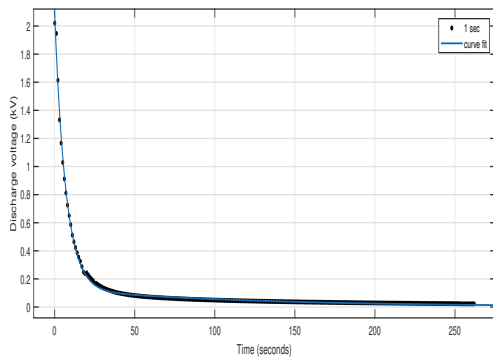
(a) Plot of discharge voltage Vs.time ;  $d = 3.2 \text{ cm}$  ;  $T = 22^\circ\text{C}$  ; Charging time  $t_c = 1 \text{ min}$



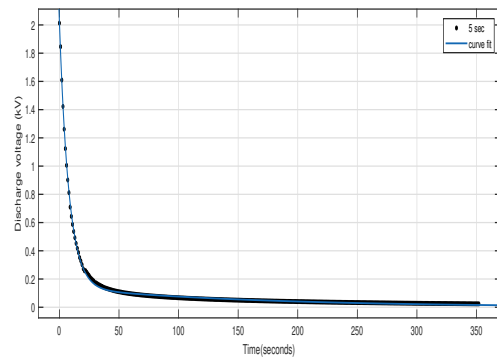
(b) Plot of discharge voltage Vs.time ;  $d = 3.2 \text{ cm}$  ;  $T = 22^\circ\text{C}$  ; Charging time  $t_c = 10 \text{ min}$

Figure A.3: Exponential curve fitting using curve fitting tool on discharge voltage curve varying over time

The following plot of the discharge voltage corresponds to the measurements given under Table 3.4

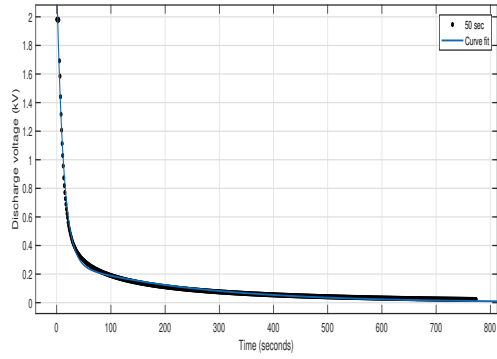


(a) Plot of discharge voltage Vs.time ;  $d = 3.2 \text{ cm}$  ;  $T = 22^\circ\text{C}$  ; Charging time  $t_c = 1 \text{ sec}$

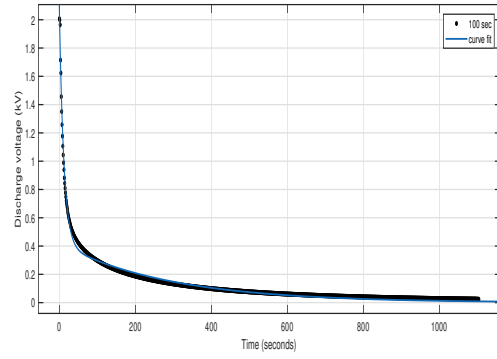


(b) Plot of discharge voltage Vs.time ;  $d = 3.2 \text{ cm}$  ;  $T = 22^\circ\text{C}$  ; Charging time  $t_c = 5 \text{ sec}$

Figure A.4: Exponential curve fitting using curve fitting tool on discharge voltage curve varying over time

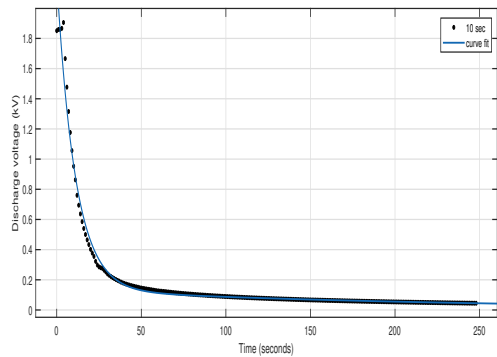


(a) Plot of discharge voltage Vs.time;  $d = 3.2$  cm ;  $T = 22^{\circ}\text{C}$  ; Charging time  $t_c = 50$  sec



(b) Plot of discharge voltage Vs.time;  $d = 3.2$  cm ;  $T = 22^{\circ}\text{C}$  ; Charging time  $t_c = 100$  sec

Figure A.5: Exponential curve fitting using curve fitting tool on discharge voltage curve varying over time



(a) Plot of discharge voltage Vs.time;  $d = 3.2$  cm ;  $T = 22^{\circ}\text{C}$  ; Charging time  $t_c = 10$  sec

# B

## APPENDIX

### B.1. Dissipation factor ( $\tan \delta$ ) of the test samples

#### B.1.1. Values of dissipation factor obtained from DC measurements on individual test samples of oil, paper and pressboard

The following Table presents the values of  $\tan \delta$  obtained from IDAX measurements of the individual test samples of oil, paper and pressboard. The moisture content (%) presented in the Tables is only an estimate calculated from the  $\tan \delta$  values as per the IDAX 300 manual.

<b>Test sample</b>	<b><math>\tan \delta</math> %</b>	<b>Moisture content %</b>
<b>Oil</b>	0.13	less than 1%
<b>Paper</b> ( 0.25 mm thickness )	4.9	more than 4%
<b>Pressboard</b> ( 1 mm thickness )	1.3	more than 1%
<b>Pressboard</b> ( 2mm thickness )	4.32	more than 1%

Table B.1: Tan delta values for individual test samples

### B.2. Values of dissipation factor obtained from DC measurements on composite test samples of oil, paper and pressboard

The following table presents the estimated values of  $\tan \delta$  obtained from IDAX measurements of the test samples given under Tables 5.10, 5.11 and 5.12. The moisture content in the test sample can be estimated

from the computed  $\tan \delta$  values as per IDAX 300 manual.

Test Sample	Distance between the electrodes	$\tan \delta$ %	Moisture content %
<b>Oil</b> + <b>Paper</b> ( 0.25 mm thickness ) + <b>Pressboard</b> ( 1 mm thickness )	15 mm	0.187	less than 1%
	20 mm	0.247	
	25 mm	0.246	

Table B.2: Test case:1  $\tan \delta$  values for the composite test sample of oil, paper and pressboard; Thickness of pressboard = 1 mm

Test Sample	Distance between the electrodes	$\tan \delta$ %	Moisture content %
<b>Oil</b> + <b>Paper</b> ( 0.25 mm thickness ) + <b>Pressboard</b> ( 2 mm thickness )	21 mm	0.284	less than 1%
	26 mm	0.260	
	31 mm	0.260	

Table B.3: Test case:2  $\tan \delta$  values for the composite test sample of oil, paper and pressboard; Thickness of pressboard = 2 mm

Test Sample	Distance between the electrodes	$\tan \delta$ %	Moisture content %
<b>Oil</b> + <b>Paper</b> ( 0.25 mm thickness ) + <b>Pressboard</b> ( 5 mm thickness )	20 mm	0.387	1 -2 %
	25 mm	0.254	
	30 mm	0.177	

Table B.4: Test case:3  $\tan \delta$  values for the composite test sample of oil, paper and pressboard; Thickness of pressboard = 5 mm

### B.3. Estimated Values of oil to paper/pressboard ratio in the composite test samples of oil, paper and pressboard

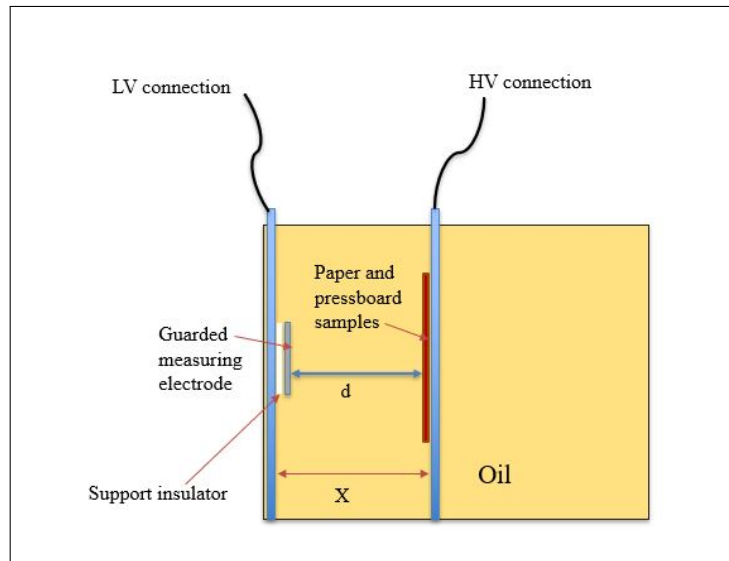


Figure B.1: Test aquarium with test dielectrics

The distance 'X' stands for the distance between the metallic plates [figure B.1]. To calculate the distance between the electrodes 'd' is calculated as follows:

$$X = 5.5 \text{ mm} + d_{oil} + d_{pap} + d_{pb}$$

$$d = d_{oil} + d_{pap} + d_{pb}$$

where  $d_{oil}$ ,  $d_{pap}$  and  $d_{pb}$  represents oil gap, thickness of paper and pressboard in the composite test sample.

Test sample	Distance between the parallel plates X	Distance between the electrodes d	Oil gap $d_{oil}$	Thickness of paper $d_{pap}$	Thickness of pressboard sample $d_{pb}$	Oil to paper-pressboard ratio
<b>Oil</b>	15 mm	9.5 mm	8.25 mm	0.25 mm	1 mm	6
<b>+ Paper</b> (0.25 mm thickness)	20 mm	14.5 mm	13.25 mm	0.25 mm	1 mm	10
<b>+ Pressboard</b> (1 mm thickness)	25 mm	19.5mm	18.25 mm	0.25 mm	1 mm	14

Table B.5: Estimation of oil to paper-pressboard ratio (Rounded off to nearest decimal point); Thickness of pressboard in composite insulation = 1 mm

<b>Test sample</b>	Distance between the parallel plates X	Distance between the electrodes d	Oil gap $d_{oil}$	Thickness of paper $d_{pap}$	Thickness of pressboard sample $d_{pb}$	Oil to paper-pressboard ratio
<b>Oil</b> + <b>Paper</b> (0.25 mm thickness) + <b>Pressboard</b> (2 mm thickness)	21 mm	15.5 mm	13.25 mm	0.25 mm	2 mm	6
	26 mm	20.5 mm	18.25 mm	0.25 mm	2 mm	8
	31 mm	25.5 mm	23.25 mm	0.25 mm	2 mm	10

Table B.6: Estimation of oil to paper-pressboard ratio (Rounded off to nearest decimal point); Thickness of pressboard in composite insulation = 2 mm

In the following test case [Test case 5.12], 'X' is given by:

$$X = 8 \text{ mm} + d_{oil} + d_{pap} + d_{pb}$$

<b>Test sample</b>	Distance between the parallel plates X	Distance between the electrodes d	Oil gap $d_{oil}$	Thickness of paper $d_{pap}$	Thickness of pressboard sample $d_{pb}$	Oil to paper-pressboard ratio
<b>Oil</b> + <b>Paper</b> (0.25 mm thickness) + <b>Pressboard</b> (5 mm thickness)	20 mm	12 mm	7.25 mm	0.25 mm	5 mm	1
	25 mm	17 mm	12.25 mm	0.25 mm	5 mm	2
	30 mm	22 mm	17.25 mm	0.25 mm	5 mm	3

Table B.7: Estimation of oil to paper-pressboard ratio (Rounded off to nearest decimal point); Thickness of pressboard in composite insulation = 5 mm

# C

## APPENDIX

### C.1. MATLAB CODE FOR CALCULATING THE MODEL PARAMETERS

The following MATLAB code is used for the calculation of geometric resistance  $R_0$  and geometric capacitance  $C_0$  of oil and pressboard in the equivalent R-C model for composite insulation.

```
% Composite insulation of oil, paper and pressboard
% Pressboard thickness = 1mm
% Distance between electrodes=15mm
```

```
clc
clear all
```

```
U0=500
relative_permittivity=3.27
ep0=8.854*10(-15)
```

```
C_m=4.27*10(-12)
ipol=351.64*10(-12)
x= (ep0*relative_permittivity)/(C_m*U0)
```

```
epoil=3.1
d=8.25
A=pi*(22.75)(2)
```

```
C0=((ep0*A)/d)
```

```
C_oil=C0*epoil
```

```
Sigma_oil=x*ipol
```

```
Roil=(ep0*epoil)/(Sigma_oil*C0)
%sigma pressboard
```

```
d_pb=1;
```

```
d_pap=0.25;
d_tot=d+d_pb+d_pap
```

```

idc=58*10(-12)

R_p=12.95*10(-12)

Sigma_r= ((idc*ep0)/(C0*U0))

Sigma_pap= (d_pb/(R_p*A));

a=(d_tot/Sigma_r);
b=(d/Sigma_oil);
c=(d_pap/Sigma_pap);

Y=a-b-c;
Sigma_PB= (d_pb/Y)
C_pb=((ep0*A)/d_pb)
Cpb=4.2*C_pb

R_pb=(d_pb/(Sigma_PB*A))

%end

```

## **C.2. MATLAB CODE FOR CALCULATING THE RELATIVE PERMITTIVITY OF COMPOSITE INSULATION**

```

%15mm1mm

ep_oil=3.18;
ep_pap=3.4;
ep_pb=4.3;
dtot=9.5
x=dtot*ep_oil*ep_pap*ep_pb

doil=8.25
dpap=0.25
d_pb=1

y=(doil*ep_pap*ep_pb)+(dpap*ep_oil*ep_pb)+(d_pb*ep_pap*ep_oil)

Relativepermittivity=x/y

%%end

```

# Bibliography

- [1] Idax series. URL <https://us.megger.com/insulation-diagnostic-analyzer-idax-series>.
- [2] Tettex for precision measurements. URL <https://ieeexplore.ieee.org/stamp/stamp.jsp?arnumber=4070189>.
- [3] High-Voltage test techniques-Part-3:Definitions and requirements for on-site testing. Standard NEN-EN-IEC: 60060-3:2006, International Electrotechnical Commission, Geneva, Switzerland, 2006.
- [4] Power transformers- Part3: Insulation levels , dielectric tests and external clearances in air. Standard IEC: 60076-3:2013, International Electrotechnical Commission, Geneva, Switzerland, 2013.
- [5] Kraft paper insulation, 2018. URL <http://precisionwires.com/tape-ktf/>. Last accessed 16 September 2020.
- [6] Abdelghaffar Abdelmalik, John Fothergill, and S. Dodd. Electrical conduction and dielectric breakdown characteristics of alkyl ester dielectric fluids obtained from palm kernel oil. *Dielectrics and Electrical Insulation, IEEE Transactions on*, 19:1623–1632, 10 2012. doi: 10.1109/TDEI.2012.6311509.
- [7] O. Aljohani, A. Abu-siada, and S. Islam. Impact of insulating oil degradation on the power transformer frequency response analysis. In *2015 IEEE 11th International Conference on the Properties and Applications of Dielectric Materials (ICPADM)*, pages 396–399, 2015.
- [8] S Bhumiwat. Application of polarisation depolarisation current (pdc) technique on fault and trouble analysis of stator insulation. In *CIGRE SCA1 & D1 Joint Colloquium, Gyeongju, Korea*, pages 79–87, 2007.
- [9] Sivaji Chakravorti, Debangshu Dey, and Biswendu Chatterjee. Frequency domain spectroscopy. In *Recent Trends in the Condition Monitoring of Transformers*, pages 193–225. Springer, 2013.
- [10] Sivaji Chakravorti, Debangshu Dey, and Biswendu Chatterjee. Recent trends in the condition monitoring of transformers. *Power Systems Springer-Verlag: London, UK*, 2013.
- [11] Gu Chao, Zhu Mengzhao, Zhu Wenbing, Jian Hao, and Runhao Zou. Thermal ageing condition assessment for transformer using natural ester-paper insulation based on polarization and depolarization current. In *2018 International Conference on Diagnostics in Electrical Engineering (Diagnostika)*, pages 1–4. IEEE, 2018.
- [12] Vahe Der Houhanessian. *Measurement and analysis of dielectric response in oil-paper insulation systems*. PhD thesis, ETH Zurich, 1998.
- [13] Sobhy Dessouky, Adel El-Faraskoury, Sherif Ghoneim, and Ahmed Haassan. Further contribution for evaluating the aging of transformer oil of power transformer. *Journal of Engineering Sciences -Assist University*, 43:211–226, 03 2015.
- [14] D. Dey, A. Sarkar, S. Pal, A. Kumar, D. Mishra, A. Baral, N. Haque, and S. Chakravorti. Effect of measurement temperature on interfacial charge freed from deep traps located at the interface of oil-paper insulation. In *2018 IEEE Applied Signal Processing Conference (ASPCON)*, pages 346–350, 2018.
- [15] Mahnaz Farahani, H. Borsi, and Ernst Gockenbach. Dielectric response studies on insulating system of high voltage rotating machines. *Dielectrics and Electrical Insulation, IEEE Transactions on*, 13:383 – 393, 05 2006. doi: 10.1109/TDEI.2006.1624283.
- [16] Issouf Fofana and Yazid Hadjadj. Power transformer diagnostics, monitoring and design features, 2018.

- [17] U. Gafvert, L. Adeen, M. Tapper, P. Ghasemi, and B. Jonsson. Dielectric spectroscopy in time and frequency domain applied to diagnostics of power transformers. In *Proceedings of the 6th International Conference on Properties and Applications of Dielectric Materials (Cat. No.00CH36347)*, volume 2, pages 825–830 vol.2, 2000.
- [18] Uno Gafvert. Condition assessment of insulation systems: analysis of dielectric response methods. In *Proc. of Nordic Insulation Symposium NORD IS*, volume 96, pages 1–19, 1996.
- [19] Uno Gafvert and Ering Ildstad. Modelling return voltage measurements of multi-layer insulation systems. In *Proceedings of 1994 4th International Conference on Properties and Applications of Dielectric Materials (ICPADM)*, volume 1, pages 123–126. IEEE, 1994.
- [20] SGB-SMIT Group. Smit group - transformatorhersteller aus europa. URL <https://www.sgb-smit.com/>.
- [21] X. Guoqiang and W. Guangning. Quantitative assessment of moisture content in transformer oil-paper insulation based on extended debye model and pdc. In *2016 China International Conference on Electricity Distribution (CICED)*, pages 1–5, 2016.
- [22] Kassim R Hameed and Ibraheem J Jabur. "fem application for evaluating and improving the insulation system of the 33kv wound-core type distribution transformer". *Modern Applied Science*, 12(9), 2018.
- [23] Wolfgang Hauschild and Eberhard Lemke. *High-voltage test and measuring techniques*, volume 1. Springer, 2014.
- [24] Jaroslav Hornak, Pavel Trnka, Pavel Totzauer, and Miroslav Gutten. The effect of space charge accumulation in high voltage insulation systems. In *2017 18th International Scientific Conference on Electric Power Engineering (EPE)*, pages 1–5. IEEE, 2017.
- [25] Vahe Der Houhanessian and Walter S Zaengl. Time domain measurements of dielectric response in oil-paper insulation systems. In *Conference Record of the 1996 IEEE International Symposium on Electrical Insulation*, volume 1, pages 47–52. IEEE, 1996.
- [26] E. Ildstad, U. Gafvert, and P. Tharning. Relation between return voltage and other methods for measurements of dielectric response. In *Proceedings of 1994 IEEE International Symposium on Electrical Insulation*, pages 25–28, 1994.
- [27] R. Islam and Z. H. Mahmood. Characterization of transformer oil for breakdown voltage, transmittance heat dissipation capability. In *2nd International Conference on Green Energy and Technology*, pages 54–58, 2014.
- [28] R. B. Jadav, C. Ekanayake, and T. K. Saha. Dielectric response of transformer insulation - comparison of time domain and frequency domain measurements. In *2010 Conference Proceedings IPEC*, pages 199–204, 2010.
- [29] AK Jonscher and K Andrzej. Dielectric relaxation in solids (chelsea, london, 1983).
- [30] T. Judendorfer, A. Pirker, and M. Muhr. Conductivity measurements of electrical insulating oils. In *2011 IEEE International Conference on Dielectric Liquids*, pages 1–4, 2011.
- [31] Muhammad Saufi Kamarudin, Erwan Sulaiman, Md Zarafi Ahmad, Saiful Aizam Zulkifli, and Ainul Faiza Othman. Impulse generator and lightning characteristics simulation using orcad pspice software. 2008.
- [32] Fred H Kreuger. *Industrial high voltage. 1, Fields. 2, Dielectrics. 3, Constructions*. Delft University Press.
- [33] Frederik H Kreuger. *Industrial high dc voltage: 1. fields, 2. breakdowns, 3. tests*. 1995.
- [34] Andreas Küchler. *High Voltage Engineering: Fundamentals-Technology-Applications*. Springer, 2017.
- [35] T. Leibfried and A. J. Kachler. Insulation diagnostics on power transformers using the polarisation and depolarisation current (pdc) analysis. In *Conference Record of the the 2002 IEEE International Symposium on Electrical Insulation (Cat. No.02CH37316)*, pages 170–173, 2002.

- [36] Libretexts. Dielectric polarization, Jul 2020. URL [https://eng.libretexts.org/Bookshelves/Materials\\_Science/Supplemental\\_Modules\\_\(Materials\\_Science\)/Optical\\_Properties/Dielectric\\_Polarization](https://eng.libretexts.org/Bookshelves/Materials_Science/Supplemental_Modules_(Materials_Science)/Optical_Properties/Dielectric_Polarization).
- [37] Ji Liu, Daning Zhang, Xinlao Wei, and Hamid Reza Karimi. Transformation algorithm of dielectric response in time-frequency domain. *Mathematical Problems in Engineering*, 2014, 2014.
- [38] Q Liu and ZD Wang. Streamer characteristic and breakdown in synthetic and natural ester transformer liquids under standard lightning impulse voltage. *IEEE Transactions on Dielectrics and Electrical Insulation*, 18(1):285–294, 2011.
- [39] Q Liu, ZD Wang, P Dyer, and D Walker. Accumulative effect on streamer propagation of lightning impulses on oil/pressboard interface. In *2011 IEEE International Conference on Dielectric Liquids*, pages 1–4. IEEE, 2011.
- [40] Qiang Liu. *Electrical performance of ester liquids under impulse voltage for application in power transformers*. PhD thesis, The University of Manchester (United Kingdom), 2011.
- [41] R Lopatkiewicz, Z Nadolny, and P Przybylek. The influence of water content on thermal conductivity of paper used as transformer windings insulation. In *2012 IEEE 10th International Conference on the Properties and Applications of Dielectric Materials*, pages 1–4. IEEE, 2012.
- [42] D Mishra, N Haque, A Baral, and S Chakravorti. Assessment of interfacial charge accumulation in oil-paper interface in transformer insulation from polarization-depolarization current measurements. *IEEE Transactions on Dielectrics and Electrical Insulation*, 24(3):1665–1673, 2017.
- [43] D. Mishra, S. Dutta, A. Baral, N. Haque, and S. Chakravorti. Use of interfacial charge for diagnosis and activation energy prediction of oil-paper insulation used in power transformer. *IEEE Transactions on Power Delivery*, 34(4):1332–1340, 2019.
- [44] NA Muhamad, BT Phung, TR Blackburn, and KX Lai. Polarization and depolarization current (pdc) tests on biodegradable and mineral transformer oils at different moisture levels. In *2009 Australasian Universities Power Engineering Conference*, pages 1–6. IEEE, 2009.
- [45] N.A. Muhamad, Toan Phung, and Trevor Blackburn. Test cell for polarization and depolarization current test of transformer insulation oil. *Jurnal Teknologi (Sciences and Engineering)*, 54:343–359, 01 2011. doi: 10.11113/jt.v54.820.
- [46] Manas Ranjan Patra and Nageshwar Rao Burjupati. Effect of moisture and geometrical parameter on dielectric behavior of ester oil impregnated insulation using dielectric spectroscopy measurement. In *2018 12th International Conference on the Properties and Applications of Dielectric Materials (ICPADM)*, pages 423–428. IEEE, 2018.
- [47] R. Patsch, J. Menzel, and D. Kamenka. Dielectric time constants the key to the interpretation of return voltage measurements on cellulose-oil insulated power equipment. In *2010 IEEE International Symposium on Electrical Insulation*, pages 1–6, 2010.
- [48] Rainer Patsch, Johannes Menzel, and Dieter Kamenka. Dielectric time constants the key to the interpretation of return voltage measurements on cellulose-oil insulated power equipment. In *2010 IEEE International Symposium on Electrical Insulation*, pages 1–6. IEEE, 2010.
- [49] T. A. Prevost and T. V. Oommen. Cellulose insulation in oil-filled power transformers: Part i - history and development. *IEEE Electrical Insulation Magazine*, 22(1):28–35, 2006.
- [50] Trek product precision electrostatic charge monitoring instruments. Non-contacting voltmeters, 2020. URL <http://www.trekinc.com/products/esvm.asp>. Last accessed 26 July 2020.
- [51] T. K. Saha and P. Purkait. Investigation of polarization and depolarization current measurements for the assessment of oil-paper insulation of aged transformers. *IEEE Transactions on Dielectrics and Electrical Insulation*, 11(1):144–154, 2004.

- [52] T. K. Saha, M. K. Pradhan, and J. H. Yew. Optimal time selection for the polarisation and depolarisation current measurement for power transformer insulation diagnosis. In *2007 IEEE Power Engineering Society General Meeting*, pages 1–7, 2007.
- [53] Tapan K Saha and Prithwiraj Purkait. Effects of temperature on time-domain dielectric diagnostics of transformers. *Australian Journal of Electrical and Electronics Engineering*, 1(3):157–162, 2004.
- [54] Fabian Schober, Stephan Harrer, Andreas K uchler, Frank Berger, Marcus Liebschner, Christoph Krause, and Wolfgang Exner. Conductivity of pressboard for hvdc insulation systems. *International journal of electrical and computer engineering systems*, 4(2.):35–41, 2013.
- [55] Fabian Schober, Andreas K uchler, and Christoph Krause. Oil conductivity—an important quantity for the design and the condition assessment of hvdc insulation systems. 2014.
- [56] Wenxia Sima, Potao Sun, Ming Yang, Qing Yang, and Jingyu Wu. Effect of space charge on the accumulative characteristics of oil paper insulation under repeated lightning impulses. *IEEE transactions on dielectrics and electrical insulation*, 22(5):2483–2490, 2015.
- [57] CF Ten, MARM Fernando, and ZD Wang. Dielectric properties measurements of transformer oil, paper and pressboard with the effect of moisture and ageing. In *2007 Annual Report-Conference on Electrical Insulation and Dielectric Phenomena*, pages 727–730. IEEE, 2007.
- [58] Genyo Ueta, Toshihiro Tsuboi, Jun Takami, and Shigemitsu Okabe. Insulation characteristics of oil-immersed power transformer under lightning impulse and ac superimposed voltage. *IEEE Transactions on Dielectrics and Electrical Insulation*, 21(3):1384–1392, 2014.
- [59] Behrooz Vahidi and Ashkan Teymouri. *Quality Confirmation Tests for Power Transformer Insulation Systems*. Springer, 2019.
- [60] Jan Peter van Bolhuis. Applicability of recovery voltage and on-line partial discharge measurements for condition assessment of high-voltage power transformers. 2004.
- [61] K. Wu, Q. Zhu, H. Wang, X. Wang, and S. Li. Space charge behavior in the sample with two layers of oil-immersed-paper and oil. *IEEE Transactions on Dielectrics and Electrical Insulation*, 21(4):1857–1865, 2014.
- [62] Zhaoliang Xing, Chong Zhang, Haozhe Cui, Yali Hai, Qingzhou Wu, and Daomin Min. Space charge accumulation and decay in dielectric materials with dual discrete traps. *Applied Sciences*, 9(20):4253, 2019.
- [63] Runhao Zou, Jian Hao, and Ruijin Liao. Space/interface charge analysis of the multi-layer oil gap and oil impregnated pressboard under the electrical-thermal combined stress. *Energies*, 12(6):1099, 2019.